กระบวนการไฮบริดด้วยไฮโดรไซโคลน โคแอกกูเลชัน ฟลอกกูเลชัน
และการลอยตะกอน ในกระบวนการผลิตน้ำประปา

นางสาววรศิริ เสียงสนั่น

HYBRID PROCESS: HYDROCYCLONE, COAGULATION FLOCCULATION AND FLOTATION IN WATER TREATMENT PROCESS

Miss Vorasiri Siangsanun

A Dissertation Submitted in Partial Fulfillment of the Requirements
for the Degree of Doctor of Philosophy Program in Environmental Engineering
Department of Environmental Engineering
Faculty of Engineering
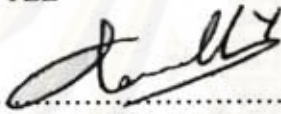Chulalongkorn University
Academic Year 2009

Thesis Title   HYBRID PROCESS : HYDROCYCLONE, COAGULATION, FLOCCULATION AND FLOTATION IN WATER TREATMENT PROCESS

By   Miss Vorasiri Siangsanun

Field of Study   Environmental Engineering

Thesis Advisor   Chaiyaporn Puprasert, Ph.D.

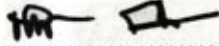Thesis Co-Advisor   Professor Gilles Hébrard, D.Eng

---

Accepted by the Faculty of Environmental Engineering, Chulalongkorn University in Partial Fulfillment of the Requirements for the Doctoral Degree
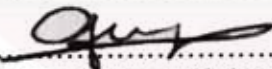
....Dean of the Faculty of Engineering
(Associate Professor Boonsom Lerdhirunwong, Dr.Ing.)

THESIS COMMITTEE
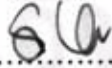
....Chairman
(Professor Yves Aurelle, D.Eng)

....Thesis Advisor
(Chaiyaporn Puprasert, Ph.D.)

....Thesis Co-Advisor
(Professor Gilles Hébrard, D.Eng)

....Examiner
(Assistant Professor Christelle Guigui, Ph.D.)

....Examiner
(Srayut Rachu, Ph.D.)

....Examiner
(Associate Professor Sutha Khaodhair, Ph.D.)

....External Examiner
(Professor Alain Grasmick. D.Eng)

วรศิริ เสียงสนั่น : กระบวนการไฮบริดด้วยไฮโครไซโคลน โคแอกูเลชัน ฟลอกกูเลชัน และการลอยตะกอนในกระบวนการผลิตน้ำประปา. (HYBRID PROCESS: HYDROCYCLONE, COAGULATION FLOCCULATION AND FLOTATION IN WATER TREATMENT PROCESS) อ. ที่ปรึกษาวิทยานิพนธ์ หลัก : อ.คร.ชัยพร ภู่ประเสริฐ, อ. ที่ปรึกษาวิทยานิพนธ์ร่วม : Professor Gilles Hébrard, 176 หน้า.

เป้าหมายของงานวิจัยนี้คือการพัฒนากระบวนการไฮบริด ซึ่งเป็นการรวมกระบวนการ โคแอกูเลชัน ฟลอกกูเลชัน และการลอยตะกอนให้เกิดขึ้นในถังปฏิกรณ์เพียงถังเดียวคือ ไฮโครไซโคลนด้วยการไหลแบบต่อเนื่อง เพื่อใช้ในกระบวนการผลิตน้ำประปา โดยศึกษาให้ เข้าใจถึงลักษณะทางชลศาสตร์และสภาวะที่เหมาะสม ที่ใช้ในกระบวนการนี้

การศึกษาลักษณะทางชลศาสตร์ในกระบวนการไฮบริด ใช้วิธีการคำนวณทาง คณิตศาสตร์เพื่อนำมาเปรียบเทียบกับผลการทดลองจริง ด้วยวิธีการวัดความเร็วด้วยเสียง ความถี่สูงของคอปเปลอร์ (Doppler ultrasound velocimetry) ผลการศึกษาทั้งสองส่วนนี้จะ นำไปเปรียบเทียบกับผลการวิจัยการวัดความเร็วด้วยวิธีหยดน้ำมัน (Oil droplet method) อีกที หนึ่ง ซึ่งการศึกษาในส่วนนี้ จะเป็นข้อมูลและความรู้พื้นฐานที่จะนำไปอธิบายปรากฏการณ์ที่ เกิดขึ้นในถังปฏิกิริยาไฮโครไซโคลน สำหรับในส่วนการศึกษาเกี่ยวกับฟองอากาศในงานวิจัย นี้ ใช้วิธีการกระจายแสงเลเซอร์ (Laser diffraction technique) เพื่อวัดขนาดและศึกษาตัวแปรที่ ส่งผลกระทบกับขนาดของฟองอากาศนี้

การทดลองเพื่อพัฒนากระบวนการไบริดแบ่งออกเป็นสองส่วนหลักๆสำคัญคือ การศึกษากับน้ำดิบสังเคราะห์ และการศึกษากับน้ำธรรมชาติจากแม่น้ำ จุดประสงค์ของ งานวิจัยนี้เพื่อประยุกต์กระบวนการไฮบริดเพื่อนำไปใช้ในการบำบัดน้ำจริง ในการทดลองมี การเปลี่ยนค่าตัวแปรต่างๆ ที่มีผลต่อระบบ เพื่อให้สามารถระบุได้ว่ามีกระบวนการแยกเกิดขึ้น หรือสำเร็จในแง่ของการบำบัดน้ำ ตัวแปรต่างๆได้แก่ ลักษณะน้ำดิบ ชนิดและความเข้มข้นของ โคแอกูแลนท์และฟลอกกูแลนท์ สัดส่วนของอากาศที่ใช้ อัตราการจ่ายน้ำดิบเข้า เป็นต้น

ภาควิชา วิศวกรรมศาสตร์สิ่งแวดล้อม ลายมือชื่อนิสิต..
สาขาวิชา วิศวกรรมศาสตร์ ลายมือชื่ออ.ที่ปรึกษาวิทยานิพนธ์หลัก.....................
ปีการศึกษา 2552 ลายมือชื่อ อ.ที่ปรึกษาวิทยานิพนธ์ร่วม.....................

4971888621 : MAJOR   ENVIRONMENTAL ENGINEERING

VORASIRI SIANGSANUN : HYBRID PROCESS: HYDROCYCLONE, COAGULATION FLOCCULATION AND FLOTATION FOR WATER TREATMENT PROCESS. THESIS ADVISOR : CHAIYAPORN PUPRASERT, PH.D., THESIS CO-ADVISOR : PROFESSOR GILLES HÉBRARD, 176 PP.

The aim of this study is to develop a hybrid process which combines with coagulation, flocculation and flotation process in a hydroclone for water treatment process. The development is concerned with the hydrodynamics characterization and the water treatment optimum condition determination.

The hydrodynamics characterization study is carried out by the numerical simulation (Computational Fluid Dynamics) and experimental work by Doppler ultrasound velocimetry technique to study the hydrodynamics for the further research.   The results are used for validating the oil droplet experimental technique and to be the basis knowledge to explain the phenomena in the hybrid process. Laser diffraction technique is involved for determining the micro bubbles size and also study on the parameter affects to the size.

The experimental work of a developed hybrid pilot plant is studied with synthesis raw water and natural river water. The objective of this study is to apply this hybrid process for the water treatment. The parameters have been varied in many operating conditions to indicate the separation and the water treatment phenomena such as raw water characteristic, coagulant - flocculant type and concentration, air fraction and inlet flow rate.

Department :   Environmental Engineering   Student's Signature ....

Field of Study : Environmental Engineering   Advisor's Signature ....

Academic Year : 2009 ....   Co-Advisor's Signature ....

ACKNOWLEDGEMENTS

CONTENTS

LIST OF TABLES

LIST OF FIGURES

LIST OF ABBREAVIATIONS

Latin letters

A_i Inlet cross section area, m^2

c   Sound speed, m/s

C_s Saturation concentration of gas in water, g/m^3

$\bar{d}$ Average diameter

d_p Particle diameter, m

g   Acceleration gravity, m/s^2

F_c Centrifugal force, $kg.m/s^2$

f_e Emits waves frequency

f_d Doppler frequency (Shift frequency)

f_r Reflected wave frequency

G   Average velocity gradient, s^{-1}

G^* Optimum velocity gradient, s^{-1}

K_H Henry's law constant

K   Constant

SS   Suspended solid,mg/L

me   Electrophoresis mobility

P   Power dissipated, m^2kg/s^3

P_T Total pressure, atm

p_g Mole fraction of gas in air

Q   Flow rate,L/hr

R   Hydrocyclone radius

r_i Rotating radius, m

T   Turbidity, NTU

t   Retention time, s

V	Volume, m^3
V_{TOT}	Total volume
v_i	Tangential velocity at any radius, m/s
v_p	Terminal velocity, m/s
v_y	Tangential velocity, m/s
v_z	Axial velocity, m/s
x_g	Mole fraction of gas in water

Greek letters

ϵ	Dielectric constant of the medium
ζ	Relative centrifugal acceleration in hydrocyclone
δv	Fluid velocity difference, m/s
δS	Distance difference, m
ρ_w	Density of water, kg/m^3
ρ_p	Density of solid particle, kg/m^3
ρ_m	Density of dispersion phase, kg/m^3
η	Dynamic viscosity
μ	Dynamic viscosity, N/m^2

CHAPTER I

INTRODUCTION

1.1   Thesis title

Hybrid process: Hydrocyclone, Coagulation – Flocculation and Flotation in a water treatment process

1.2   Key words

Hybrid process

Hydrocyclone

Coagulation – Flocculation process

Flotation process

Oil droplet method

Computational Fluid Dynamics

Doppler Ultrasound Velocimetry

1.3   Introduction

Hydrocyclone is a type of separation equipment used for solid-liquid and liquid-liquid systems. It is used to separate dispersed particles from a continuous fluid from the effect of a swirl flow and has been used in many mineral processing and mining industries. The hydrocyclone advantages are that it is simple to maintain and operate. It costs are economical and uses a compact area.

In the environmental engineering field, the hydrocyclone is not widely used. In industrial work, the hydrocyclone is used for separation microsand which is used as the contacting nuclease in coagulation – flocculation, before being fed   into the water treatment system.   There are some works that use hydrocyclones to separate the components of coagulant and particles which are called "floc" in order to decrease the amount of floc before the sedimentation process.   However, in the environmental engineering field, using the hydrocyclone is still limited because of the understanding of the phenomenon inside the hydrocyclone.

The conventional water supply system is composed with the main unit, coagulation – flocculation processes.   These systems combine the suspended solids to be the floc which will be separated from the clear water.   The separation methods such as sedimentation or

flotation system and also filtration system eliminate the turbidity in the water. Then the disinfection process eliminates the microbial. To decrease the turbidity in the water, the conventional process has to use many units in the system.

This study is to create a new process which is called a Hybrid process combining four processes; coagulation, flocculation, flotation and floc separation by the vortex flow which is the main mechanism in the hydrocyclone. All the processes will occur in one hybrid reactor. For that the number and size of the reactor will be decreased. Moreover, to modify the hydrocyclone operation, it is necessary to understand the hydrodynamics inside the reactor. Consequently, this study will also study the hydrodynamics in terms of velocity profile.

In this study of water treatment, it is aimed to develop a hybrid process by changing the geometry and verifying the hydrodynamic phenomena inside the reactor by experimental methods; Doppler ultrasound velocimetry is used to verify the oil droplet method. Computational fluid dynamic simulation by the software package, FLUENT 6.3.26 is utilized for the velocity profile inside hydrocyclone.

Moreover, a laser diffraction technique is involved to determine the micro bubble size from the Dissolved Air Flotation technique. The process will be done in a continuous operation by controlling the parameters and reactor geometry.

1.4 The expecting advantages

1. To know the possibility of creating new water treatment process, a so called Hybrid process: hydrocyclone, coagulation, flocculation and flotation processes for water treatment in a continuous operation.

2. To know the effects of the parameters of the Hybrid process: hydrocyclone, coagulation, flocculation and flotation processes.

3. To have unique research about a hybrid process to be applied to natural water treatment.

1.5 Objective and scope of this study

1.5.1 Objective

1. To characterize the hydrodynamic conditions inside a new hydrocyclone built from the results of previous studies in terms of the velocity profile by a numerical method, Computational Fluid Dynamics and an experimental method; oil droplet and Doppler velocimetry technique.

2. To determine the micro bubble size from the Dissolved Air Flotation technique used in the hybrid process.

3. To investigate the modified hybrid process for water treatment with synthetic raw water and natural water

4. To find the optimum operating conditions of the hybrid process

1.5.2 Scope of the study

This study is a test in the pilot plant scale at room temperature. The experiment will be tested in the laboratory of the Institut National des Sciences Appliquées (INSA) Toulouse in France and the Centre of Research Annet sur Marne of Veolia Company in France between November 2007 and October 2009.

1. There are two types of the raw water usage in this study

    I. The synthetic water is a suspension of bentonite particle in tap water

    II. The natural water is from La Marne River which is adjacent to the Annet sur Marne water treatment plant.

2. The results will be mainly from observation of the phenomenon in the treatment process which will be monitored by taking photo, VDO recordings by a digital camera and a high speed camera.

3. The chemical substances used in this study are cationic polymer FO107, anionic polymer AN905 and Aluminum sulfate WAC HB. These chemical substances will be used as the coagulant and the flocculant.

4. The numerical simulation will be done with computational fluid dynamic (CFD) techniques by the commercial software package FLUENT 6.3.26.

5. Laser diffraction for micro bubble size measurement is done by Spraytec Malvern Instruments.

.

CHAPTER II

BIBLIOGRAPHY

This study is concerned with Hydrocyclone, Coagulation – Flocculation and the flotation processes. Moreover the Computational Fluid Dynamics will be studied to simulate and compare the results to the previous study. The experimental method; the oil droplet method and Doppler velocimetry method will be used in this study. Consequently, each subject will be described as follow.

2.1 The Hydrocyclone

2.1.1 The Hydrocyclone introduction

The classical hydrocyclone is the separation equipment. It separates solid-solid, solid-liquid or liquid-liquid mixtures. The separation action of hydrocyclones is based on the effect of centrifugal forces created within the cyclone body. In contrast to sediment centrifuges, however, hydrocyclones have no rotating parts and the necessary vortex is produced by injecting the fluid tangentially into a stationary cylindrical body. The mixture which can be separated needs to have the density difference. The conventional hydrocyclone is composed of three flow components (Rushton et al., 2000)

1. Feed inlet
2. Overflow
3. Underflow
   These three flow components are shown in Figure II-1
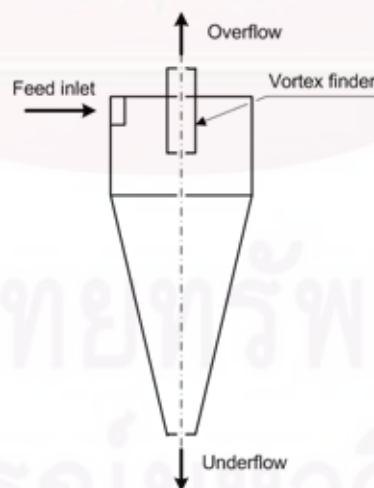
Figure II-1   A schematic diagram of a conventional cylindrical hydrocyclone

The hydrocyclone mechanism is to feed the mixture into the tangential inlet duct. The motion of the fluid within the cyclone body creates the ‚outer vortex‟ flow or

„primary vortex" downward to the underflow orifice. The underflow carries most of the solids, which leaves through the opening in the apex of the cone. The rest flows reversely in a vertical direction and goes up via the „inner vortex" flow or „secondary vortex" and out through the vortex finder, or so called overflow.

As mentioned above, in a hydrocyclone there are two swirl flows; the primary and secondary vortex. The formal flow spins close to the hydrocyclone wall downward to the underflow orifice. The underflow carries most of the solids or high density material through the underflow apex. The latter flow, the secondary vortex, spins upward with the clear water or low density solid through the overflow vortex finder. The velocity of the secondary vortex flow presents low pressure at the hydrocyclone axis and produces the „air core".

The hydrocyclone can be both a clarifier and/or thickener. Considering the overflow dilutes or carries low density particles while the underflow presents concentrated solid or high density particles.

The hydrocyclone diameter range is between 10mm. to 2.5m. The separated particle range is between $2 - 250\mu m$. and the feed flow rate range is between 0.1 to 7200m^3/hr. The pressure drop between the feed inlet duct and underflow apex range is 0.34 – 6 bars (Svarovsky, 1984).

Designing the vortex finder affects the short-circuit flow. Instead of a flow downward through the outer vortex, the short – circuit flow goes along the top of hydrocyclone and leaves through the vortex finder without being separated by the vortex flow.

The hydrocyclone's advantages

1. The hydrocyclone can be used widely, to separate liquid – solid, liquid – liquid and gas – liquid.

2. The hydrocyclone is simple to install and operate. It is economically and has a low cost of maintenance.

3. The hydrocyclone uses a compact area compared to the other separation systems and a low retention time.

The hydrocyclone's disadvantages

1. The separation in the hydrocyclone is never completed. There is some fine escaping with the overflow and there is certainly liquid discharging with underflow.

2. Inner wall hydrocyclone corrosion happens from the impact from the mixture injection.

2.1.2 Fluid flow and Particle Motion in Hydrocyclone

The mechanism of treatment or separation by the hydrocyclone mainly uses the centrifugal force. The vortex flow line in the hydrocyclone is produced from the tangentially attached feed inlet.
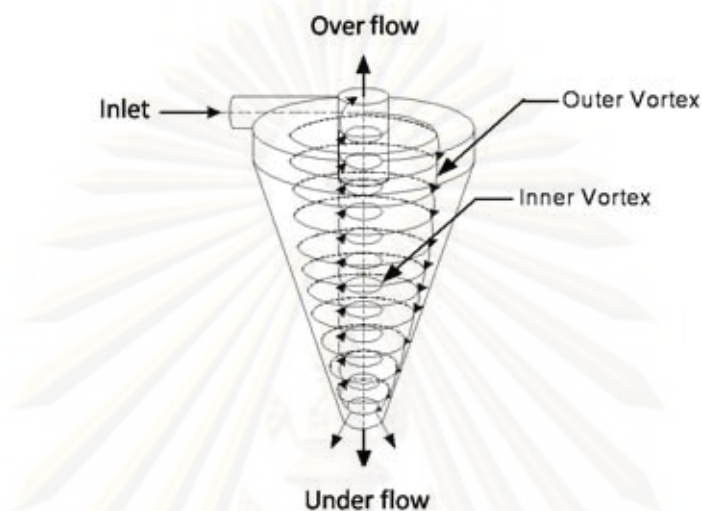
**Figure II-2   A perspective view of a hydrocyclone showing
the vortex flow inside schematically**

Figure II-2 shows the conventional hydrocyclone. The cylindrical part is closed at the top by a cover, through which the liquid overflow pipe (called „*vortex finder*") protrudes some distance into the cyclone body. The underflow part which carries the solids leaves through the opening in the apex of the cone. The fluid is fed through the inlet aperture tangentially. The size of the inlet aperture controls the inlet flow rate.

Except for the region in and just around the tangential inlet duct, the motion of the fluid is shown in Figure II-2

At the top of the cylindrical section, there exists some secondary flow pattern which moves across the top cover to the base of the vortex finder and along the outer wall of the tube until it joins the rest of the fluid in the overflow. This secondary, „short-circuit" flow is due to the presence of the cyclone cover and the outer wall of the vortex finder, which slows down the spin velocity in their immediate vicinity and thus provides areas of lower resistance to flow from the outer regions to high pressure to the inner regions of lower pressure.
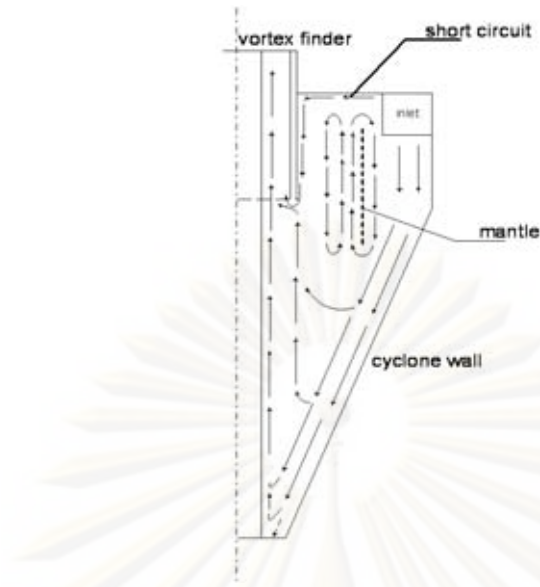
Figure II-3   A simplified diagram of the axial and radial flows in a hydrocyclone

Figure II-3 gives a simplified diagram of the axial and radial flows in a conventional hydrocyclone. The short circuit flow can be clearly seen. There are also one or more circulation eddies marked as „mantle" which provide a buffer between the downward moving outer vortex and the upward moving inner vortex. The mantle eddies prevent any radial flow through a cylindrical surface within the flow.

Another important feature of the flow in the hydrocyclone is the formation of the central air core. The strong vortex flow creates an area of low pressure in the centre which normally results in the formation of a rotating free liquid surface, cylindrical in shape and running the whole length of the cyclone. If either or both outlets are connected directly into atmosphere, the core is filled with air. Any dispersed or even dissolved gases in the incoming fluid will also report to this central core which may exist even when the outlets are not connected into the atmosphere. The air core is quite a desirable phenomenon. It is an indication of vortex stability and it should be reasonably straight and constant in diameter throughout the cyclone length.

2.1.3   The velocity in the hydrocyclone

When the fluid is fed tangentially into the hydrocyclone, the velocity of flow in a hydrocyclone can be conveniently resolved into three velocity components: tangential, axial and radial.

2.1.3.1   Tangential Velocity, V_y

The tangential velocity is the linear velocity which is fed into the inlet aperture in a tangentially direction to the hydrocyclone wall. It relates to the inlet flow rate and the cross section area as shown in the Equation II-1.

$$V_y = \frac{Q}{A_i}$$
Equation II-1

In the cyclone the condition nearly approaches that which has conservation of angular momentum as implied by Equation II-2

$$V_i r_i = \text{Constant}$$
Equation II-2

Considering the angular momentum,

$$V_y R^n = \text{Constant}$$
Equation II-3

Where n is an empirical exponent, which normally has values between 0.5 and 0.9. and $n = 1$ when the resistance force is negligible. (Kelsall, 1952 cited in Svarovsky, 1984)

The most important velocity component is the tangential velocity because it is the one which creates the vortex flow which promotes the separation mechanism inside the hydrocyclone. Thus Equation II-3 is the basic hydrocyclone calculation.

Tangential velocity distribution was confirmed by the flow measurements by Kelsall (1952). Kelsall's work measured clean water flow with fine aluminum particles and used an optical microscope within a transparent, 76 mm diameter hydrocyclone. The results are summarized in Figure II-4, which shows the tangential velocity in the cone section only.
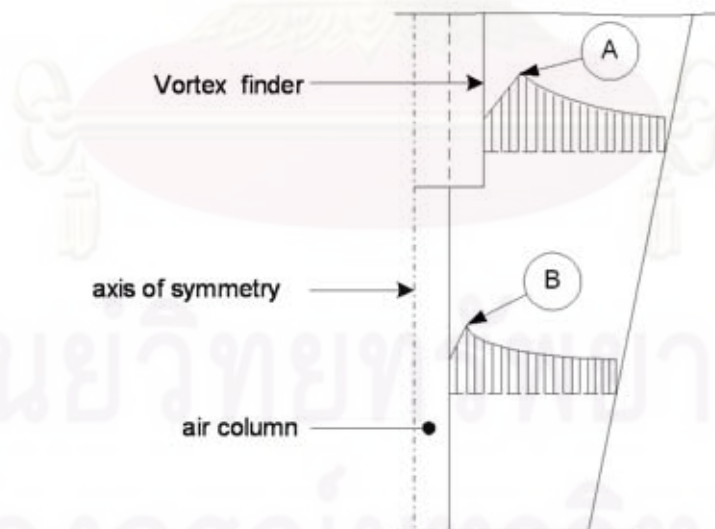
Figure II-4   Tangential velocity distribution in a hydrocyclone (V_y)

Figure II-4, the tangential velocity increases with the decreasing radius as predicted by Equation II-3. In the inner vortex zone, the velocity decreases which cannot be described by Equation II-3. The radius of the peak of tangential velocity (point B) is

smaller than the inside radius of the vortex finder. At levels above the rim of the vortex finder (point A), the break in the rising tangential velocity occurs at a larger radius. Apart from this phenomenon, the tangential velocity is independent of the vertical position in the cyclone.

2.1.3.2 Axial velocity, V_z

Axial velocity is the velocity on the axis of the hydrocyclone direction, which can be upward or downward flow as shown in Figure 3.5. The flow in the outer vortex moves downward and the inner vortex moves upward. There is a well defined *Locus of Zero Vertical Velocity* (LZVV) between the two vortices which roughly follow the profile of the cyclone. The short-circuit flow alongside the vortex finder wall can be seen clearly as well.
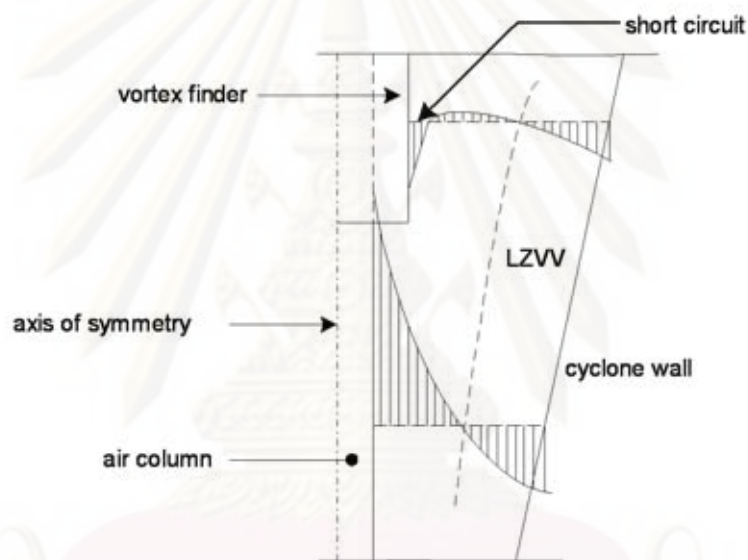
**Figure II-5   Axial velocity distribution in a hydrocyclone.
LZVV in the locus of zero vertical velocity**

2.1.3.3 Radial velocity, v_x

Radial velocity has the perpendicular direction to the cyclone axis. Radial velocity is the smallest velocity component and is the least important of the three of them. The highest radial velocity is above the vortex finder close to the hydrocyclone wall as shown in Figure II-6.
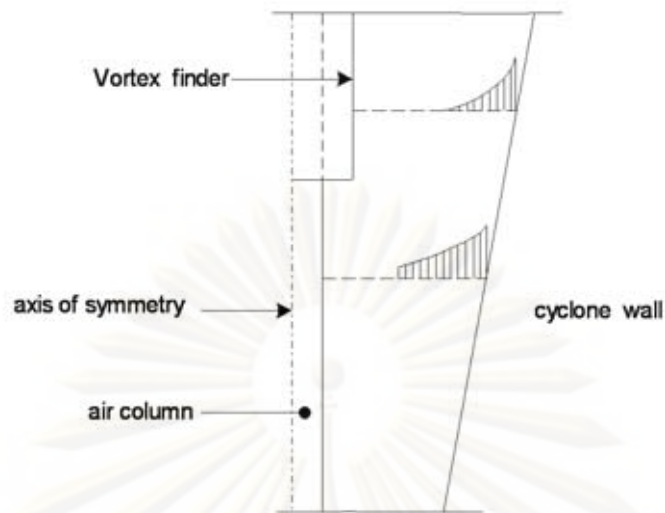
Figure II-6   Radial velocity distribution in a hydrocyclone

2.1.4   Particle motion in a hydrocyclone

The separation process is created in the hydrocyclone by tangential injection of the solution to the hydrocyclone. Since this process is carried out by centrifugal force, the density of the particles has to be different from that of the water. This way, they are separated immediately by the centrifugal force, which is created by the fluid rotation in the hydrocyclone. The applied forces on the particles are detailed in the Figure II-7.

F_1 = Centrifugal force in x-axis
F_2 = Drag force in x-axis
F_3 = Buoyancy force in z-axis
F_4 = Drag force in z-axis
F_5 = Tangential force in y-axis
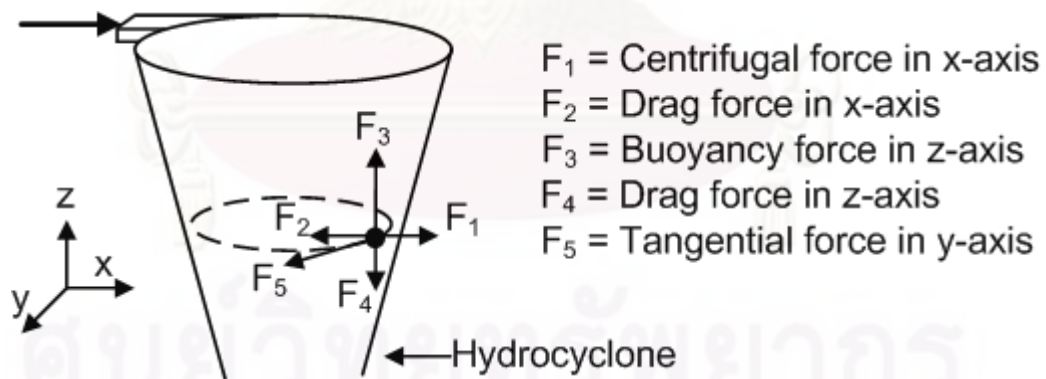
Figure II-7   Various forces applied on particle from different axes

From Figure II-7, it can be concluded that there are many forces acting on particle motion in the hydrocyclone such as the centrifugal force, drag force, buoyancy force, and weight force. These forces are related to the different parameters such as particle size, liquid density, radius distance, and viscosity.

Table II-1   Expression of various forces on the different axes

Force	Expression	Equation
F_1	Centrifugal force (on the x-axis)	$(\rho_p - \rho_m)\dfrac{V_y^2}{R}\dfrac{\pi d_p^3}{6}$
F_2	Drag force (on the x-axis)	$\dfrac{1}{2}\rho_L V_x^2 \dfrac{\pi d_p^2}{4} C_D$
F_3	Buoyancy force	$(\rho_p - \rho_m)g\dfrac{\pi d_p^3}{6}$
F_4	Drag force (on the z axis)	$\dfrac{1}{2}\rho_L V_z^2 \dfrac{\pi d_p^2}{4} C_D$

The centrifugal force along the x-axis (F1), which is proportional to particle volume, is opposed by the drag force (F2), which according to Stokes' law is proportional to the particle area. Assuming a steady state condition for one particle along the x-axis, an increase in particle diameter involves an increase in the centrifugal force that is greater than the increase in the drag force. In that case the particle is projected into the underflow via the external vortex. In an opposite situation, a decrease in particle size leads to a larger decrease in the centrifugal force than in the drag force; in this case, the particle is brought into the overflow via the internal vortex. This comment allows understanding the cut size notion in the hydrocyclone.

2.1.5   Physical-chemical parameters

Stoke's law is the fundamental theory to find the terminal velocity of the separation process such as sedimentation. There is a force acting on the small sphere particle when it moves in the fluid. Gravitational force moves the particle to settle while the particle's moving downward has the drag force (frictional force) against the movement and the viscosity force (buoyant force) of the fluid. The gravitational force which acts on the particle can be determined by the particle density. High density causes a high gravitational force.

To determine the terminal velocity from Stoke's law in this research is to understand and indicates the possibility of separation.

Stoke's law Equation (Metcralf and Eddy, 2003)

$$v_p = \frac{g(\Delta\rho)d_p^{\,2}}{18\mu} \qquad\qquad \text{Equation II-4}$$

Equation II-4 shows the important parameters for particle separation as follows:

1. Acceleration due to gravity

The conventional sedimentation for the water treatment is normally based on gravitational force. For other separation equipment, the gravity force can be increased to raise the terminal velocity. Though, the relation between the acceleration in the hydrocyclone, ζ and the gravitational acceleration, g can be described as the Equation II-5 (Chaiyaporn Puprasert, 2004; Warren, Julian and Peter, 1993: 1061)

$$\zeta = \frac{v_y^2}{R \cdot g}$$

Equation II-5

2. The density difference of the two phases ($\Delta\rho = \rho_p - \rho_w$)

This parameter is important for the Stoke's law in order to separate the two phases. This research separates solids from liquid in the hydrocyclone. If there is no density difference between two phases ($\Delta\rho = 0$), the terminal velocity will be zero ($v_p = 0$). Consequently, the separation process will not occur. Thus, hydrocyclone separation needs the density difference.

3. Liquid viscosity (μ)

This parameter affects the terminal velocity (v_p) in which high liquid viscosity decreases the terminal velocity. The liquid temperature also affects to the viscosity, high temperature decreases the viscosity. Thus, to increase the terminal velocity, the fluid viscosity should be high and the temperature should be low.

4. Particle size diameter (d_p)

This is also an important parameter. It is the power of two. For that, the large particle diameter size causes a very high terminal velocity. Consequently, increasing the particle size promotes a good separation process in hydrocyclone.

Consequently, it is implied that the hybrid process should be modified the geometry which concerning to the radius (R) in order to provide the optimum acceleration. Besides, it is necessary to produce a lighter phase: aerated floc in order to govern the density difference between water phase and aerated floc.

2.2 Coagulation and Flocculation processes

2.2.1 The role of coagulation-flocculation

The coagulation-flocculation processes facilitate the removal of suspended solids and colloids by gathering the solids to be floc. The colloid size is between 10^{-6}mm to 10^{-3}mm or 1μm. Its size is unable to settle by gravitational force in the limited time. The colloids are stable as their surface electric charge. For that, to form a particle group of

suspended solids is necessary. The definition of coagulation is to destabilize the colloid particle. The destabilized particle is called micro floc. Then the flocculation process is to gather the micro floc to form a larger size for the sedimentation separation.

2.2.2   Coagulation process

2.2.2.1   Colloid stability

Since colloids are the particles that cannot settle naturally, there are two main forces that can determine the stability of colloidal suspensions.

- Van der Waals attraction, which relates to the structure and form of colloids as well as to the type of medium (E_A)

- the electrostatic repulsive force, which relates to the surface charges of the colloids (E_B)

The stability of a colloidal suspension depends on the balance between the forces of attraction and repulsion, the energy level of which is:

$$E = E_A + E_B$$ Equation II-6

In order to destabilize the suspension, it is necessary to overcome the energy barrier E. To accomplish this and promote the agglomeration of the colloids, it is necessary to reduce the electrostatic repulsive forces. This destabilization is brought about by coagulation.

2.2.2.2   The double layer theory

In natural water, the colloids invariably carry a negative charge. In order to neutralize this negative surface charge, positive ions, which are present in raw water or are introduced into it, come together to form a layer around the colloid. Various theories have been put forward (Monod, 1991).

- **The Helmholtz theory**: A layer of positive ions covers the entire surface of the colloid and ensures the neutrality of the entire mass (bound layer).

- **The Gouy-Chapman theory**: The layer of positive ions is spaced unevenly around the colloid; neutrality is obtained at a greater distance (diffuse layer).

- **The Stern theory** brings together the two preceding theories and introduces the idea of a double layer. The first layer, which is attached to the colloid, rapidly loses its potential. The second layer, which is more diffuse, undergoes a slower loss of potential.
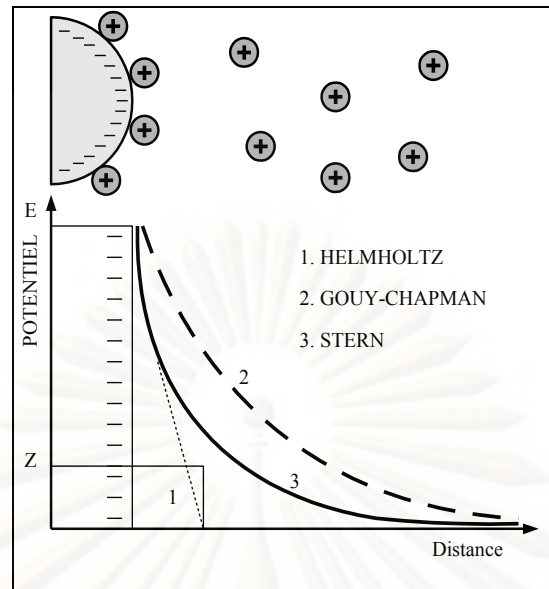
Figure II-8   The double layer theory

2.2.2.3   The zeta potential

The colloid moves with part of its double layer. The colloid has two potentials as shown in Figure II-8.

- E: The surface potential of the colloid or the thermodynamic potential.

- Z: The potential at the shear surface or the electrokinetic potential.

The Z potential, so called the zeta potential, indicates the movement of the colloids and their mutual interaction. It can be defined through electrophoresis: when a particle is subjected to an electrical field, it almost instantly attains a velocity so that there is a balance between the electrical force of attraction and the friction due to the viscosity of the medium.   The following relationship between the zeta potential and the electrophoretic mobility is obtained by the calculation.

$$me = \frac{\in Z}{k\eta}$$
Equation II-7

Where, me = Electrophoresis mobility

$\in$ = Dielectric constant of the medium

η = Dynamic viscosity

Those particles that have the same electrokinetic zeta potential possess the same electrophoretic mobility regardless of their diameter.

In the double layer theory, coagulation nullifies the zeta potential.

2.2.2.4 The chemical theory

Since the covalent forces of attraction are 20 to 50 times greater than the electrostatic forces. Chemical theory has been introduced to interpret the destabilization of colloidal suspensions. This theory puts forth the idea that the primary charge carried by a colloidal particle is due to the direct ionization of chemical groups on its surface (hydroxyl, carboxyl, phosphates, sulphates, etc.). The destabilization is achieved through a covalent reaction between these groups and the polyvalent metallic ions of the coagulants.

This theory shows that the simultaneous precipitation of metallic hydroxides and the interparticular bridging are significant factors in coagulation.

2.2.3 Flocculation

Flocculation is the agglomeration of destabilized particles into microfloc, and later into bulky floccules which can be settled, called *floc*. The introduction of another reagent, called a *flocculant* or a *flocculant aid* may promote the formation of the floc.

Two transport factors determine flocculation:

2.2.3.1 Perikinetic flocculation

Perikinetic flocculation is connected to Brownian diffusion (thermal agitation). The flocculation rate or the variation in the number of particles in a period of time is given. This flocculation only occurs in cases where the particles are smaller than 1 micron. It promotes the formation of microfloc.

2.2.3.2 Orthokinetic flocculation

Orthokinetic flocculation is tied to dissipated energy. The effectiveness of flocculation in this case, which promotes the formation of bulky separable floc. This flocculation is practical. The particle must be larger than $0.1 - 1$ micron and the concentration should be more than 50mg/L. The turbulent conditions can be defined with velocity gradient G.

For the small particle (≤ 1 micron) the perikinetic flocculation is more significant and does not need to promote the orthokinetic flocculation for the colloid system. However, the 1 micron particle size has higher and/or equals the microfloc formation rate to the orthokinetic flocculation when the velocity gradient $G \geq 10s^{-1}$. Consequently, this condition should be orthokinetic flocculation. It can be concluded that the small colloid size should be formed larger than 1 micron by perikinetic flocculation. Later, produce the orthokinetic flocculation of 1 micron floc size by mixing.

2.2.4 The importance of the velocity gradient

The velocity gradient G can be defined in laminar flow, as the difference in velocity between two adjacent liquid veins in the orthogonal plane with respect to their movement:

$$G = \frac{\delta v}{\delta S}$$
Equation II-8

Gradient velocity can indicate the agglomeration of destabilized particles but not accuracy. In the practical method, the velocity gradient should not be high enough to break the floc with the water shear force. The typical range of velocity gradient is between $400 - 1000s^{-1}$ for the coagulation process and $100s^{-1}$ for the flocculation process.

2.2.5 Reagents for coagulation and flocculation processes

Coagulant destabilizes the suspended colloid in the water. The higher the valency the more effective the coagulating action will be (Schultz-Hardy theory: a trivalent ion is ten times more effective than a divalent ion) (Monod, 1991). For that the trivalent cations is considerable.

The neutralization of the negative surface charge of the colloid is accomplished by the addition of cations in the case of inorganic coagulants. When choosing a coagulant, its harmlessness and its cost must be taken into account. Thus, trivalent iron or aluminum salts have been and continue to be widely used in all water coagulation treatments.

2.2.5.1 Flocculant

To agglomerate the destabilized colloid or micro floc from the coagulation by adding the flocculant or coagulant aids. Inorganic polymers (activated silica) and natural polymers (starches, alginate) were the first to be used. But the appearance of widely varying synthetic polymers has changed flocculation results considerably. In fact, a flocculant usually does not take effect until the coagulation stage is over (Less than 1 minute). The length of the coagulation stage depends on the type of colloid as well as on the temperature of the raw water. The main factors that should be borne in mind are the size of the floc, its cohesion and its settling rate.

The use of synthetic flocculants often results in a minimum amount of sludge. Combined with modern separation techniques, this can lead to the production of a very dense sludge that can be directly treated in a dewatering unit.

2.2.5.2 Coagulation mechanisms

There are four coagulation mechanisms

- Coagulation with alum and iron compound

- Adsorption-destabilization coagulation

- Sweep coagulation

- Polymer or coagulant aids bridging

For a hybrid process: using the hydrocyclone coagulation-flocculation and flotation in this research, the coagulation process will approach adsorption-destabilization and polymer bridging mechanisms that will be described as follows.
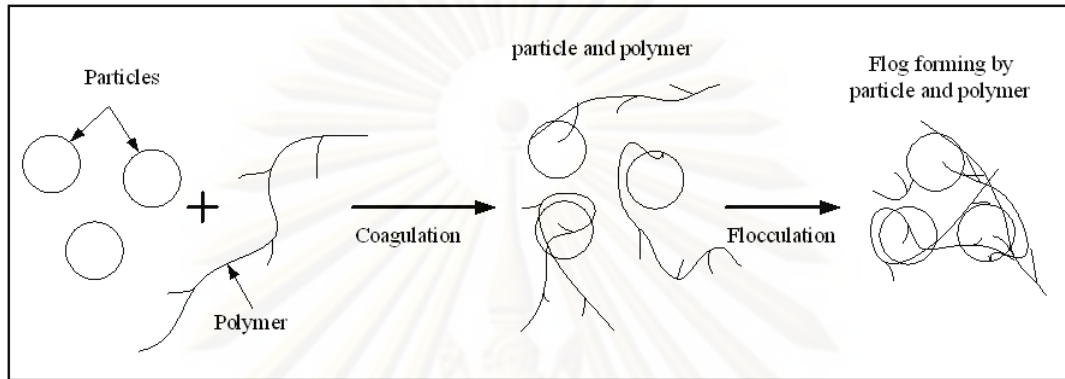
Figure II-9   Polymer bridging mechanism

The synthetic organic polymer which is used as the coagulant to destabilize the colloid mostly has a large molecular weight. Cationic, anionic and non-ionic polymers are all possible to use in polymer bridging mechanism. Figure II-9 shows how the polymer links with the colloid on its surface. The adsorption is from the different ions of the polymer and colloid or the chemical reaction between the same ion of the polymer and colloid. The connected colloid-polymer which still has the free bond to connect with another colloid is a *destabilized colloid*. This colloid is able to connect to another particle with the polymer as a bridge. This linkage occurs whenever the polymer and the colloid surface are available. Using an over dose polymer can cause the *restabilization* because many polymer molecules link with the same colloid particle. They lose the surface for another colloid-polymer to link. The colloid stabilization is not neutralized. The floc breakage problem can happen from the high shear force mixing.

The alternative destabilization mechanism is to reduce the stern layer, destabilization of the colloid ion surface, sweep coagulation and coagulation with alum and iron compound. These mechanisms are concerned about the coagulant ion which has to be opposite of the colloid ion. The optimum coagulant dosage and pH of the water are important for the coagulation process.

This research intends to use polymer as the coagulant and uses a polymer bridging mechanism because pH is not considered. The coagulant dosage will be tested by Jar test method.

2.2.6 Coagulation and flocculation control

For the coagulation, an intense mixing is the required parameter for dispersing the coagulant uniformly throughout the basin and for allowing an adequate contact time between the coagulant and the suspended particle. A rational approach for evaluating the mixing and design of the basin has been developed by Camp and Stein (1943). The mixing intensity is measured by the global velocity gradient. The equation used to calculate the average velocity gradient is presented in Equation II-9.

$$G = \sqrt{\frac{P}{\mu V}} \qquad\qquad \text{Equation II-9}$$

The coagulation is a very rapid phenomenon therefore, a low contact time is required. Therefore, whatever the operating parameters, the average gradient velocity has to be greater than 100s^{-1} and the mean residence time lower than 60s. For the instantaneous mixing, the velocity gradient can reach 1000 s^{-1} as reported in Table II-2.

In flocculation, the growth of small floc sizes is performed by the adequate mixing intensity. They are contacted slowly to create the large flocs. However, floc structure may be broken if very high mixing intensity is used. The average velocity gradient has to be lower than 100s^{-1} and the mean residence time is required to be higher than 600s^{-1}.

The recommended global velocity gradient for the coagulation and flocculation process is summarized in Table II-2.

Table II-2 The recommended criteria for the coagulation and flocculation process

Process	Detention time, s	$G_{a,m}$ Value, s^{-1}	References
Coagulation stage			
Typical rapid mixing operations in waste water treatment	5-20	250-1500	Tchobanoglous (2004)
Coagulation	-	400-1000	Degrémont (2005)
Mixing condition	300	200	Chaiyaporn Puprasert (2004)
Coagulation mixing basins	20 30 40 50 or more	1000 900 790 700	Reynolds and Richards (1995)

Process	Detention time, s	$G_{a,m}$ Value, s^{-1}	References
Flocculation stage			
Typical flocculation process used in wastewater treatment	600-1800	20-80	Tchobanoglous (2004)
Flocculation	-	100	Degrémont (2005)
Coagulation-flocculation phase 1	1800	75	Chaiyaporn Puprasert (2004)
Coagulation-flocculation phase 2	600	30	

Table II-2, the recommended values for the detention time of the coagulation tank range from 5 - 300s, and the recommended velocity gradient should be within the range of 200-500s^{-1}. In the flocculation process, the recommended contact time and velocity gradient ranges from 600 - 1800s^{-1} and 20 - 100s^{-1}, respectively.

It could be noticed that the criteria of the detention times and the averaged velocity gradients in Table II-2 is valid for the conventional coagulation and flocculation process. These processes are followed by the setting which is not used for separation in this study. Therefore, these criteria could be used as the roughly guideline.

In the coagulation and flocculation process, solid particles are destabilized and agglomerated together to form large flocs. A first step with coagulation stage is necessary to neutralize the colloidal particles. A second, the flocculation stage is carried out to form the large floc. After floc formation, the next step at a water treatment plant is the separation process used to remove flocs formed in the water. Therefore, there are many types of separator used such as a settling tank, hydrocyclone, or flotation tank. In this study, the separation process involve with the flotation process and the hydrocyclone mechanism. The following section will explain the technique of micro bubble generation by a flotation process: dissolved air flotation.

2.3 The flotation process

Flotation is a gravity separation process in which air or gas bubbles are attached to solid particles. The bubble-particle agglomerates have a density lower than the liquid and rise to the surface where they accumulate as a *float*. The success of the process depends on two separate factors, one the formation of an ample supply of suitable small bubbles and the other the attachment of the bubbles to solid particles.

Bubbles may be generated by any of five methods:

1. Dispersed-air flotation, wherein a high-speed mechanical agitator is combined with some form of air injection system.

2. Dissolved-air (vacuum) flotation, wherein water is saturated with air at atmospheric pressure then passed to a flotation chamber where the pressure is reduced to below atmospheric pressure. The air, now super-saturated, precipitates out of the solution.

3. Microflotation, where pumped air is dissolved into water under a hydrostatic head of, say, 15 m. As the water flows to the surface the air precipitates out of solution.

4. Electroflotation, where a direct (low voltage) current is passed across two plate electrodes immersed in water. From the electrolytic dissociation of water, bubbles of hydrogen and oxygen are produced.

5. Dissolved-air (pressure) flotation, where air is dissolved into a stream of liquid under pressures higher than atmospheric. On reduction of the pressure to atmospheric, air precipitates out of solution.

As a general propose solid-liquid separation tool, the two flotation techniques which have found increasing value in recent years are dissolved-air and electrolytic flotation. With dissolved-air flotation, the only chemical additives required are those commonly used for colloidal destabilization purposes, e.g. metal coagulants and polyelectrolyte. With activated sludge, dissolved-air flotation operates successfully with no chemical addition whatsoever required for efficient bubble particle attachment.

For hybrid process, this research used adissolved air flotation will be used for the micro bubbles production technique. This technique will be described in the next part.

2.4 Dissolved-air flotation: DAF

2.4.1 Dissolved-air flotation mechanism

The dissolved-air flotation mechanism is to dissolve the air into water under 2-3 atmospheric pressure. On reduction of the pressure to atmospheric, air precipitates out of solution. This method has two systems; recirculation and non-recirculation systems.

In the flotation system, there is the flotation unit and the air saturator. The solid phase – liquid phase separation process occurs in the flotation unit. The air saturator conducts the air into water under the pressure to become air saturated water by passing the relief valve into the flotation unit. Pressure reduction from 2-3atm to atmospheric pressure causes the air to precipitate out of the solution in micro bubble form and attach to the colloid particle and form a bubble-particle agglomerate whose density is lower than water. The buoyancy force lifts the bubble-particle agglomerate up to the water surface where they gather with each other called *floated floc* or *aerated floc* on the surface.

The released air bubbles become attached to the suspended particles by one of the following mechanisms:

1. **In the adsorption mechanism**, air in excess of atmospheric saturation comes out of solution by formation on the surface of the suspended particle. This is not the dominant mechanism. . Hence, it is necessary to first achieve near complete air release by turbulence before attachment to the particles.

2. **The entrapment mechanism** is perhaps the most significant in the flotation process. In this mechanism, the air-to-solids bond is created by collision during random motion. Air bubble and particle size must be controlled to some extent to ensure that there is a sufficient radius of attachment to maintain the bond until separation. Particle size is controlled by the amount of energy added during the enflocculation process.

3. **The absorption mechanism**, which provides a "permanent" air-to-solids bond, can be the predominant mechanism when the final step of chemical flocculation occurs after air release. This occurs as the air bubbles become embedded in the floc mass.

After the air-to-solids bond is complete, flotation will occur if the net combined specific gravity of the air-to-solids agglomerate is less than 1.0. Rise rate of the undisturbed agglomerate is governed by Stokes' Law.

Actual separation of the suspension in the flotation unit will also be governed by the solids and air concentration; and, the degree of turbulence.

The flotation process is employed where separation of particles having specific gravities close to that of water is desired. The flotation process will provide faster separation and higher ultimate solids concentration.

Sludge volume generated by the DAF process will be nearly equal to other system processes, but the DAF will have more air volume entrapped with the sludge; therefore, less water entrapment.

2.4.2 Air dissolution mechanism

The parameter which affects the bubble-particle agglomerate floating rate is the air/solid ratio. It is concerned to the parameters as follow.

1. Pressure to compress the air into water

2. Saturator feed/ wastewater feed

If the air dissolved into water is inefficient, the recirculation ratio should be increased to reach the optimum air/solid ratio. Thus, the flotation tank will be increased which increases the cost.

There are three air dissolution methods.

2.4.2.1   Sparged air system

Air is compressed into water in bubble form by passing through the saturator using a fine bubble diffuser. The saturation level depends on the compressed air flow rate and the hydraulic retention time in the saturator. The system efficiency can be improved by violent agitation of the saturator contents such as high velocity impellers.

2.4.2.2   Air injection system

Air is introduced at the suction side of a centrifugal pump and is intimately mixed with the water by the shearing action of the impeller. The air-water mixture is passed to a saturator to allow sufficient time for dissolution. With this method only about 25% of the air required for saturation is dissolved into the water because of the risk of air binding in the pump. Full saturation can only be achieved by introducing air in a supplementary fashion, e.g. by also injecting air downstream of the pump or by sparging air in the saturator.

2.4.2.3   Packed column system

Water is distributed evenly over some form of proprietary packing media under pressure in a saturator. Of these three methods, the packed column system was found to be markedly superior in performance. It is not necessary (nor desirable) to pass air counter-currently through the packing, since a decrease in the rate of percolation will result. Air is introduced at the top of the saturator, at a rate sufficient to replace that dissolved and removed in the saturator feed. For packing depths exceeding 300mm and pressures above 3 atmospheres, full saturation is obtained up to the maximum surface loading rate possible through the packing before ponding occurs (Bratby and Marais, 1974)

In this hybrid process, the packed column system with the air-water mixing media is chosen to produce the micro bubbles.

2.5   Air flow rate calculation

In this research, there will be an air pressurized water flow rate. It will be injected into the reactor together with the raw water. In order to calculate the amount of air compare to all inlet flow rates, Henry"s law is used to calculate the air in the system.

The equilibrium or saturation concentration of gas dissolved in a liquid is a function of the type of gas and the partial pressure of the gas in contact with the liquid. The relationship between the mole fraction of the gas in the atmosphere above the liquid and the mole fraction of the gas in the liquid is given by the following form of Henry"s law (Metcalf and Eddy, 2004)

$$p_g = \frac{K_H}{P_T} x_g$$ Equation II-10

In this research, Henry's law is used for air fraction calculation in which the air pressurized water under pressure for the aerated floc production.

2.6 Literature reviews of coagulation and flocculation in hydrocyclone

Plitt and Ligle (1967 cited in Roldan-villasana et al., 1999: 1229) studied a 32mm hydrocyclone and used polyacrylamide as the flocculant to treat clay slurry which had the average size 5μm and silica which had the average size 25μm.

The results show the overflow concentration decreased 72% with clay slurry and 50% with silica.

This study concluded that the treated particle by flocculation process is able to be separated better than the untreated (and fine) particle such as clay.

Visman and Hamza (1973 cited in Roldan-villasana et al., 1999:1229) used a hydrocyclone in an industrial factory to treat (separate) coal which passed the flocculation process. The results showed that the shear force inside the 10-50mm hydrocyclone did not affect the floc. However, this study did not compare between the flocculated system and non-flocculated system.

Wallace et al. (1980 cited in Roldan-villasana et al., 1999: 1229) studied six hydrocyclones with a 10mm diameter in parallel to treat 2% by weight kaolinite with an average size 0.77μm. The results showed that the total efficiency is higher with the polyacrylamide flocculant solution.

Borts et al. (1982 cited in Roldan-villasana et al., 1999: 1229) improved the 150mm hydrocyclone efficiency by adding polyacrylamide as the flocculant to treat the slurry. The results showed that with the polyacrylamide the solid removal efficiency was 94%. Without the polyacrylamide, the efficiency was 53%. But the slurry mixture detail was not explained.

Williams and Roldan-Villasana (1991 cited in Roldan-villasana et al., 1999) developed the efficiency of 10mm hydrocyclone and 2.6mm vortex finder diameter. 6 hydrocyclones in parallel treated kaolin which passed the flocculation process by using polyacrylamide as the flocculant.

The above researches have shown that chemical agents as the flocculant are used in hydrocyclone. This research attempts to use them in the coagulant process.

Woodfield and Bickert (2004) studied the separation of flocs in hydrocyclones-significance of floc breakage and floc hydrodynamics. The experimental work used 22

mm hydrocyclone. Particles were suspended in water by alumina trihydrate flocculated using polymer flocculant before being fed into the hydrocyclone with 100kPa pressure.

The results found that limited floc breakage occurs within hydrocyclones for flocs formed using appropriate polymeric flocculants. Further, the overflow floc size distribution is quite similar to the underflow floc size distribution. The reason for the differing separation of the underflow and overflow, even though the floc size distribution is similar, is the difference in floc density caused by differences in composition of primary particles within the flocs.

The reason for the improvement in overall separation is the inclusion of fine particles in underflow flocs containing coarse particles. The experimental results suggest that floc hydrodynamics and density are more important than breakage in determining hydrocyclone separation performance.

This research has shown that it is possible to use flocculant to agglomerate the fine particles before being separated by the hydrocyclone. Bidault et al.(1997) and Woodfield and Bickert (2004) showed that the floc remained in the hydrocyclone if the floc was build efficiently enough for the shear force in the hydrocyclone.

Rubio J. and Rosa J. (2004) used flocculation and flotation process to produce the aerated polymeric floc and separated by the separator.

The flocculation-flotation system is composed of a turbulent "flocculator" to generate aerated polymeric flocs coupled with solid/solid, solid/liquid/liquid$_2$ or liquid/liquid$_2$ separation devices (columns, tanks, centrifuges). The basic concept was that of a reactor of flocculator and a floc flotation separation (Figure II-10)
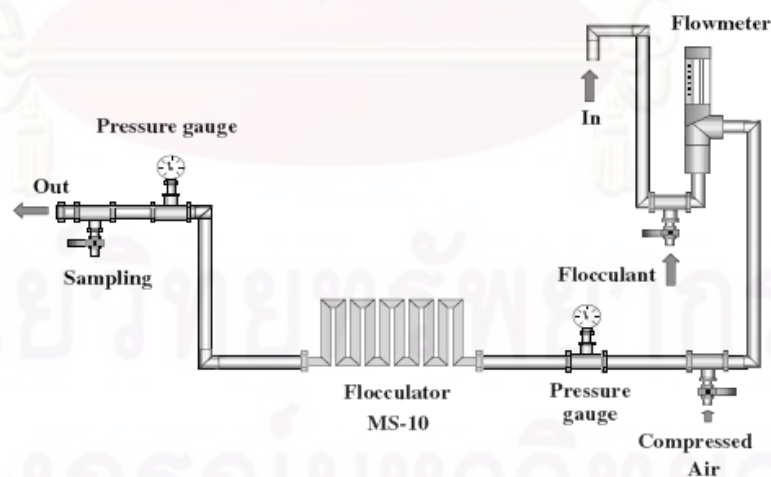
Figure II-10 The FF-flocculation-flotation system.

The lay out of the aerated floc generation system, MS10 is for the flocculator with 10 zigzags units. The outlet connects with the floc flotation separation unit
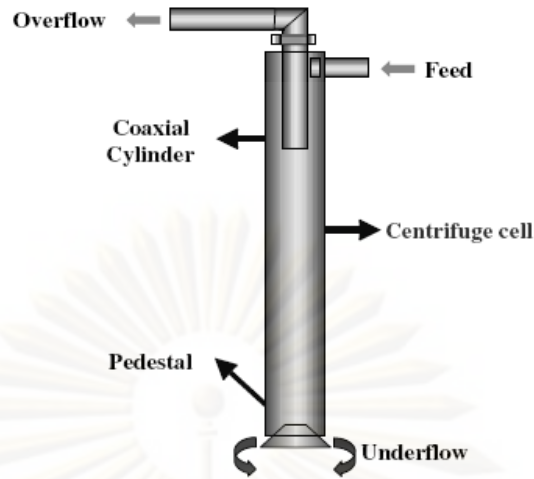
Figure II-11 The aerated floc flotation separator

After flocculation-flotation, FF% values were calculated from the dry weights of dispersions, before and after the separation: %FF = $(100)(D_o-D_f/D_o)$ where D_o is the degree of dispersion ("dispersibility") calculated from the feed dispersed solids content (by weight) before FF (D_o=initial dispersion degree) and D_f is the dispersion degree after FF, using the cationic polymer. Particles were ground to 100% less than 37μm. The idea of this research is similar to the hybrid process which produces aerated floc.
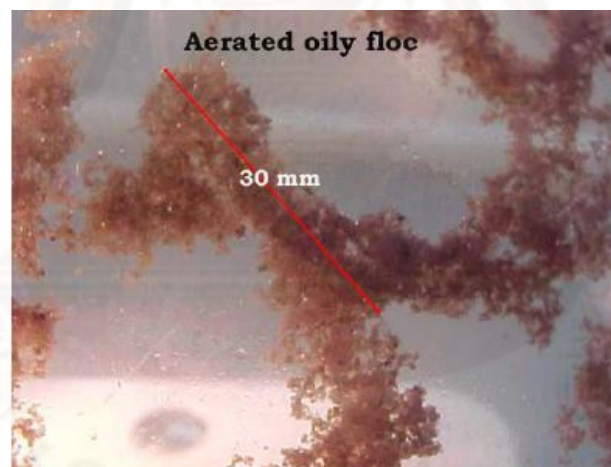
Figure II-12 The aerated oil floc formed with cationic polyacrelamide in the FF process

It was believed that the small bubble formation and their rapid occlusion (entrapment) within flocs was nucleation of bubbles at floc/water interfaces and bubbles entrainment. Qualitative measurements of the bubble size generated in the FF system, using the technique developed by Rodrigues and Rubio (2003), yielded values of the order of 100μm bubble diameter. These values are considered very fine (microbubbles) and of the order of those generated in DAF units, were formed at head losses (measured by the pressure differences before and after the flocculator) of the order of 3 atmospheres and at 4L/min for the feed rate and 7L/min for the air flow rate.

The uprising rates of the aerated flocs (more than 130m/hr) were faster than the rising bubbles sizes alone (30-40m/hr), it was believed that air was entrapped (occluded) inside the flocs, highly decreasing the aggregate density as a function of the incorporated air volume.

Because some air must be dissolved in water following the flow pressure inside the flocculator, these microbubbles behaved as in DAF. Thus, a very important feature concerned with the mechanisms of bubble/particle (aggregates) interactions other than the common adhesion through hydrophobic forces (Rubio et al., 2002). Apart from particles-bubbles collisions and adhesion, part of the dissolved air in water, which did not convert into bubbles, remained in solution and "nucleate" at the particle surface. This mechanism is independent of the surface hydrophobicity and allows flotation of hydrophilic particles. In addition, entrainment by the rising bubbles might be also operating.

Even this research is having the same idea about aerated-floc in the hybrid process but still the units are separated (flocculation and flotation). Moreover, there was no study to create aerated floc to treat natural water yet.

2.7 Hybrid process concept

The hybrid process is a new water treatment process. It is aimed to combine three processes; coagulation, flocculation and flotation processes present in one reactor which is the hydrocyclone as shown in Figure II-13
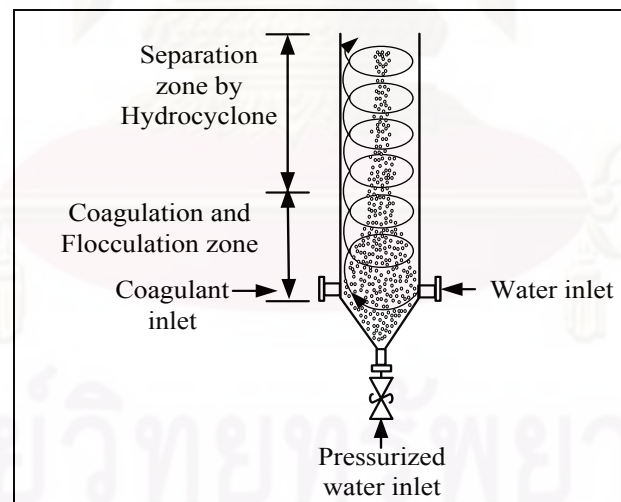
Figure II-13 Conception of Hybrid process

In the bottom part of hydrocyclone, there are three injection apertures which are raw water inlet, the coagulant solution inlet and the pressurized water inlet. The two former inlets are installed tangentially to the cyclone wall. The velocity gradient is controlled by the inlet feed flow rate. In this zone, coagulation and flocculation processes are expected. The colloid particle will be destabilized and agglomerated. Spontaneously, the air pressurized water from the dissolved air flotation technique passes through the

reactor with atmospheric pressure, the saturated air precipitated into the water as micro bubbles. These bubbles attach inside the floc structure, from a coagulation-flocculation process, and become the *aerated floc*.

In the upper part of the reactor, the centrifugal force in hydrocyclone causes the separation between the floc and water. The aerated floc has a density lower than water because it contains the micro bubbles inside its structure and can be separated to the hydrocyclone reactor axis.

2.8 The hybrid process studies

The hybrid process has been studied since 2004. With the same objective, it has been researched by many researchers as following reviews.

Chaiyaporn Puprasert C. (2004) studied of the feasibility of a hybrid process for water treatment. A 5cm hydrocyclone was used to be the reactor with a bentonite suspension and EM470 coagulant solution.

The experiment was done in 5cm diameter hydrocyclone. The raw water and coagulant solution were fed tangentially into hydrocyclone. Simultaneously, the pressurized water was fed from the bottom cone apex in vertical direction as shown in Figure II-14. When the pressurized water passes to the hydrocyclone with atmospheric pressure, the saturated air precipitates to be micro bubble at the feed inlet point (bottom part). It was found that this process could produce the floc which contained the micro bubbles inside.
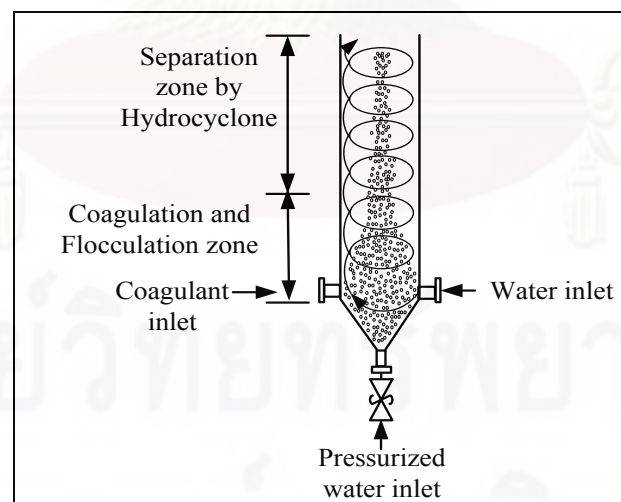
Figure II-14 The expected phenomenon of Chaiyaporn Puprasert (2004)

This research was done in three parts.

Firstly, the feasibility of the hybrid process with continuous operation. The results did not reach the expected phenomenon because the water in the hydrocyclone was still

turbid of bentonite and there was no separation. However, with batch operation; which fed the three flow rates and then stopped the operation, water was still spinning with a lower velocity and the floc occurred in the hydrocyclone and those flocs tended to gather in the hydrocyclone axis and floated up to the top of reactor. The floc was looked at through a microscope and it was found the special floc which contained air bubbles inside.

The second part, floc observation, from the first part the floc did not float up to the top of cyclone. There were some settled flocs. This experiment varied the air pressurized water flow rate at 14, 21, 28 and 36L/hr. The results showed that increasing the air pressurized water increased the float floc. With 36L/hr flow rate, all the floc floated up to the top of hydrocyclone. This flow rate is 9% of the raw water inlet flow rate. Compare to the dissolved air flotation technique this flow rate was lower as the DAF technique requires 30-50% air pressurized water.

The last part was to vary the velocity gradient for the coagulation and flocculation processes by controlling the raw water inlet flow rate. The velocity gradient in the lower part was controlled for the coagulation process. In the middle of the hydrocyclone, the velocity gradient was controlled for the flocculation process. The top part was expected to separate the special floc by centrifugal force and gather in the hydrocyclone axis.

The results did not reach the expected phenomenon. When the flow rate in the lower part was controlled for the coagulation process, the vortex flow for flocculation process in the upper part was to strong. Contrary, when the flow rate in the upper part was controlled for the flocculation process, the lower part had inadequate velocity gradient to produce the micro floc.

Conclusions from this research

1. The special floc was produced by a hybrid process by containing the air bubbles inside its structure.

2. The expected phenomenon (Figure II-14) was successful only in batch operation.

Vorasiri Siangsanun (2006) studied the Hybrid process with hydrocyclone coagulation flocculation and flotation in water treatment process. It was aimed to operate with continuous operation by using 1mg/L bentonite as the suspended solid in the tap water.

To achieve continuous operation the parameters which affected to hybrid process were studied.

- The hydrocyclone reactor geometry

- Polymeric coagulant type

- Velocity gradient at the inlet point

- Air pressurized water to inlet flow ratio

- Inlet flow velocity

There were two hydrocyclones reactor geometries. The first hydrocyclone was a cylindrical reactor with two diameter sizes; 50mm for the lower part and 100mm for the upper part. The lower part was designed to have higher velocity gradient from tangential inlet flow with small cyclone radius (5cm). The upper part was designed to decrease the velocity gradient by increasing the cyclone radius (10cm) as shown in Figure II-15. The second hydrocyclone was a conical reactor (see Figure II-16) where its diameter increases along the reactor height. It was designed to slightly decrease the velocity gradient inside the reactor and to compare the result to the cylindrical one.
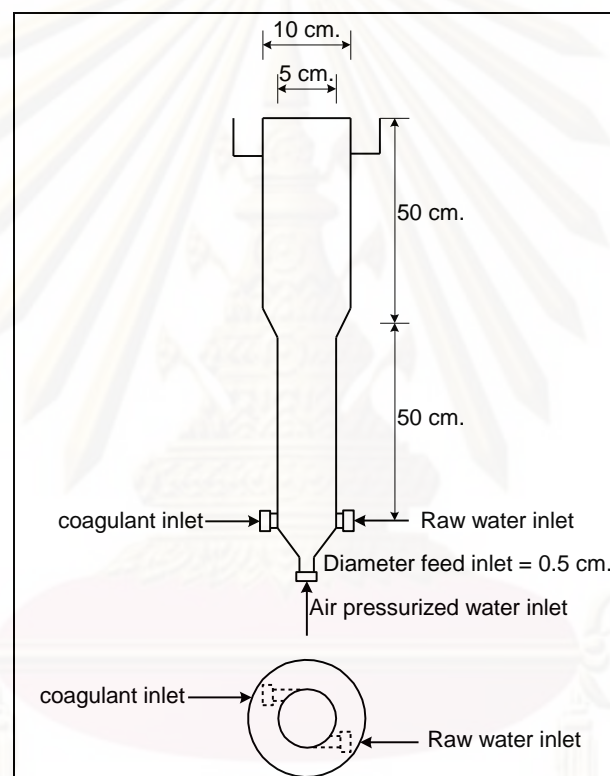
Figure II-15 Cylindrical hybrid reactor size and details

The results found in the cylindrical hydrocyclone that separation could occur only with the batch operation that was after stop all the feed inlets, the floated flocs were observed inside the reactor and the treated water was less turbid.

Coagulation and flocculation processes by hybrid process could produce the special floc which contained the air-bubbles inside (*aerated floc*).

The coagulant polymer did not present the different of percent turbidity significantly in each type. The coagulation process mechanism was the polymer bridging for that ion of the coagulant did not affect differently in the process.

The air flow rate to inlet flows ratio was the important parameter to produce the special floc. Increasing the inlet raw water flow rate caused the air fraction to decrease. That in turn affected the special floc production.

The diameter change position of the reactor disturbed the flow spin up. This flow, so called vortex flow, was important to separate the floc from the clear water after the coagulation and flocculation processes. There was not the separation process between the floc and water because the vortex flow was too weak and disturbed when it passed the diameter change point.
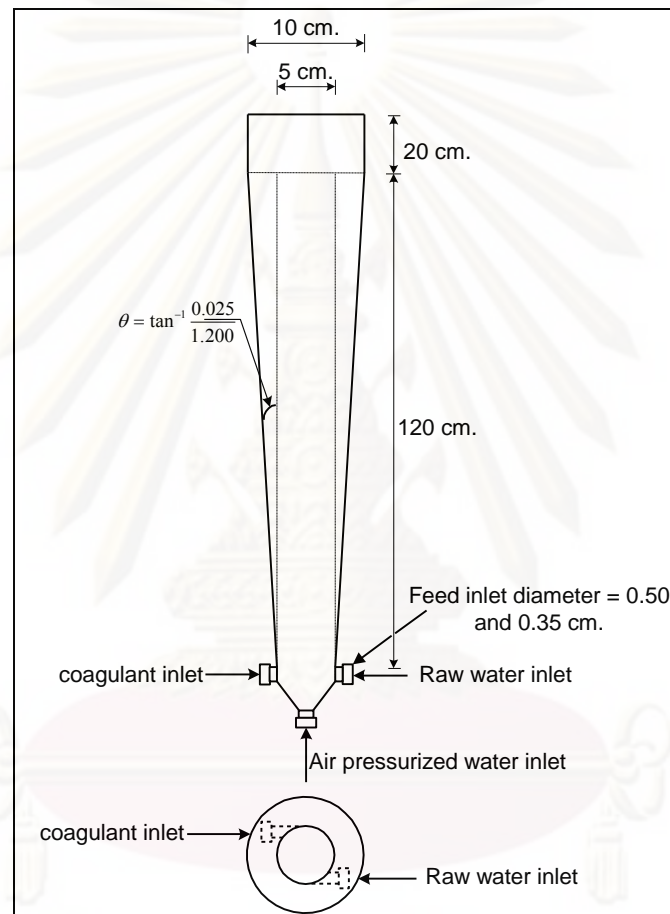
Figure II-16 Conical hybrid reactor size and details

In the conical hydrocyclone, the experimental results found that the type of coagulant polymers were not different significantly in the floc producing term. The separation between floc and clear water occurred only in batch operations.

Increasing the inlet flow rate caused the amount of floated floc to decrease because the total air volume was inadequate to produce the special floc. With a low flow rate (150L/hr) all the floc floated up to the top but there was not the vortex flow which was important to separate the floc from the water. With a high inlet flow rate (450L/hr), the produced floc settled down to the bottom of reactor after stopping the operation. It was there is expected there was not enough air volume to produce the special floc.

With the conical hybrid reactor, increasing the inlet flow rate caused the air-bubbles to coalescence to each other. The air bubbles became larger in size and were not able to insert themselves into the floc structure.

The conclusion of comparing between the cylindrical hybrid reactor and the conical hybrid reactor is the two hybrid reactors could produce the special floc which contained the air-bubble inside but the cylindrical hybrid reactor produced the floc and it got larger at the diameter change point. This point changed the flow direction and disturbed the vortex flow in the reactor.

This study needs to be explored to approach the separation with continuous operation. For that Pradipat Bamrungsri (2008a) studied the phenomenon inside these hybrid reactors.

Pradipat Bamrungsri (2008a) studied two main parts. First, the development of a simple experimental method used for the determination of the liquid field velocity in a conical and cylindrical hydrocyclone by using red oil droplets. Secondly, she studied the optimum conditions for the hybrid process with different operating conditions and reactor geometry.

In the first part, velocity measurement using simple method, the oil droplet was injected by a small syringe into the hydrocyclone at different zones. The trajectory line of the injected droplets and velocity of water in terms of tangential and axial velocity of the liquid (clean water) and the average velocity gradient in the hydrocyclone could be investigated.
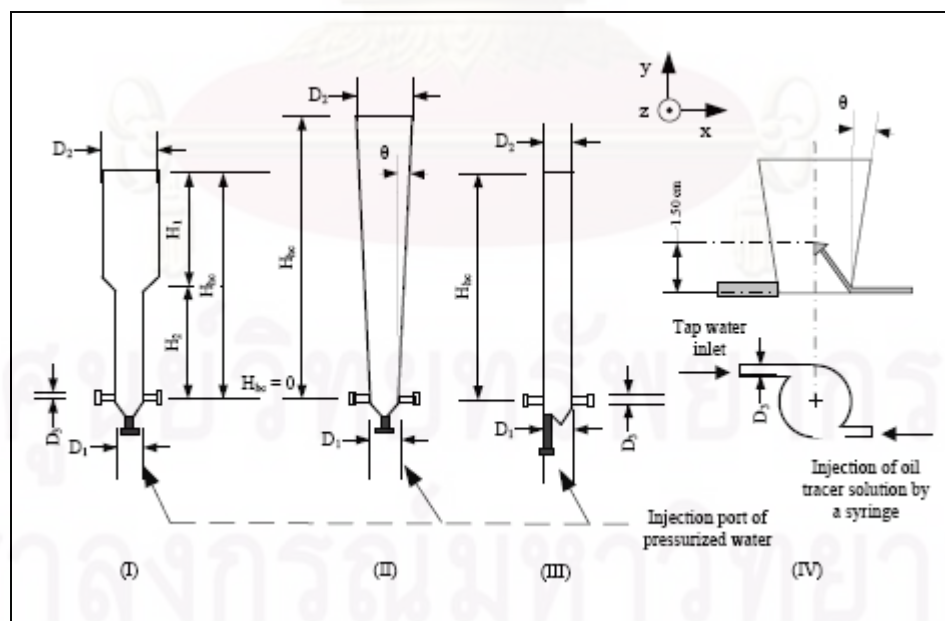
**Figure II-17   The diagram of each hydrocyclone from this research
and the oil droplet method measurement**

In each hydrocyclone, the oil droplets were injected at the centre of the hydrocyclone, they moved down to the bottom part. On the contrary, the droplets were injected close to the wall of the hydrocyclone they raised up rapidly to the upper part of the hydrocyclone. Beyond that, the average axial velocity of water at the centre of the conical hydrocyclone which had the downward direction to the bottom of the hydrocyclone was greater than the average axial velocity of water at the centre of the cylindrical hydrocyclone.

The tangential velocity of water in both hydrocyclones presented the average velocity gradient of the water at the centre of the hydrocyclone was significantly lower than the average velocity gradient of water close to the wall of hydrocyclone. It was concluded that the external vortex close to the wall of the hydrocyclone was stronger than the internal vortex at the centre of the hydrocyclone.

The trajectory lines of droplets at the internal zone ($0 \leq r \leq 1$cm) of the hydrocyclone were downward to the bottom of hydrocyclone. In contrast, they moved upward to the upper part of hydrocyclone when injected close to the wall of hydrocyclone ($1 < r < 2.5$cm).

In all hydrocyclones, the water flow direction was downward at the internal zone ($0 \leq r \leq 2$cm) and it changed to an upward direction at the wall of hydrocyclone which was concerned with the axial velocity of liquid. In both hydrocyclones, the water flow of the small water inlet aperture moved downward to the bottom faster than the water flow of the larger water inlet aperture. However, the water flow of the conical hydrocyclone moved downward to the bottom of the hydrocyclone faster than water flow in cylindrical.

The radius of the downward flow of the cylindrical hydrocyclone is smaller than the radius of downward flow in conical hydrocyclone when they are operated at the water inlet diameter equal to 0.50cm.

In the second part, the studies of the hydrodynamics in the hydrocyclones were done with the different conditions and different geometries. It was found that there were three conditions which were interesting from the results of oil droplet method in the hydrocyclone III (HC3).

Condition	Inlet diameter,D (cm)	Inlet flow rate,Q (l/hr)	Water inlet velocity, v (m/s)
1	0.3	200	7.86
2.	0.5	200	2.83
3.	0.5	400	5.66

The optimum conditions from this research were concluded as follow

Hydrocyclone geometry	HC3
The raw water flow rate	200L/hr
The raw water inlet diameter	0.50cm
Coagulant concentration	3.0 – 4.0mg/L
Total pressure	3.5bars
Air fraction	0.0082 – 0.0100

The floc sizes in the wall zone of the optimum operating condition, 70% separation efficiency, were still large, 0.1 to 0.5cm. The higher separation efficiency was difficult in this hydrocyclone geometry (HC3). For that, the enlargement of the hydrocyclone diameter was proposed to improve the hybrid process with the continuous flow in order to be a guide line for designing the hybrid process and applying it for industrial scale. The modified hydrocyclone reactor geometry and the parameters will be explained in the next chapter.

In terms of the optimum conditions, results from the oil droplet method, even the oil droplet method is the new simple way to understand the hydrodynamics inside the hydrocyclone. On the other hand, the rapid development of computer and computational fluid dynamic (CFD) techniques, the use of numerical simulations to predict the performance of the cyclone has received much attention.

For that, it is interesting to use numerical simulation method by FLUENT as one of the method to simulate the tangential and axial velocity profiles on the same conditions from the result of oil droplet method. With the oil droplet method, there are three conditions of the experimental results which are interesting.

2.9 Computational Fluid Dynamics with FLUENT

FLUENT is a computational fluid dynamics (CFD) software package to simulate fluid flow problems. It uses to solve the governing Equations for a fluid. It provides the capability to use different physical models such as incompressible or compressible, inviscid or viscous, laminar or turbulent, etc. Geometry and grid generation is done using GAMBIT which is the preprocessor bundled with FLUENT.

It is used for modeling fluid flow and heat transfer in complex geometries. FLUENT provides complete mesh flexibility including the ability to solve the flow problems using unstructured meshes that can be generated about complex geometries with relative ease. Supported mesh types include 2D triangular/quadrilateral, 3D tetrahedral/ hexahedral/ pyramid/wedge/ polyhedral, and mixed (hybrid) meshes. FLUENT also refines or coarsens the grid based on the flow solution.

FLUENT is theoretically based on Navier's stoke Equation (Byron *et al.*, 1960)

The general Equations of motion for a Newtonian fluid with varying density and viscosity

$$\rho \frac{Dv_x}{Dt} = -\frac{\partial p}{\partial x} + \frac{\partial}{\partial x}\left[2\mu\frac{\partial v_x}{\partial x} - \frac{2}{3}\mu(\nabla \cdot v)\right]$$

$$+ \frac{\partial}{\partial y}\left[\mu\left(\frac{\partial v_x}{\partial y} + \frac{\partial v_y}{\partial x}\right)\right] + \frac{\partial}{\partial z}\left[\mu\left(\frac{\partial v_z}{\partial x} + \frac{\partial v_x}{\partial z}\right)\right] + \rho g_x \qquad \text{Equation II-11}$$

$$\rho \frac{Dv_y}{Dt} = -\frac{\partial p}{\partial x} + \frac{\partial}{\partial x}\left[\mu\left(\frac{\partial v_y}{\partial x} + \frac{\partial v_x}{\partial y}\right)\right] + \frac{\partial}{\partial y}\left[2\mu\frac{\partial v_y}{\partial x} - \frac{2}{3}\mu(\nabla \cdot v)\right]$$

$$+ \frac{\partial}{\partial z}\left[\mu\left(\frac{\partial v_z}{\partial y} + \frac{\partial v_y}{\partial z}\right)\right] + \rho g_y \qquad \text{Equation II-12}$$

$$\rho \frac{Dv_z}{Dt} = -\frac{\partial p}{\partial z} + \frac{\partial}{\partial x}\left[\mu\left(\frac{\partial v_z}{\partial x} + \frac{\partial v_x}{\partial z}\right)\right] + \frac{\partial}{\partial y}\left[\mu\left(\frac{\partial v_z}{\partial x} + \frac{\partial v_y}{\partial z}\right)\right]$$

$$+ \frac{\partial}{\partial z}\left[2\mu\frac{\partial v_z}{\partial z} - \frac{2}{3}\mu(\nabla \cdot v)\right] + \rho g_z \qquad \text{Equation II-13}$$

These equations, along with the Equation of continuity, the Equation of state *p=p(ρ)*, the density dependence of viscosity *μ=μ(ρ)*, and the boundary and initial conditions, determine completely the pressure, density, and velocity components in a flowing isothermal fluid.

For constant ρ and constant μ, equation II-11 to II-13 may be simplified by means of the Equation of continuity $[(\nabla \cdot v) = 0)]$ to give

$$\rho \frac{Dv}{Dt} = -\nabla p + \mu\nabla^2 v + \rho g \qquad \text{Equation II-14}$$

The Cartesian components of this equation are given in Table II-3. Equation II-14 is the celebrated *Navier-Stokes Equation* (Byron *et al.*, 1960)

Table II-3   The equation of motion in rectangular coordinates (x,y,z)

In terms of η	
x-component	$$\rho\left(\frac{\partial v_x}{\partial t} + v_x\frac{\partial v_x}{\partial x} + v_y\frac{\partial v_x}{\partial y} + v_z\frac{\partial v_x}{\partial z}\right) = -\frac{\partial p}{\partial x}$$ $$-\left(\frac{\partial \tau_{xx}}{\partial x} + \frac{\partial \tau_{yx}}{\partial y} + \frac{\partial \tau_{zx}}{\partial z}\right) + \rho g_x \qquad (A)$$
y-component	$$\rho\left(\frac{\partial v_y}{\partial t} + v_x\frac{\partial v_y}{\partial x} + v_y\frac{\partial v_y}{\partial y} + v_z\frac{\partial v_y}{\partial z}\right) = -\frac{\partial p}{\partial y}$$ $$-\left(\frac{\partial \tau_{xy}}{\partial x} + \frac{\partial \tau_{yy}}{\partial y} + \frac{\partial \tau_{zy}}{\partial z}\right) + \rho g_y \qquad (B)$$
z-component	$$\rho\left(\frac{\partial v_z}{\partial t} + v_x\frac{\partial v_z}{\partial x} + v_y\frac{\partial v_z}{\partial y} + v_z\frac{\partial v_z}{\partial z}\right) = -\frac{\partial p}{\partial z}$$ $$-\left(\frac{\partial \tau_{xz}}{\partial x} + \frac{\partial \tau_{yz}}{\partial y} + \frac{\partial \tau_{zz}}{\partial z}\right) + \rho g_z \qquad (C)$$

In terms of velocity gradients for a Newtonian fluid with constant ρ and μ

x-component	$$\rho\left(\frac{\partial v_x}{\partial t} + v_x\frac{\partial v_x}{\partial x} + v_y\frac{\partial v_x}{\partial y} + v_z\frac{\partial v_x}{\partial z}\right) = -\frac{\partial p}{\partial x}$$ $$+\mu\left(\frac{\partial^2 v_x}{\partial x^2} + \frac{\partial^2 v_x}{\partial y^2} + \frac{\partial^2 v_x}{\partial z^2}\right) + \rho g_x \qquad (D)$$
y-component	$$\rho\left(\frac{\partial v_y}{\partial t} + v_x\frac{\partial v_y}{\partial x} + v_y\frac{\partial v_y}{\partial y} + v_z\frac{\partial v_y}{\partial z}\right) = -\frac{\partial p}{\partial y}$$ $$+\mu\left(\frac{\partial^2 v_y}{\partial x^2} + \frac{\partial^2 v_y}{\partial y^2} + \frac{\partial^2 v_y}{\partial z^2}\right) + \rho g_y \qquad (E)$$
z-component	$$\rho\left(\frac{\partial v_z}{\partial t} + v_x\frac{\partial v_z}{\partial x} + v_y\frac{\partial v_z}{\partial y} + v_z\frac{\partial v_z}{\partial z}\right) = -\frac{\partial p}{\partial z}$$ $$+\mu\left(\frac{\partial^2 v_z}{\partial x^2} + \frac{\partial^2 v_z}{\partial y^2} + \frac{\partial^2 v_z}{\partial z^2}\right) + \rho g_z \qquad (F)$$

$\rho \dfrac{Dv}{Dt}$ is the mass per unit volume times acceleration

ρv is the mass velocity vector of the components $\rho v_x, \rho v_y, \rho v_z$

g is the gravitational acceleration for g_x, g_y, g_z

∇p is the gradient of p is composed with $\dfrac{\partial p}{\partial x}, \dfrac{\partial p}{\partial y}, \dfrac{\partial p}{\partial z}$

FLUENT provides the following choices of turbulence models:

- Spalart-Allmaras model

- k-ε models

  - Standard k-ε model

  - Renormalization-group (RNG) k-ε model

  - Realizable k-ε model

- k-ω models

  - Standard k- ω model

  - Shear-stress transport (SST) k- ω model

- υ^2-f model (addon)

- Reynolds stress model (RSM)

  - Linear pressure-strain RSM model

  - Quadratic pressure-strain RSM model

  - Low-Re stress-omega RSM model

The solution process requires a geometry modeler and grid generator. GAMBIT is used for geometry modeling and grid generation. Then the grid will be imported to FLUENT.

It is recommended in the modeling basic fluid flow that the modeling turbulent flow with a significant amount of swirl (e.g., cyclone flows, swirling jets) should consider using one of FLUENT"s advanced turbulence models: the RNG k-ε model, realizable k-ε model, or Reynolds stress model (RSM). The appropriate choice depends on the strength of the swirl, which can be gauged by the swirl number.

Table II-4   The turbulence Model-features and usage (Fluent Inc., 1999)

Models	Features
Spalart-Allmaras	• Economical for large meshes • Suitable for mildly complex 2D flows • Performs poorly for 3D flows, free shear flows, and flows with strong separation
Standard -	• It is robust • Suitable for initial iterations, initial screening of alternative designs, and parametric studies • Performs poorly for complex flows involving severe separation
RNG -	Suitable for complex shear flows involving rapid strain, moderate swirl, vortices, and locally transitional flows.
Realizable -	• Similar benefits and applications as RNG • Cannot be used with multiple rotating reference frames (MRF) • Possibly more accurate and easier to converge than RNG
Standard -	• Superior performance for wall-bounded, free-shear and low Reynolds number flow. • Suitable for complex boundary layer flows under adverse pressure gradient and separation. • Separation is typically predicted to be excessive and early.
SST -	• Similar benefits as standard - model • Less suitable for free shear flows
RSM	• Physically the most balanced model • Avoids isotropic eddy-viscosity assumption • Suitable for complex 3D flows • Requires more CPU time and memory • Tougher to converge due to close coupling of Equations

In this study, the model physic will be chosen to simulate the velocity profile are; standard k-ε Model and Reynolds Stress Model. These two models are explained as follow.

2.9.1 Standard k-ε Model

The simplest "complete models" of turbulence are two-equation models in which the solution of two separate transport equations allows the turbulent velocity and length scales to be independently determined. The standard k-ε model in FLUENT falls within this class of turbulence model and has become the workhorse of practical engineering flow calculations in the time since it was proposed by Launder and Spalding. Robustness, economy, and reasonable accuracy for a wide range of turbulent flows explain its popularity in industrial flow and heat transfer simulations. It is a semi-empirical model, and the derivation of the model equations relies on phenomenological considerations and empiricism.

As the strengths and weaknesses of the standard k-ε model have become known, improvements have been made to the model to improve its performance. Two of these variants are available in FLUENT: the RNG k-ε model and the realizable k- ε model. The standard k- ε model is a semi-empirical model based on model transport equations for the turbulence kinetic energy (k) and its dissipation rate (ε). The model transport equation for k is derived from the exact equation, while the model transport equation for ε was obtained using physical reasoning and bears little resemblance to its mathematically exact counterpart.

In the derivation of the k- ε model, the assumption is that the flow is fully turbulent, and the effects of molecular viscosity are negligible. The standard k- ε model is therefore valid only for fully turbulent flows.

2.9.2 Transport equations for the Standard k- ε Model

The turbulence kinetic energy, k, and its rate of dissipation, ε, are obtained from the following transport equations:

Kinetic energy: k

$$\frac{\partial}{\partial t}(\rho k) + \frac{\partial}{\partial x_i}(\rho k u_i) = \frac{\partial}{\partial x_j}\left[\left(\mu + \frac{\mu_t}{\sigma_k}\right)\frac{\partial k}{\partial x_j}\right] + G_k + G_b - \rho\varepsilon - Y_M + S_k \qquad \text{Equation II-15}$$

And dissipation: ε

$$\frac{\partial}{\partial t}(\rho\varepsilon) + \frac{\partial}{\partial x_i}(\rho\varepsilon u_i) = \frac{\partial}{\partial x_i}\left[\left(\mu + \frac{\mu_t}{\sigma_\varepsilon}\right)\frac{\partial\varepsilon}{\partial x_j}\right] + C_{1\varepsilon}\frac{\varepsilon}{k}(G_k + C_{3\varepsilon}G_b) - C_{2\varepsilon}\rho\frac{\varepsilon^2}{k} + S_\varepsilon$$

Equation II-16

In these equations, G_k represents the generation of turbulence kinetic energy due to the mean velocity gradients. G_b is the generation of turbulence kinetic energy due to buoyancy. Y_M represents the contribution of the fluctuating dilatation incompressible turbulence to the overall dissipation rate. $C_{1\varepsilon}$, $C_{2\varepsilon}$, and $C_{3\varepsilon}$ are constants. ζ_k and ζ_ε are the turbulent Prandtl numbers for k and ε, respectively. S_k and S are user-defined source terms.

The model constants C_2, ζ_k, and ζ_ε have been established to ensure that the model performs well for certain canonical flows. The model constants are

$C_{1\varepsilon} = 1.44$; $C_{2\varepsilon} = 1.9$; $\zeta_k = 1.0$; $\zeta_\varepsilon = 1.2$

2.9.3   Reynolds Stress Model (RSM) Theory

The Reynolds stress model (RSM) is the most elaborate turbulence model that FLUENT provides. Abandoning the isotropic eddy-viscosity hypothesis, the RSM closes the Reynolds-averaged Navier-Stokes Equations by solving transport Equations for the Reynolds stresses, together with an equation for the dissipation rate. This means that five additional transport Equations are required in 2D flows and seven additional transport equations must be solved in 3D.

Since the RSM accounts for the effects of streamline curvature, swirl, rotation, and rapid changes in strain rate in a more rigorous manner than one-equation and two-equation models, it has greater potential to give accurate predictions for complex flows. However, the fidelity of RSM predictions is still limited by the closure assumptions employed to model various terms in the exact transport equations for the Reynolds stresses. The modeling of the pressure-strain and dissipation-rate terms is particularly challenging, and often considered to be responsible for compromising the accuracy of RSM predictions.

The RSM might not always yield results that are clearly superior to the simpler models in all classes of flows to warrant the additional computational expense. However, use of the RSM is a must when the flow features of interest are the result of anisotropy in the Reynolds stresses. Among the examples are cyclone flows, highly swirling flows in combustors, rotating flow passages, and the stress-induced secondary flows in ducts.

The exact form of the Reynolds stress transport equations may be derived by taking moments of the exact momentum equation. This is a process wherein the exact momentum equations are multiplied by the fluctuating property, the product then being Reynolds-averaged. Unfortunately, several of the terms in the exact equation are unknown and modeling assumptions are required in order to close the equations.

2.9.4   Reynolds Stress Transport Equations

The exact transport equations for the transport of the Reynolds stresses, $\rho \overline{u_i' u_j'}$, may be written as follows:

$$\frac{\partial}{\partial t}\left(\rho \overline{u_i' u_j'}\right) + \frac{\partial}{\partial x_k}\left(\rho u_k \overline{u_i' u_j'}\right) = -\frac{\partial}{\partial x_k}\left[\rho \overline{u_i' u_j' u_k'} + \overline{p\left(\delta_{kj} u_i' + \delta_{ik} u_j'\right)}\right] + \frac{\partial}{\partial x_k}\left[\mu \frac{\partial}{\partial x_k}\left(\overline{u_i' u_j'}\right)\right]$$

$$-\frac{\partial}{\partial x_k}\left[\mu \frac{\partial}{\partial x_k}\left(\overline{u_i' u_j'}\right)\right] - \rho\left(\overline{u_i' u_k'}\frac{\partial u_j}{\partial x_k} + \overline{u_j' u_k'}\frac{\partial u_i}{\partial x_k}\right) - \rho\beta\left(g_i \overline{u_j' \theta} + g_j \overline{u_i' \theta}\right)$$

$$+ \overline{p\left(\frac{\partial u_i'}{\partial x_j} + \frac{\partial u_j'}{\partial x_i}\right)} - 2\mu\overline{\frac{\partial u_i'}{\partial x_k}\frac{\partial u_j'}{\partial x_k}} - 2\rho\Omega_k\left(\overline{u_j' u_m'}\varepsilon_{ikm} + \overline{u_i' u_m'}\varepsilon_{jkm}\right) + S_{user} \qquad \text{Equation II-17}$$

Local Time Derivate $+$ $C_{ij} = D_{T,ij} + D_{L,ij} + P_{ij} + G_{ij} + \phi_{ij} - \varepsilon_{ij} + F_{ij} +$ User-Defined Source Term

Where, C_{ij} = convection-term

          $D_{T,ij}$ = turbulent diffusion

          $D_{L,ij}$ = molecular diffusion

          P_{ij} = term for Stress Production

          G_{ij} = Buoyancy Production

          ϕ_{ij} = pressure strain

          ε_{ij} = dissipation

          F_{ij} = production by system rotation.

          S_{user} = User-Defined source term

The simulation will be included turbulence 3D model selection for simulating the tangential and axial velocity profiles on different inlet diameter and inlet velocity in hydrocyclone with one phase of water liquid and compare to the experimental results. Choosing the model physic, it is considered that this operation will be the turbulent flow and 3D.

2.9.5 GAMBIT grid division

Gambit is the main preprocessor of Fluent, is used to create geometry, meshing and specifying boundary types of hydrocyclone. With the available dimensions of the hydrocyclone three-dimensional geometry is created. For meshing, hexahedral and tetrahedral meshes were used for all the part of hydrocyclone.   Boundary types are considered as inlet velocity, outlet pressure and wall. Using Fluent the created geometry by Gambit can be read and simulation is done. For analysis of the results the contour plots

and vector plots are analyzed. Residual plot is observed continuously during simulation. Accuracy and convergence are very important during simulation. Current study involves two things: one is to create three-dimensional geometry in Gambit along with the meshing, and second is to know the general procedure to simulate this hydrocyclone. Analysis of the result is also important to know the flow field and pressure distribution. The convergence and accuracy is important during solution. This can be seen by the residual plots. A general convergence criterion is 10^{-7} and more than that is desirable. If not then it has to be change the solution parameters and sometimes solution method also. Currently, modified k–ε method and water as the fluid medium is used for the hydrodynamic study of the hydrocyclone I. On the other hand, Hydrocyclone II, simulation was performed with RSM which is more appropriate to swirling flows. Here, only one phase is considered for the study, water. Results of residual plot will be observed until the x, y, z component reach a stable value.

Another experimental method which is interesting to measure the velocity inside the hydrocyclone is Doppler. As the oil droplet method is a new simple way to measure the velocity, it is needed to be verified with existing method. Consequently, Doppler is considered to be used in this study.

2.10 Doppler ultrasound velocimetry (Signal Processing, 1998)

2.10.1 Doppler ultrasound technique

Doppler ultrasound technique was originally applied in the medical field and dates back more then 30 years. The use of pulsed emissions has extended this technique to other fields and has open the way to new measuring techniques in fluid dynamics. The term "Doppler ultrasound velocimetry" implies that the velocity is measured by finding the Doppler frequency in the received signal, as it is the case in Laser Doppler velocimetry. In fact, in ultrasonic pulsed Doppler velocimetry, this is never the case. Velocities are derived from shifts in positions between pulses, and the Doppler Effect plays a minor role. Unfortunately, many publications fail to make the distinction, resulting in erroneous system description and fallacious interpretation of the influence from various physical effects.

Consider an ultrasonic transducer which emits waves of frequency f_e and remains fixed in a medium where the speed of sound is given by c. A receptor, or target in the medium, moves with a velocity v. By convention, v is considered negative when the target is moving toward the transducer. If the trajectory of the target forms an angle with respect to the propagation direction of the ultrasonic wave, the frequency of the waves perceived by the target will be:

$$f_g = f_e \pm \frac{f_e v \cos\theta}{c} \qquad \text{Equation II-18}$$
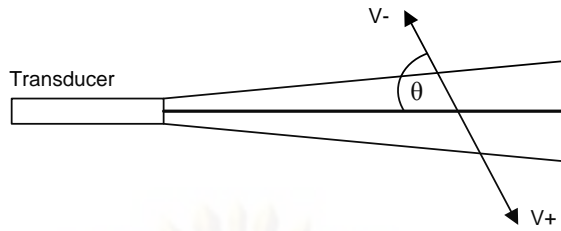
Surrounding medium, the waves will be partially reflected. In this way, the target acts as a moving source of ultrasonic signals. The frequency of the waves reflected by the target, as measured by a stationary transducer, is:

$$f_r = \frac{c}{c \mp v\cos\theta} f_g \qquad\qquad \text{Equation II-19}$$

By combining the two above equations, the frequency of the signal received by transducer is:

$$f_r = \left(\frac{c \pm v\cos\theta}{c \mp v\cos\theta} \right) f_e \qquad\qquad \text{Equation II-20}$$

This equation may be simplified by knowing that the velocity of the target is much smaller than the speed of sound (v<<c). By expanding the denominator of the above equation into a geometric series, and neglecting the terms of order two and greater, one may obtain the difference between the frequencies of the emitted and received signals. This frequency shift, called the Doppler frequency, is given by:

$$f_d = \pm \frac{2f_e v\cos\theta}{c} \qquad\qquad \text{Equation II-21}$$

T_s=observation time
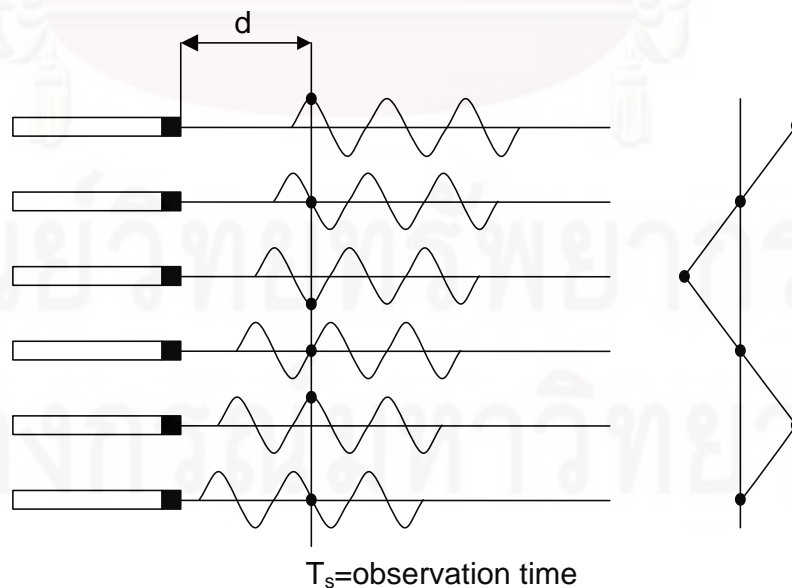
The principle for measuring the velocity of a target using a pulsed signal is illustrated above. If the target is moving toward the transducer, the time delay between the emitted and received signals T_v=2d/c will diminish. If, instead of following the time delay, one examines the amplitude of the received signal after a fixed time delay T_s after the emission of regularly timed pulses, ideally a sinusoidal signal will result. The sampling times are t_n=nT_{prf}+T_s, where n is an integer and T_{prf} is the time between emitted pulses. This is only valid if the observation time T_s is chosen in order to receive the proper echo.

2.10.2 Functioning principles of pulsed Doppler ultrasound

In pulsed Doppler ultrasound, instead of emitting continuous ultrasonic waves, an emitter sends periodically a short ultrasonic burst and a receiver collects continuously echoes issues from targets that may be present in the path of the ultrasonic beam. By sampling the incoming echoes at the same time relative to the emission of the bursts, the shift of positions of scatters are measured. Let assume a situation, as illustrated in the Figure below, where only one particle is present along the ultrasonic beam.
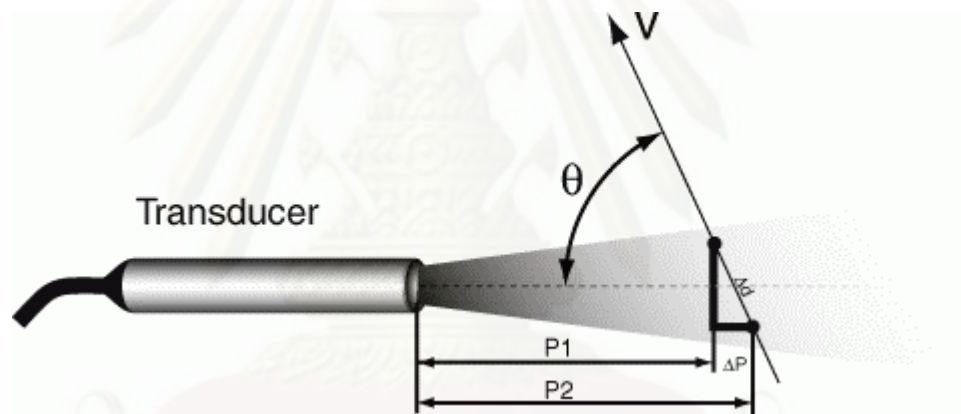
From the knowledge of the time delay T_d between an emitted burst and the echo issue from the particle, the depth p of this particle can computed by:

$$p = \frac{c \cdot T_d}{2}$$

Equation II-22

where *c* is the sound velocity of the ultrasonic wave in the liquid. If the particle is moving at an angle q regarding the axis of the ultrasonic beam, its velocity can be measured by computing the variation of its depth between two emissions separated in time by T_{prf}:

$$(P_2 - P_1) = v \cdot T_{prf} \cdot \cos\theta = \frac{c}{2} \cdot (T_2 - T_1)$$

Equation II-23

The time difference (T_2-T_1) is always very short, most of the time lower than a microsecond. It is advantageous to replace this time measurement by a measurement of the phase shift of the received echo.

$$\delta = 2\pi \cdot f_e (T_2 - T_1) \qquad \text{Equation II-24}$$

where f_e is the emitting frequency. With this information the velocity of the target is expressed by:

$$v = \frac{c \cdot \delta}{4\pi \cdot f_e \cos\theta \cdot T_{prf}} = \frac{c \cdot f_d}{2 \cdot f_e \cdot \cos\theta} \qquad \text{Equation II-25}$$

This last equation gives the same result as the Doppler equation. But one should always be aware that the phenomena involved are not the same. Assume that the particles are randomly distributed inside the ultrasonic beam. The echoes issue from each particle is then combined together in a random fashion, giving a random echo signal. Hopefully, a high degree of correlation exists between different emissions. This high correlation degree is put in advance in all digital processing techniques used in Signal Processing's Ultrasonic Doppler velocimeter to extract information, such as the velocity.

2.10.3 Advantages and limitations

The main advantage of pulsed Doppler ultrasound is its capability to offer spatial information associated to velocity values. Unfortunately, as the information is available only periodically, this technique suffers from the Nyquist theorem. This means that a maximum velocity exists for each pulse repetition frequency (Prf):

$$v_{\max} = \frac{c}{4 \cdot T_{prf} \cdot f_e \cdot \cos\theta} \qquad \text{Equation II-26}$$

In addition to the velocity limitation, there is a limitation in depth. The ultrasonic burst travels in the liquid at a velocity which depends on the physical properties of the liquid. The pulse repetition frequency gives the maximum time allowed to the burst to travel to the particle and back to the transducer. This gives a maximum depth of:

$$P_{\max} = \frac{T_{prf} \cdot c}{2} \qquad \text{Equation II-27}$$

From the above two equations, we can see that increasing the time between pulses (TPRF) will increase the maximum measurable depth, but will also reduce the maximum velocity which can be measured. The maximum velocity and maximum depth are thus related according to the following Equation:

$$P_{max}V_{max} = \frac{c^2}{8f_e\cos\theta}$$

Equation II-28

The ultrasonic waves generated by the transducer are more or less confined in a narrow cone. As they travel in this cone they may be reflected or scattered when they touch a particle having different acoustic impedance. The acoustic impedance is defined by:

$$z = \rho \cdot c$$

Equation II-29

where ρ is the density and c the sound velocity.

If the size of the particle is bigger than the wave length, the ultrasonic waves are reflected and refracted by the particle. In such a case the direction of propagation and the intensity of the ultrasonic waves are affected. But if the size of the particle is much smaller than the wave length and other phenomena appear, which is named scattering. In such a case, a very small amount of the ultrasonic energy is reflected in all direction. The intensity and the direction of propagation of the incoming waves are practically not affected by the scattering phenomena. Ultrasonic Doppler velocimetry needs therefore particles smaller than the wave length.

2.11 Literature reviews of Computational Fluid Dynamics in Hydrocyclone and Doppler Ultrasound Velocimetry

Sripriya et al. (2007) studied the performance of a hydrocyclone and modeling for flow characterization in the presence and absence of an air core. The work was done in a 10cm diameter hydrocyclone with a 58.1cm cyclone body length. There was an experimental study and Computational Fluid Dynamics stimulation. The latter was studied by using three-dimensional geometry and hydrodynamics studies of a hydrocyclone using Gambit and FLUENT. Only one phase was considered using a k-epsilon model physic. The results from the simulation part found that the flow pattern and pressure distribution were the same as that of the theoretical study.

For that, the hybrid process study considers the model physic k-ε standard to simulate the velocity inside the hydrocyclone reactor and compare to the experimental method.

Bai et al. (2008) used a two component laser Doppler velocimeter to measure the velocity inside a 35mm deoiling hydrocyclone. They focused on the air core occurring in the hydrocyclone. The results found that when the inlet flow rate was more than 2m³/h, the air core occurred because the static pressure energy of liquid could not compensate for the loss of energy when inlet flow rate was higher. The velocity fluctuations were greater near the core and near the wall. The turbulence fluctuations were greater at the core region were due to velocity grads. The collision between the wall and fluid made the

turbulence fluctuations strengthen near the wall. The turbulence fluctuations near the core were a disadvantage to separation because the fluctuation made the oil droplet return to liquid. The results showed that the axial and tangential velocity magnitudes were dependent on the inlet flow rate and the flow characters were not changed by changes in the inlet flow rate.

The hybrid process of this study trended to use the Doppler Ultrasound Velocimetry method to measure the velocity inside the hydrocyclone as the work of Bai *et al.* (2008).

2.12 Conclusion of the bibliography for the study of hybrid process

All previous literature reviews relating to the study of hybrid process are summarized in this section. The principles for performing coagulation and flocculation, the main principle of hydrocyclone, computational fluid dynamic study and Doppler technique are included.

2.12.1 The principles of the coagulation and flocculation process

Coagulation involves the addition and rapid mixing of a coagulant, the resulting destabilization of the colloidal and fine suspended solid, and the initial aggregation at the destabilized particle. A coagulant such as the high molecular weight polymer is needed for the destabilization process. Flocculation involves slow stirring to aggregate the destabilized particle before the floc settles. The practical ways of utilizing coagulation and flocculation are through sweep coagulation and polymer bridging mechanism. To carry out these processes, specific operating conditions are required with regard to the type and dosage of the coagulant, flocculant contact time and mixing turbulence.

2.12.2 The required properties for the coagulation and flocculation process

The rapid mixing condition and slow mixing condition are required for coagulation and flocculation, respectively. Therefore, the velocity gradient, an important parameter that controls the mixing intensity in the container, is necessary for both processes. The rapid mixing at a high velocity gradient is required for a contact between the colloidal particle and the added coagulant since the high velocity gradient provides the high collision opportunities between the particles. The recommended range for the velocity gradient in a coagulation process is $100 - 1000s^{-1}$.

2.12.3 The separation potential of the hydrocyclone

A hydrocyclone separates an immiscible solution with different densities by using the centrifugal force of the vortex flow. In a classical hydrocyclone, the mixed solution containing heavy and light phases are injected tangentially from the top of the hydrocyclone to create the vortex flow, then the heavy phase is separated from the light phase following the external vortex, and then moves towards the bottom of hydrocyclone. Finally, it is discharged out at the underflow channel. Meanwhile, the light phase moves

toward to the top of hydrocyclone by following the internal vortex at the hydrocyclone core. It is then discharged through the overflow channel at the top of the hydrocyclone. According to this principle, the heavy phase and the light phase in an immiscible solution can be separated by a hydrocyclone.

2.12.4 Micro bubble generation

The micro bubbles in this study were produced by the principle of dissolved air flotation (DAF). This process is performed by pumping clean water and air flow into the saturated tank. The air flow is dissolved into the liquid under a pressure (3-6bars) because air pressurized water. Afterwards, it enters the reactor through the relief valve, where the pressure is reduced to atmospheric pressure. The large pressure difference across the relief valve produces micro bubble from the air-liquid phase to the gas phase. DAF systems indicate bubbles maintain a steady state size range of 10 to 100μm. A reasonable estimate of the average bubble diameter is 40μm. In this hybrid process, the packed column system with the air-water mixing media of DAF was chosen to produce the micro bubbles. Moreover, Henry"s law was used for air fraction calculation in which the air pressurized water under pressure for the aerated floc production.

2.12.5 Numerical simulation by computational fluid dynamics

FLUENT is a computational fluid dynamics (CFD) software package to simulate fluid flow problems. It is theoretically based on Navier"s stoke equation. It is recommended in the modeling basic fluid flow that the modeling turbulent flow with a significant amount of swirl should consider using one of FLUENT"s advanced turbulence models.

2.12.5.1 Standard k-ε model

A hydrocyclone in this study was simulated the velocity profile by Standard k-ε model. It is a semi-empirical model based on model transport equations for the turbulence kinetic energy (k) and its dissipation rate (ε). It is the simplest complete models of turbulence are two equation models in whish the solution of two separate transport equations allows the turbulent velocity and length scales to be independently determined. The model transport equation for k is derived from the exact equation, while the model transport equation for ε is obtained using physical reasoning and bears little resemblance to its mathematically exact counterpart. The assumption of this model is that the flow is fully turbulent, and the effects of molecular viscosity are negligible. The standard k-ε model is therefore valid only for fully turbulent flows.

2.12.5.2 Reynolds Stress Model (RSM)

The Reynolds Stress Model is the most elaborate turbulence model that FLUENT provides. Abandoning the isotropic eddy-viscosity hypothesis, the RSM closes the Reynolds-averaged Navier-Stokes equations by solving transport equations for the Reynolds stresses, together with an equation for the dissipation rate. Since the RSM

accounts for the effects of streamline curvature, swirl, rotation, and rapid changes in strain rate in a more rigorous manner than one-equation and two-equation models, it has greater potential to give accurate predictions for complex flows.

2.12.6 Doppler Ultrasound Velocimetry

Doppler ultrasound velocimetry implies that the velocity is measured by finding the Doppler frequency in the received signal. Velocities are derived from shifts in positions between pulse, and the Doppler Effect plays a minor role. The principle for measuring the velocity of a target uses a pulse signal. An ultrasonic transducer emits waves with a frequency in a medium. A receptor, or target in the medium moves with a velocity. If the trajectory of the target forms an angle with respect to the propagation direction of the ultrasonic wave, the frequency of the wave perceived by the target can be determined. The frequency shift is called the Doppler frequency. The target velocity can be calculated from the shift frequency and the time reflection delay between the emitted and received signals.

CHAPTER III

GENERAL MATERIALS AND CHEMICAL SUBSTANCES

The study is provided in four main parts. First two parts are to study the hydrodynamics and phenomenon inside hydrocyclone. Seconds two parts are the experimental work on hybrid process with synthetic raw water and natural water. The study will be presented as the four publications form.

Part I: Hydrodynamics studies and Micro bubble size measurement

1. The velocity measurement by oil droplet, Doppler ultrasound velocimetry and CFD modeling (under review in Chemical Engineering and Sciences, submitted in October 2009).

2. Micro bubble size measurement from Dissolved Air Flotation by Laser diffraction technique.

Part II: Hybrid process experimental study

3. The hybrid process for water treatment on synthetic raw water

4. The hybrid process for water treatment on natural water (La Marne River, Research center of VEOLIA Company, Annet sur Marne, France, June – September 2009)

The experiments were done in the laboratoire d'ingenierie des procédés de l'environnement Toulouse France from the November 2007 to the October 2009. It was in co-operation between INSA, Toulouse, France and Chulalongkorn University, Bangkok, Thailand.

Part I: Hydrodynamics studies and Micro bubble size measurement

3.1 Instruments of velocity measurement by oil droplet, Doppler Ultrasound Velocimetry and CFD modeling

To compare and verify the hydrodynamics results from Oil droplet method by Pradipat Bumrungsri (2008), this study used Doppler Ultrasound Velocimetry and Computational Fluid Dynamics (CFD) modeling. The materials used in this part of study are as follow.

1. Doppler Ultrasound Velocimetry is DOP2000 model 2032 by Signal Processing 2000

2. CFD modeling simulation is done by the software package, FLUENT 6.3.26 using two model physics: k-ε standard model and Reynolds Stress Model (RSM)

3.2 Instruments of micro bubble size measurement from Dissolved Air Flotation by Laser diffraction technique

To measure the micro bubble size from the Dissolved Air Flotation system in this study, a laser diffraction technique is considered. The instrument used is Spreytec Malvern Instruments. The measurement is done with only one phase of tap water.

1) He-Ne Laser
2) Collimating optics
3) Measurement zone
4) Fourier lens
5) Silicon diode detector array
6) Rapid data acquisition system
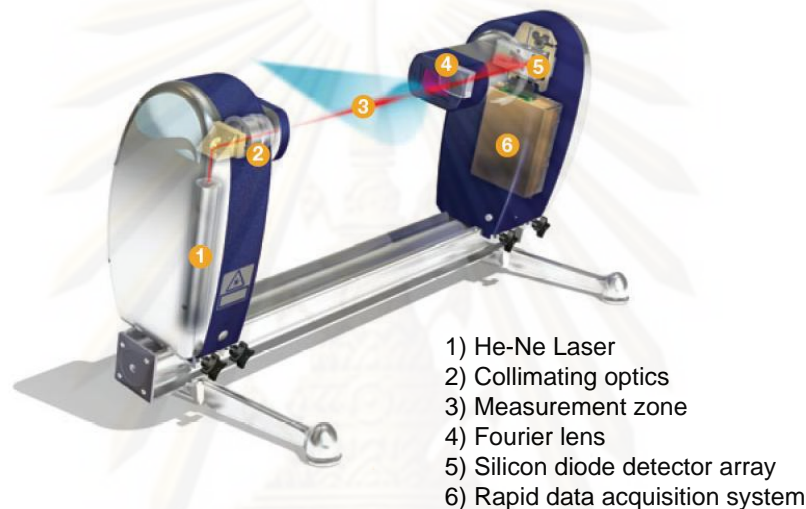
Figure III-1   Spreytec Malvern Instrument

Part II: Hybrid process experimental study

The experimental work of synthetic raw water and natural raw water are using the same pilot and hydrocyclone reactor. The material and instrument are described as follow.

3.3 Pilot plant

There are three main parts of the plant.

1. Pressurized water producer (Micro bubble generation)

2. Raw water and Coagulant solution

3. Hydrocyclone or hybrid reactor

The details has shown in Figure III-2
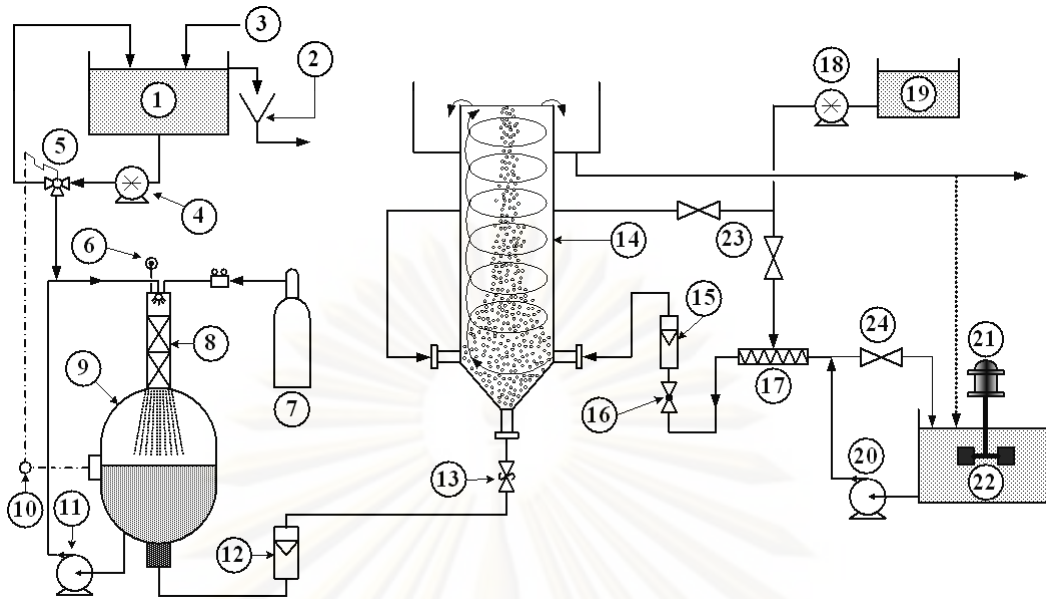
Figure III-2 Plan and instruments

1. Tap water tank	13. Releasing valve
2. Overflow tank	14. Hybrid reactor
3. Water inlet	15. Flow meter
4. Pump	16. Check valve
5. 3-ways valve	17. Static mixer
6. Pressure gage	18. Pump from coagulation tank
7. Air under pressure tank	19. Coagulation solution tank
8. Media to exchange water and air	20. Pump from raw water
9. Pressure tank	21. Mixer
10. Pressure checking in pressure tank	22. Raw water tank
11. Recirculation pump	23. Check valve
12. Flow meter	24. Flow rate adjust valve

Figure III-3   Pilot photo installation and apparatus

3.3.1   Pressurized water producer

Producing pressurized water which is used in the flotation process. According to Figure III-2, the tap water was stored in the tank (no.1) which was filled with water in order to maintain the water level (no.3). The water was pumped from the tank and fed into the pressure tank. The 3-way valve (no.5) was installed in the path to the pressure tank (no.9), which controlled the water level. If the water level was too high, which was checked by the water level checker in the pressure tank (no.10), the 3-way valve would return the water to the tank. Above the pressure tank, the media was packed in the column. Tab water passed to the media (no.8), increasing the water-air contacting, and passed to the pressure tank. If the water level was too low, the 3-way valve would increase the fed of water to the pressure tank. The recirculation pump (no.11) returned water passed the media again which increased the air dissolved in the water. The pressure was checked by the manometer. The pressurized water was fed to the reactor passing the relief valve.

3.3.2   The raw water and coagulant solution part

In this research, raw water was a mixture of bentonite and tap water for at least 24 hours.   The bentonite would become the colloid which was suspended in the water and could not settle by itself. Tank no. 22 stored the raw water and tank no. 19 stored the coagulant solution.

Polymer coagulant which was used in this research: cationic coagulant polymer FO107. The optimum concentration was tested by the Jar test method.

3.3.3 Hybrid reactor

In the hybrid reactor with 1000mm height and 100mm diameter (9.08L volume) is shown in Figure III-4. The reactor has four tangential feed inlet apertures. They are designed for raw water, coagulant solution feed inlet. Four vertical feed inlet apertures at the bottom and close to the wall of hydrocyclone are designed for air pressurized water injection. However, in this study it is used only two air-pressurized water inlets. A vertical center aperture is for draining in case of cleaning the reactor.

The top part of hydrocyclone is designed for water effluence separating between wall zone and center zone. The concentrated floc is drained out of the top part with two horizontal tubes while the clarified water is provide to the wall zone and drained out by two horizontal tubes.
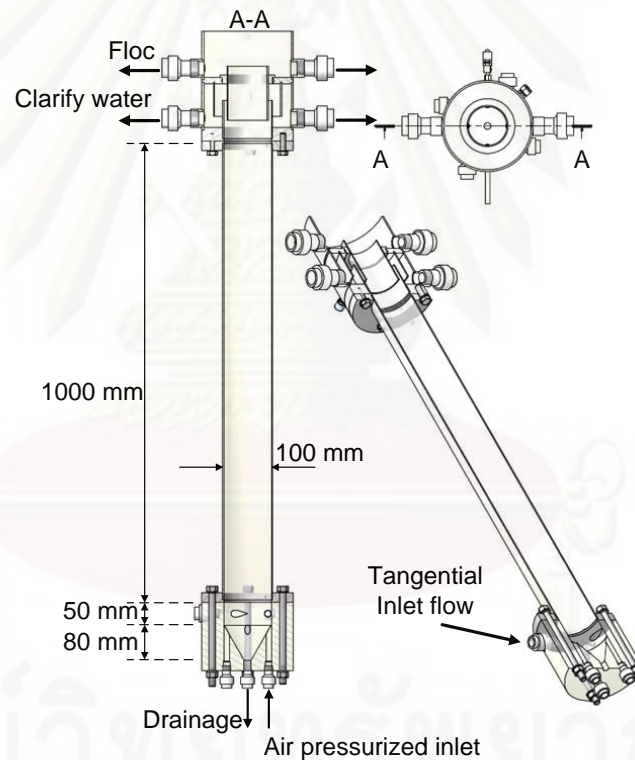
Figure III-4 Hybrid reactor dimension: Front, Top and Lateral views

3.4 Result analysis instruments

To verify the hybrid process performance, the parameters are determined to indicate the process potential. It is necessary to use the instruments as follow.

1. Digital camera (CANON, POWERSHOT S3 IS)

2. Filtration instruments and Membrane Filter 0.45 μm pore (PALL LIFE SCIENCES, LE TUFFRYN, 47mm diameter)

3. Jar test instruments (FLOCUMATIC P, SELECTA, maximum mixing speed 210rpm)

4. Turbidity meter (HACH 2100N IS)

5. Drying weight instrument (SARTORIUS MA145)

6. Spectrometer UV-254nm (HACH LANGE DR5000)

3.5 Chemical substance

The chemical substances in this study are mainly concerned to coagulation and flocculation process.

1. Bentonite (BENTONIL C15T)

2. Cationic polymer coagulant FO107

3. Anionic and Non-ionic polymer coagulant AN910 and AN905

4. Aluminum Sulfate (PROLABO)

The next chapter will explain the first part of study: Hydrodynamics study and micro bubble measurement.

CHAPTER IV

Hydrodynamics studies and Micro bubble size measurement

4.1 PART I: Velocity measurement in the hydrocyclone by oil droplet, Doppler ultrasound velocimetry and CFD modelling

4.1.1 Abstract

To develop the water treatment process, the hydrocyclone is now more used as a unit to operate. Understanding hydrodynamics is a key step to improve the separation process efficiency. The Doppler Velocimetry measurements and Computational Fluid Dynamics (CFD) have been proposed by many researchers as effective for studying the flow field of a hydrocyclone. Recently, a new simple method called the Oil droplet method was proposed by Pradipat Bumrungsri et al. (2008) and applied to velocity measurements in a hydrocyclone.

This work presents a comparison of the experimental results from these two methods along with those obtained from numerical simulations. The numerical calculations of the 3D flow field were performed with FLUENT using the k-ε model and the Reynolds Stress Model (RSM). Measurements and CFD simulations were performed for two hydrocyclone configurations (5cm and 10cm diameter).

Doppler ultrasound velocimetry data and CFD-RSM results are in close agreement. The oil droplet method is less accurate for the continuous phase velocity profiles but is promising for the validation of lagrangian tracking simulations.

Keywords: Hydrocyclone, Hydrodynamics, Imaging, Instrumentation, Simulation and Velocity field.

4.1.2 Introduction

Hydrocyclones are now more integrated in the environmental field. Using a hydrocyclone as a reactor for water treatment is being studied. The flow inside a hydrocyclone is a complex three dimensional swirling flow. One water treatment process by using a hydrocyclone is developing. This process integrates with coagulation, flocculation and also producing micro bubbles. During the research, the undesirable coalescence of the micro bubbles occurred in the special operating conditions and hydrocyclone design. Consequently, characterizing the hydrodynamics inside the specific hydrocyclone is necessary in order to develop the water treatment inside hydrocyclone. Accordingly, velocity profile determination methods are studied.

Velocity profiles in the hydrocyclone were measured by many researchers. Kelsall (1952) used a stroboscope with a rotating microscope objective lens to determine the velocities. The photographic techniques, Ohasi and Maeda (1958) used a stroboscope to determine the particle velocity. Recently, Laser Doppler Velocimetry (LDV) was used to

determine the tangential and axial velocities (Bai et al., 2008). Chiné and Concha (2000) used LDV to measure velocity in a 102-mm modular hydrocyclone. Owing to the rapid development of the computer and CFD techniques, the use of numerical simulations to predict the performance of the cyclone has received much attention. Udaya et al. (2006) worked on the comparison of experimental and simulated results generated using different turbulence models; standard k-ε, k-ε RNG and Reynolds Stress Model (RSM) in terms of water throughput and split with the help of suitably designed experiments on a 76-mm diameter hydrocyclone. The commercial software package FLUENT was used to simulate many researches in hydrocyclone (Bardow et al., 2008; Kraipech, et al., 2008; Narashimha, Brennan and Holtham, 2007b).

In the development of water treatment process by hydrocyclone, Pradipat Bumrungsri et al. (2007) has proposed a new technique called the oil droplet method to estimate the velocity field of the continuous phase in two hydrocyclone configurations. The experiment was done in a 5cm diameter hydrocyclone with a different geometry from a conventional hydrocyclone. The purpose of this work is to present the numerical velocity simulation results obtained by CFD in order to compare with the experimental method; oil droplet method and Doppler Ultrasound Velocimetry.

A comparison between the oil droplet method results and numerical simulation with k-ε model in 5cm diameter hydrocyclone is firstly presented. The second part deals with the comparison between the Doppler ultrasound velocimetry method results and the numerical simulation with RSM in 10cm diameter hydrocyclone.

4.1.3   Experimental setup

4.1.3.1   Hydrocyclone

The study was carried out with two hydrocyclone configurations. The first one was a glass hydrocyclone with a 5cm diameter and 100cm height. The tangential inlet at the bottom part varied the diameter at 0.3 and 0.5cm. The second one was a 10cm diameter hydrocyclone and 100cm height with the tangential feed inlet diameter of 1.5cm as shown in Figure IV-1
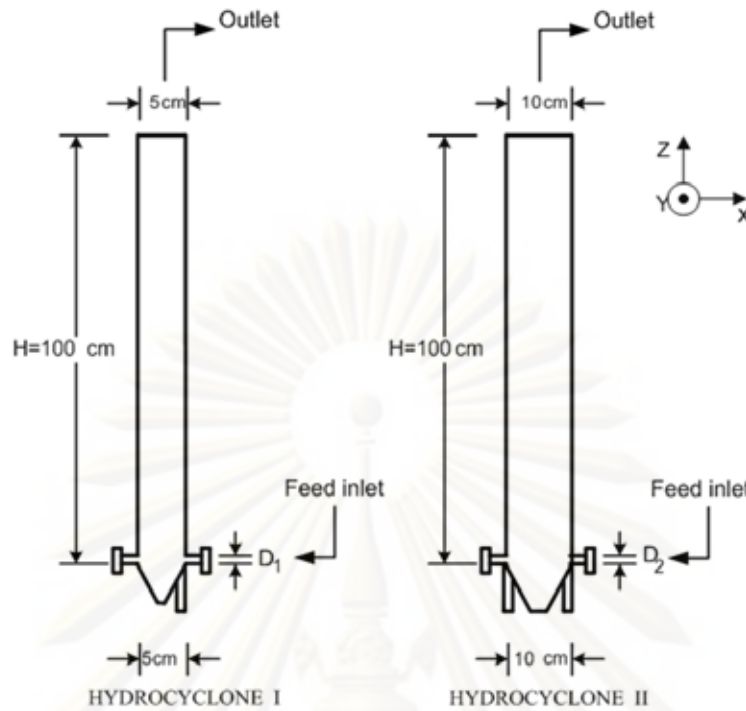
**Figure IV-1 Schematic diagram of Hydrocyclone I (D$_1$=0.3 and 0.5cm)
and Hydrocyclone II (D$_2$=1.5cm)**

4.1.3.2 Oil droplet method

The oil droplet method relies on the tracking of the red coloured oil droplet using a PCO 1200hs digital high speed camera (10 bitcmOS) taking image at 491 frames/second. The image acquisition was performed at the reactor height 7cm above the inlet level. The flow field in the hydrocyclone was studied by assigning four points to the bottom part. The four locations were at the centre, 1cm, 2cm from the centre and close to the hydrocyclone wall as shown in Figure IV-2. Three oil tracer droplets were injected continuously on a studied point by a small syringe. The droplet moved towards different directions depending upon the experimental operating conditions. This method was done in 5cm diameter hydrocyclone. Tangential and axial velocities are determined by the displacement of the droplet and also the time difference from each image. The moving distances of the droplet from t_1 to t_2 in tangential direction or Δy, and axial direction or Δx, are calculated subsequently by using Equation: $\Delta y = |y_2 - y_1|$, and $\Delta x = |x_2 - x_1|$ respectively. The relative tangential and axial velocity of each droplet can be calculated by $V_{tan} = \Delta y/\Delta t$ and $V_{axial} = \Delta x/\Delta t$ respectively. The technical details are presented in Pradipat Bumrungsri et al. (2008). The conditions investigated with the oil droplet method are shown in table IV-1. Each value of results is the average value of three experiments.
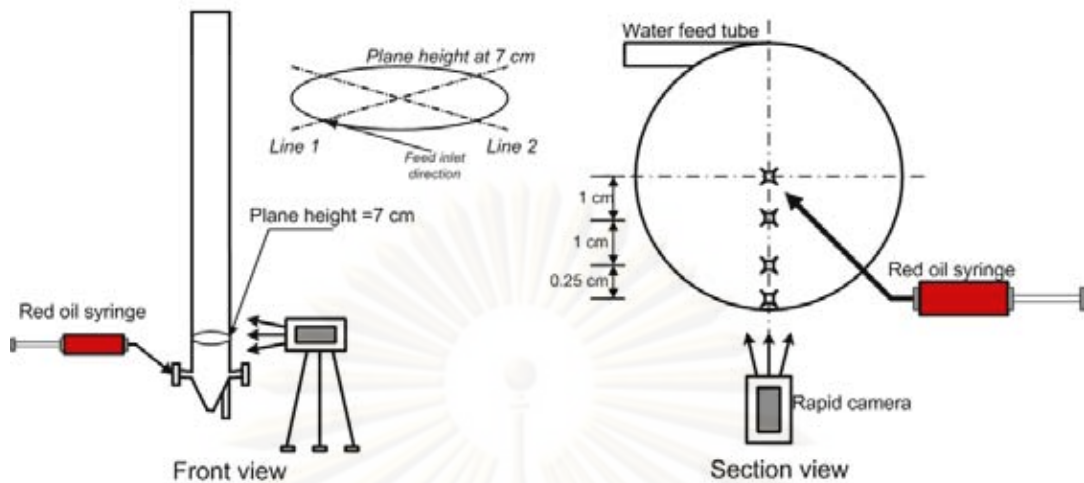
Figure IV-2 Oil droplet method

Table IV-1   The experimental conditions done in Oil droplet method

Condition	Inlet diameter, D (cm)	Inlet flow rate, Q (l/hr)	Water inlet velocity, v (m/s)
1	0.3	200	7.86
2	0.5	200	2.83
3	0.5	400	5.66

4.1.4   Doppler Ultrasound Velocimetry

The velocity measurements inside the 10-cm diameter hydrocyclone were carried out using a Doppler Ultrasound Velocimetry instrument DOP2000 model 2032. The sound speed was 1480 m/s as the medium was only water (Signal processing, 2000). The sound wave emission was 4MHz. The angle α as shown in Figure IV-3, was the angle between the sound emission direction and the diameter of cyclone, which was 10°. The Doppler signal gives the component (U_m) of the velocity in the sound direction at the distance z from the sound probe. Consequently, the tangential velocity (U_θ) can be determined by the relation between these two velocities from the angle ζ, which depends on the angular coordinate θ. The experimental conditions were 1000L/h inlet flow rate (maximum flow rate) corresponding to 1.572m/s inlet velocity. Each of the velocity values from Doppler ultrasound velocimetry is an average value among 400 measurements.
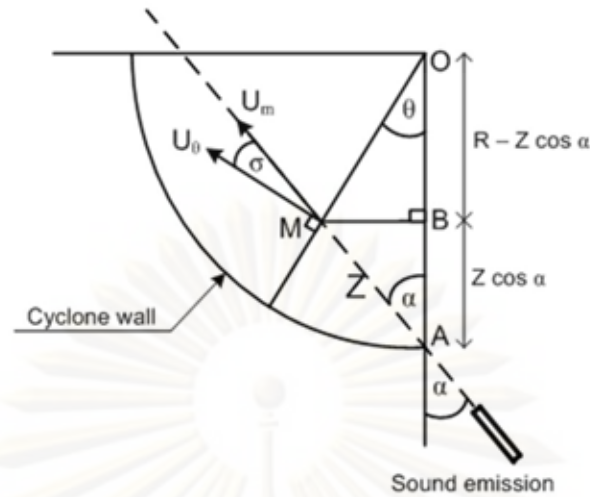
**Figure IV-3 The Doppler method and the relation of the angle between
the hydrocyclone diameter and the sound direction**

4.1.5 Turbulent model

4.1.5.1 Numerical simulation for Hydrocyclone I

Dyakowski and Williams (1996) have suggested that the k-ε model can be used on a small cyclone (<44mm radius). This model makes the assumption that the turbulence is isotropic since only one scalar velocity fluctuation is modeled (Narashimha et al., 2007a). So, for Hydrocyclone I, simulations have been conducted using the k-ε model.

k-turbulent kinetic energy

$$\frac{\partial}{\partial t}(\rho k) + \frac{\partial}{\partial x_i}(\rho k u_i) = \frac{\partial}{\partial x_j}\left[\left(\mu + \frac{\mu_t}{\sigma_k}\right)\frac{\partial k}{\partial x_j}\right] + G_k + G_b + \rho\varepsilon - Y_M + S_k \qquad \text{Equation II-15}$$

ε-transport Equation

$$\frac{\partial}{\partial t}(\rho\varepsilon) + \frac{\partial}{\partial x_i}(\rho\varepsilon u_i) = \frac{\partial}{\partial x_j}\left[\left(\mu + \frac{\mu_t}{\sigma_\varepsilon}\right)\frac{\partial\varepsilon}{\partial x_j}\right] + C_{1\varepsilon}\frac{\varepsilon}{k}(G_k + C_{3\varepsilon}G_b) - C_{2\varepsilon}\rho\frac{\varepsilon^2}{k} + S_\varepsilon$$

$$\text{Equation II-16}$$

Turbulent viscosity is modeled as $\mu_t = \rho C_\mu \dfrac{k^2}{\varepsilon}$

The value for the five calibration constants of the k-ε model defining the base line case of the presented sensitivity- based analysis correspond to those proposed in Launder and Sharma (1974) and are given by

$C_{1\varepsilon}$=1.44, $C_{2\varepsilon}$=1.92, C_μ=0.09, ζ_k=1.0, ζ_ε=1.3

4.1.5.2 Numerical simulation for Hydrocyclone II

For hydrocyclone II, simulation was performed with RSM, which is more appropriate to the swirling flows. The simulation will include turbulence 3D model selection for simulating the tangential and axial velocity profiles obtained with different inlet diameters and inlet velocities with one phase of water liquid and compared to the experimental results from the Doppler ultrasound velocimetry method.

Reynolds Stress Transport Equations: the exact transport Equations for the transport of the Reynold Stresses, $\rho \overline{u_i' u_j'}$, may be written as follows

$$\frac{\partial}{\partial t}\left(\rho \overline{u_i' u_j'}\right) + \frac{\partial}{\partial x}\left(\rho u_k \overline{u_i' u_j'}\right) = -\frac{\partial}{\partial x_k}\left[\rho \overline{u_i' u_j' u_k'} + \overline{p\left(\delta_{kj} u_i' + \delta_{ik} u_j'\right)}\right] + \frac{\partial}{\partial x_k}\left[\mu \frac{\partial}{\partial x_k}\left(\overline{u_i' u_j'}\right)\right]$$

$$-\frac{\partial}{\partial x_k}\left[\mu \frac{\partial}{\partial x_k}\left(\overline{u_i' u_j'}\right)\right] - \rho\left(\overline{u_i' u_j'}\frac{\partial u_j}{\partial x_k} + \overline{u_j' u_k'}\frac{\partial u_i}{\partial x_k}\right) - \rho\beta\left(g_i \overline{u_j' \theta} + g_j \overline{u_i' \theta}\right)$$

$$+ \overline{p\left(\frac{\partial u_i'}{\partial x_j} + \frac{\partial u_j'}{\partial x_i}\right)} - 2\mu \overline{\frac{\partial u_i'}{\partial x_k}\frac{\partial u_j'}{\partial x_k}} - 2\rho\Omega_k\left(\overline{u_j' u_m'}\varepsilon_{ikm} + \overline{u_i' u_m'}\varepsilon_{jkm}\right) + S_{user} \qquad \text{Equation II-19}$$

Local Time Derivate $+ \quad C_{ij} = D_{T,ij} + D_{L,ij} + P_{ij} + G_{ij} + \phi_{ij} - \varepsilon_{ij} + F_{ij} +$ User-Defined Source Term

4.1.5.3 Boundary condition

The circular hybrid feed inlet face was defined as „velocity inlet". The overflow outlet face was designed as „outflow". The primary water phase was allowed to enter the hybrid reactor with a density of 998.2kg/m^3 and a viscosity value of $1.003 \times 10^{-6} \text{kg/ms}$. The other inlets with no feed flow rate were set as „wall". In all cases, a second order discretization scheme was used and the convergence criterion on residuals was set to 10^{-7}.

4.1.6 Grid division

Figure IV-4 and IV-5 schematically illustrate Hydrocyclone I and Hydrocyclone II geometries and grid division. The whole mesh is an unstructured grid compound of tetrahedral control cells. The inlet tube part is meshed with fine grids because the velocity gradient in this area is the highest. The conical bottom part is meshed with the moderate grid size and the upper part (cylindrical body) is meshed with coarser grid. Hydrocyclone I with 0.3 and 0.5cm inlet diameter contained 272777 cells and 280194 cells respectively. On the other hand, hydrocyclone II contained 392729 cells. Note that

the hydrocyclone II is simulated with only one tangentially inlet. The other inlets are provided for modification and additional systems.

Inlet diameter D=0.5 cm   Inlet diameter D=0.3 cm
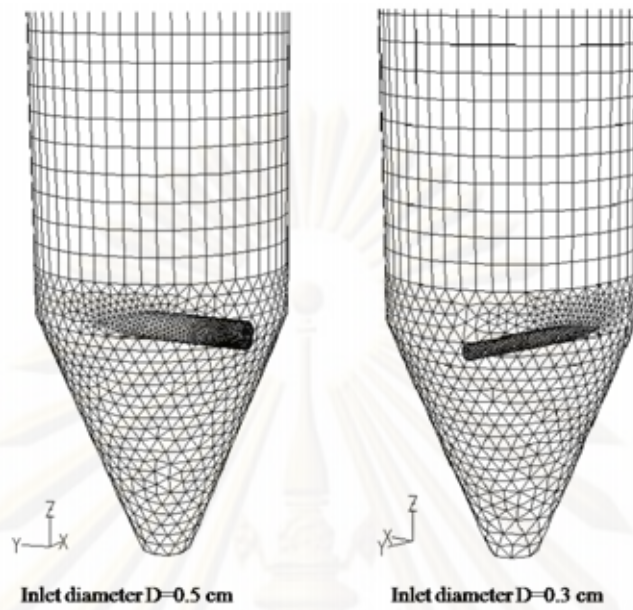
Figure IV-4 Grid system of Hydrocyclone I with 0.5 and 0.3cm inlet diameter

Figure IV-5 Grid system of Hydrocyclone II

4.1.7 Results and discussion

4.1.7.1 Hydrocyclone I

The first hydrocyclone conditions were simulated with a k-ε standard model and the experimental method was Oil droplet. Using the k-ε standard model was to justify the oil droplet method. Even this model is on the assumption that the turbulence is isotropic but it costs less than the other model.

Two lines of the results from the simulation by FLUENT are created. Line (1) and line (2) present the velocity profiles at the 7cm height from the inlet level in order to present the velocity on that surface. The first line is parallel to the flow inlet direction and the latter is perpendicular to the inlet direction in order to represent the velocity on the same section with oil droplet method.

From the Figures IV-6 and IV-7, a larger inlet diameter size presented a lower inlet velocity and also tangential velocity. With both methods the tangential velocities are low at the centre of the hydrocyclone and slightly increase close to the wall, the same trend of the oil droplet method results. The results from the oil droplet method at a 2.0cm radius did not correspond to the results from FLUENT simulation. This can be discussed by three reasons. Firstly, if the size of the oil droplet is large, the water velocities of oil droplet˝s sides are not equal. This causes the oil droplet to swirl and moves to the centre. Secondly, according to the first reason, the droplet swirling causes the droplet displacement change. The droplet trajectory is curved to the centre, it increases Δt. Consequently, the calculated tangential velocity from $\Delta y/\Delta t$ is decreased because the droplet trajectory is changed.   Finally, the vortex flow includes three velocity components; tangential velocity, axial velocity and radial velocity. The radial velocity effectively pushes the particle to the centre. From the oil droplet method, the radial velocity was not taken into account. With these three reasons, it can be discussed that the actual tangential velocity should be higher than the calculated one and the measured velocity value at 2.0cm from centre using by the oil droplet method should be closer to the centre.
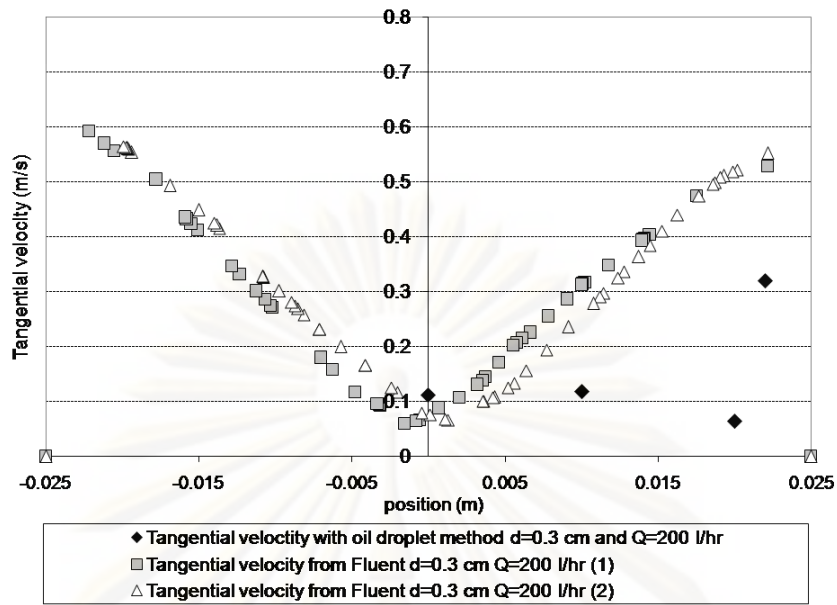
Figure IV-6 Tangential velocity with D= 0.3cm and velocity inlet 7.86 m/s
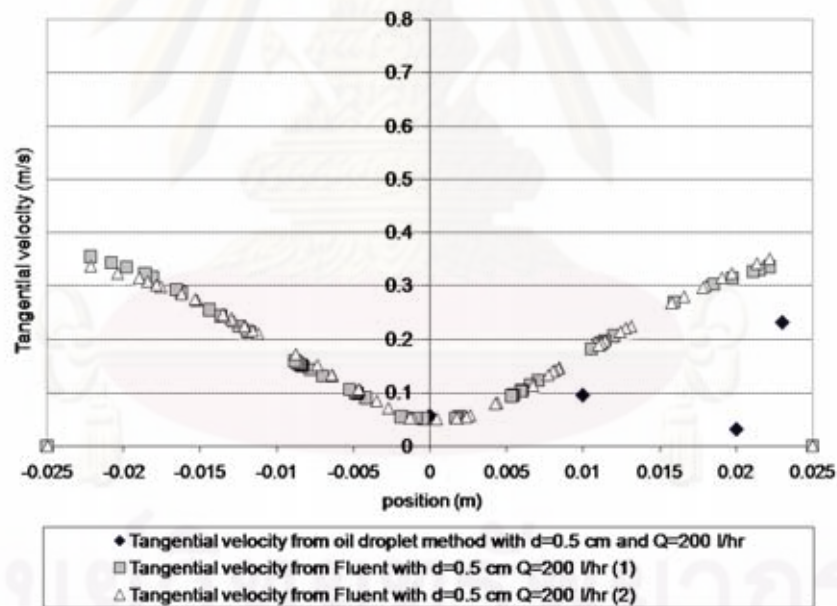
Figure IV-7 Tangential velocity with D= 0.5cm and velocity inlet 2.83 m/s

The axial velocity when changing the inlet diameter as shown in Figure IV-8 and IV-9, present the positive velocities near the hydrocyclone wall and negative at the centre. It means that water flows upwards near the wall and flows downward at the centre. The results from both methods (Oil droplet and numerical simulation) showed the same trend.
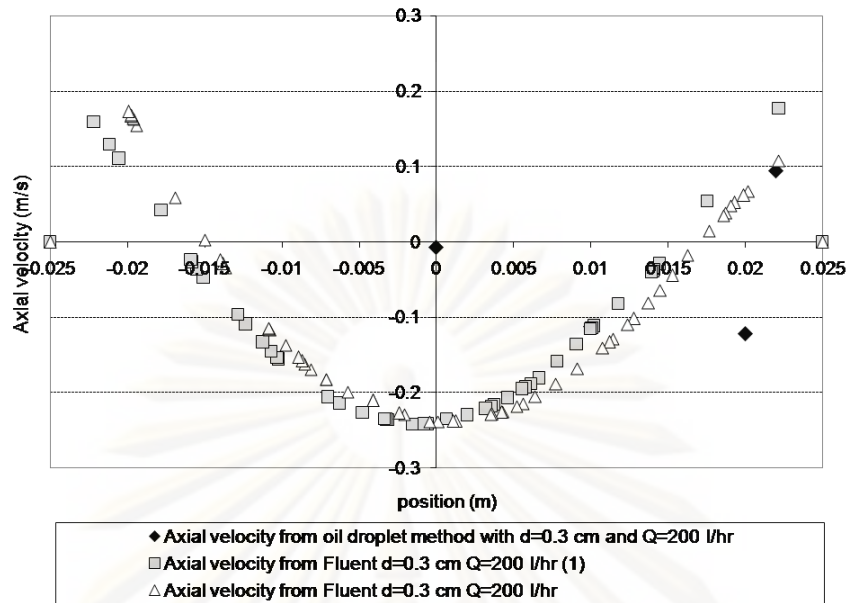
Figure IV-8 Axial velocity with D= 0.3cm and velocity inlet 7.86 m/s
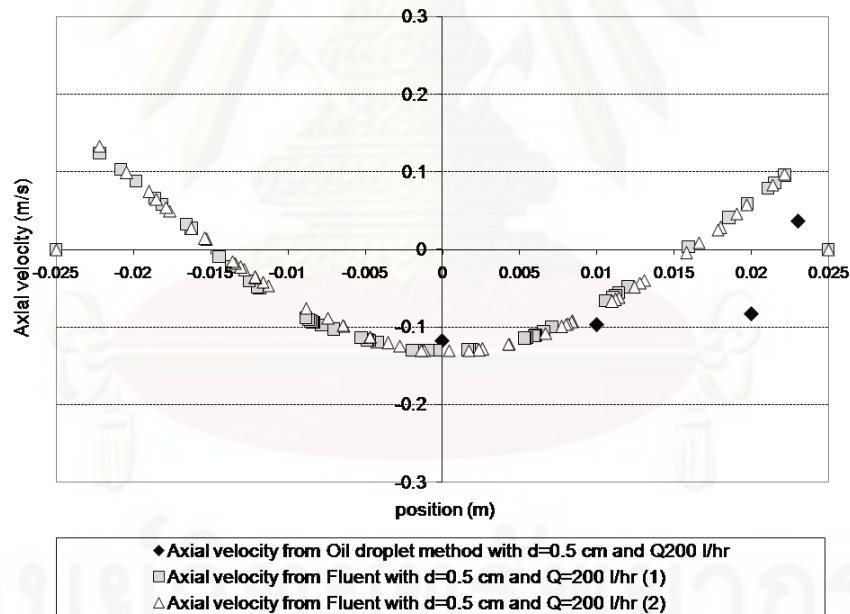
Figure IV-9 Axial velocity with D=0.5cm and velocity inlet 2.83 m/s

The results from this part explains that the bubble coalescence phenomenon that occurred in the developed process. The axial velocity moves downward at the centre. The micro bubbles are unable to move upward as they are blocked by axial velocity flow. On the other hand, the tangential velocity results show a high velocity gradient near the wall. It could be considered for the future work where the coagulation phenomenon is

attempted to occur at the hydrocyclone wall as the coagulation process requires a high velocity gradient.

The effect of changing the inlet flow rate is shown in Figure IV-10 and IV-11. The tangential velocity was obviously related to the inlet velocity. When the inlet velocity increased, the tangential velocity increased. As the review of previous tendencies observed (Jonas and Hannes, 2007), the tangential velocity in the conventional hydrocyclone is negative at the wall with high magnitude. It is in the downward direction as it has the inlet aperture on the top part. The specific hydrocyclone configuration in this study has the injection aperture in the bottom part. The liquid movement is upward. Even though the inlet position is different it presents a high tangential velocity near the wall as the conventional one.
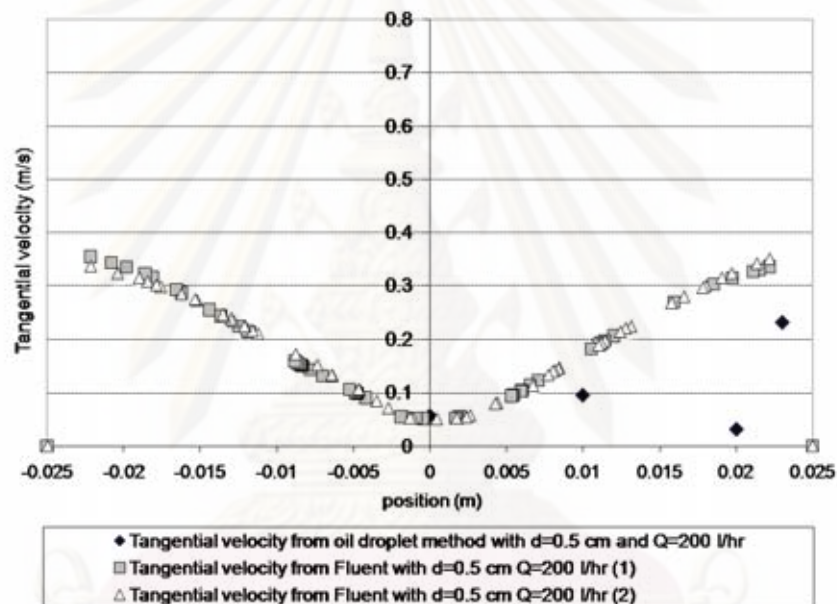
Figure IV-10 Tangential velocity with inlet flow rate 200L/h, velocity inlet 2.83m/s
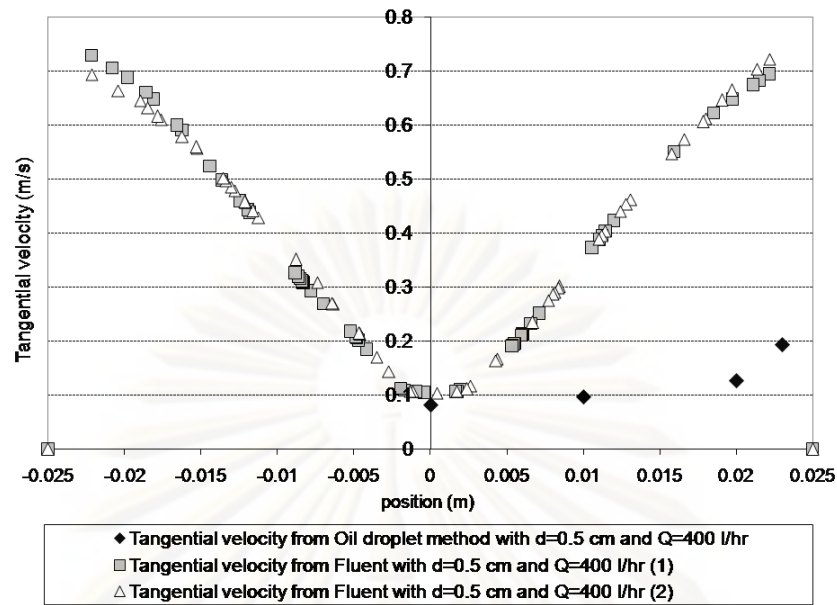
Figure IV-11 Tangential velocity with inlet flow rate 400L/h, velocity inlet 5.66m/s

4.1.7.2 Hydrocyclone II

The experimental work in the second hydrocyclone configuration, 10cm diameter and 1.5cm tangential inlet diameter, was by the Doppler Ultrasound Velocimetry method. The numerical simulation model was the Reynold Stress Model (RSM). This model is the most elaborate turbulence model that FLUENT provides.   Abandoning the isotropic eddy-viscosity hypothesis, the RSM closes the Reynolds averaged Navier-Stokes Equations by solving transport Equations for the Reynolds stresses.   Using RSM to predict the phenomena inside the hydrocyclone is widely used; Slack et al. (2000) found that the RSM model gave good predictions of velocities in gas cyclones. The present work is one of the studies for developing the hydrocyclone in the water treatment process. It is need to understand the hydrodynamic inside the hydrocyclone.   Thus, RSM is considered to simulate the velocities profile in this part of work.

Applying the Doppler method for the experimental work, the difficulties were to adjust the sound signal. There was some data that could not be counted because it was close to the hydrocyclone wall. Also the limit of this method is that the velocities on the axis zone were unable to be measured because the sound emission direction could not pass the centre point in terms of the sound reflection and the angle calculation. However, the result showed the velocity profile which was the same trend to the simulation method as shown in Figure IV-12.
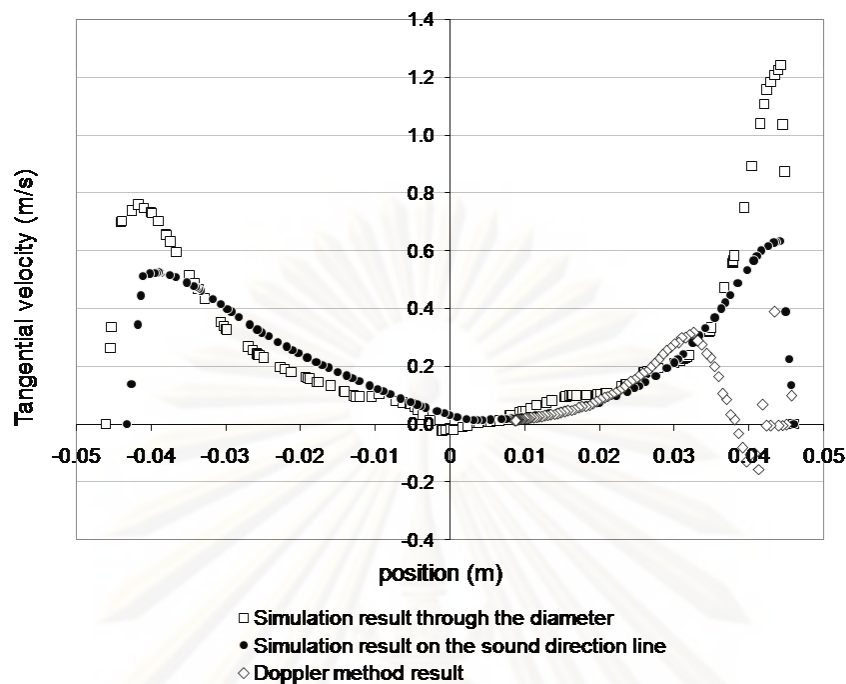
**Figure IV-12 comparison of tangential velocity result from
Doppler Ultrasound Velocimetry and CFD numerical simulation**

With a 1.512m/s inlet velocity result from Figure IV-12, the Doppler method results have shown that the tangential velocity slightly increases from the centre to the wall. At a radius larger than 3.0cm, the velocity sharply decreases and this should be marked that this zone of results were not countable because they were close to the wall. The time reflection of the sound emission was not adequate to present a good signal while the numerical simulation results through the diameter line were on the assumption that the tangential velocities were independent to the angle θ. Consequently, they were firstly compared between the Doppler results by projecting the velocity to the diameter line and the result from numerical simulation through the diameter. On the other hand, it could be seen on the graphic that the left side of velocity profile are not equal to the right side. It indicates that tangential velocities were not independent to θ. Thus, creating the sound direction line in numerical simulation was considered. Accordingly, tangential velocity simulation was done to compare the Doppler method at exactly the same position. Moreover, the θ dependence can be negligible. As a result, the simulation on the sound direction line in Figure IV-10 and IV-11 can compare with the Doppler method. Besides, these two methods gave the results with dramatically the same trend. Considering the result from the numerical simulation, there are two zones of the velocity profile. The tangential velocity slightly increases from the centre till a 30mm radius then it increases significantly close to the wall. It means the larger diameter could present higher velocity gradient comparing to hydrocyclone I. This point of result supports the coagulant process which will be developed in the hydrocyclone for the future study.
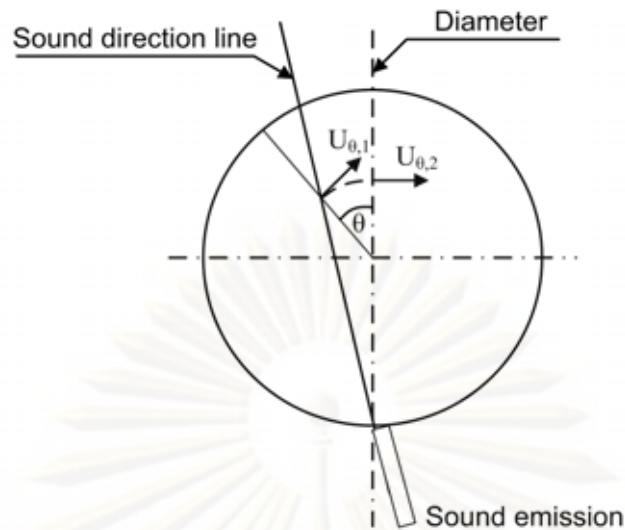
Figure IV-13 the sound direction line and diameter created in the simulation by FLUENT

4.1.8   Conclusions

Developing the water treatment process by study the hydrodynamics inside the specific hydrocyclone, the experimental method; oil droplet method and Doppler ultrasound velocimetry method are acceptable. The oil droplet method is a simple way to measure the velocity inside the hydrocyclone.   This method was used and the measurements were found to be in-line with the results simulated from the k-ε standard model. Doppler ultrasound velocimetry is also a rapid method to measure the velocity inside the hydrocyclone. It is a very interesting method as it gave result quite precise to the numerical simulation. However, the difficulties of this method are to set the sound signal weather it gives accurate data and also the limit of the relation of angle between the sound direction and the tangential velocity. Moreover, the axial velocity is unable to be measured by Doppler ultrasound velocimetry. The model physic in numerical simulation in this work, the k-ε standard model and RSM, it is known that RSM is more precise and also more expensive.   The developed velocities profiles results from this study are sufficiently to explain the phenomenon inside the hydrocyclone.   It will be further extended and used for developing a water treatment process in the hydrocyclone.

4.2 PART II: Micro bubbles measurement from Dissolved Air Flotation by laser diffraction technique

4.2.1 Abstract

A water treatment process in the hydrocyclone involves with micro bubbles produced by the Dissolved Air Flotation (DAF) technique. To develop this process, it is necessary to know the bubbles size because of its influence on to the particle-micro bubbles attachment. The measurement is done by a laser diffraction technique of Spraytec software Malvern Instruments. This work studied the influence of the reactor height and the air saturation pressure in DAF to the bubble size distribution. It appeared that the size slightly increased with the higher level of the tank and increasing air saturation pressure had an effect on bubble size. Bubble size distribution, focusing on the peak diameter of bubbles, was smaller as the pressure increased. It is believed that the bubble size measurement in this study will assist understanding and improve development of the water treatment in a hybrid process in a hydrocyclone reactor.

4.2.2 Introduction

Flotation is a process for separating solid particles by air bubbles. It is used in many fields especially in the water treatment process. There are several techniques in the flotation process; DAF is one flotation process producing the micro bubbles to attach to the particle. It has been widely studied over the last twenty years, and is now a proven technology in water treatment plants (Hudson et al., 2009). The flotation process efficiency is governed by the micro bubbles size, and therefore it is necessary to investigate the bubbles that are generated by the DAF technique.

Methods were developed to measure the bubble size distribution. Rodrigues and Rubio (2003) reviewed the basis for measuring the size distribution of bubbles. There are various methods for measuring that are useful for process control. The most widely used techniques today are based on the diffraction of light, laser diffraction technique. This method is classified as non-destructive and non-intrusive and relies on the fact that the laser diffraction angle is inversely proportional to particle size (Rawle, 2002; Xu, 2002). It has a short time of analysis, is simply to operate and can continuously measure.

A new water treatment process which is involved with DAF technique has a cylindrically dimension. The bottom part is designed for the coagulation-flotation process as shown in Figure IV-14. A velocity gradient from the tangentially inlet raw flow rate, spontaneously with coagulant solution will create the coagulation process. The created micro floc will attach to the micro bubble from air pressurized water by Dissolved Air Flotation technique (DAF), injected at the vertical tube. These micro bubbles – floc composition will be call „aerated floc". The aerated floc density is less than water since it contains the micro bubbles inside. It will be separated by the vortex flow as in the hydrocyclone mechanism. Clarified water will drain out at the wall zone and the floc concentrated will be drained out at the centre zone.
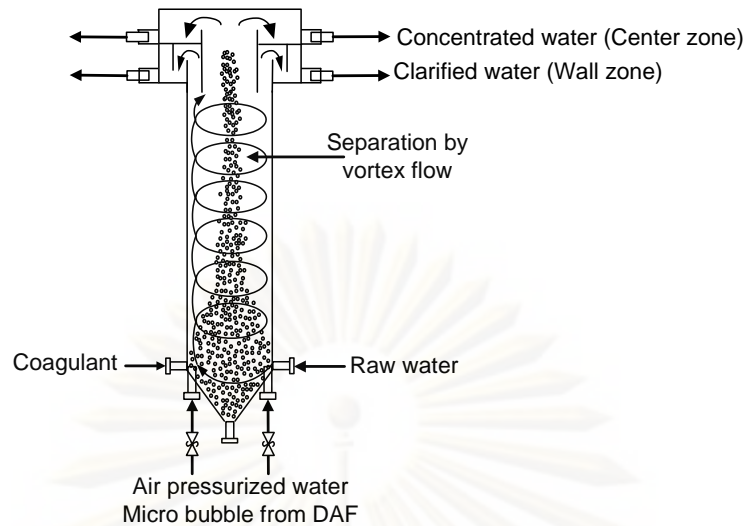
Figure IV-14 The hybrid reactor concept

Since micro bubbles play an important role in aerated floc formation, bubble coalescence is undesirable. To optimize the process, it is basically necessary to understand the effects of the reactor height and the saturation pressure to the micro bubble size and behavior. The purpose of this study is to determine the size distribution of bubbles produced by a pressure system with a laser diffraction technique and study the parameters that can influence the size of bubbles. First part presents the effect of the reactor height to the micro bubble size distribution and the second part is the study of the saturation pressure influence on the micro bubble size distribution.

4.2.3   Material and methods

The pilot used for the bubble measurement consists of three main parts; a bubble generation system, measurement column and micro bubble size measurement instrument as shown in Figure IV-15. The measurement column is a $10 \times 10 \times 55$cm glass column. The micro bubbles are generated through the water liquid medium. The water quality was 1.003Pa.s viscosity, 996.8kg/m^3 density and 72.75mN/m surface tension.

1. Laser He-Ne   5. Measuring zone
2. Receptor   6. Saturated tank
3. System acquisition   7. Relieving valve
4. Measuring column   8. Water level probes
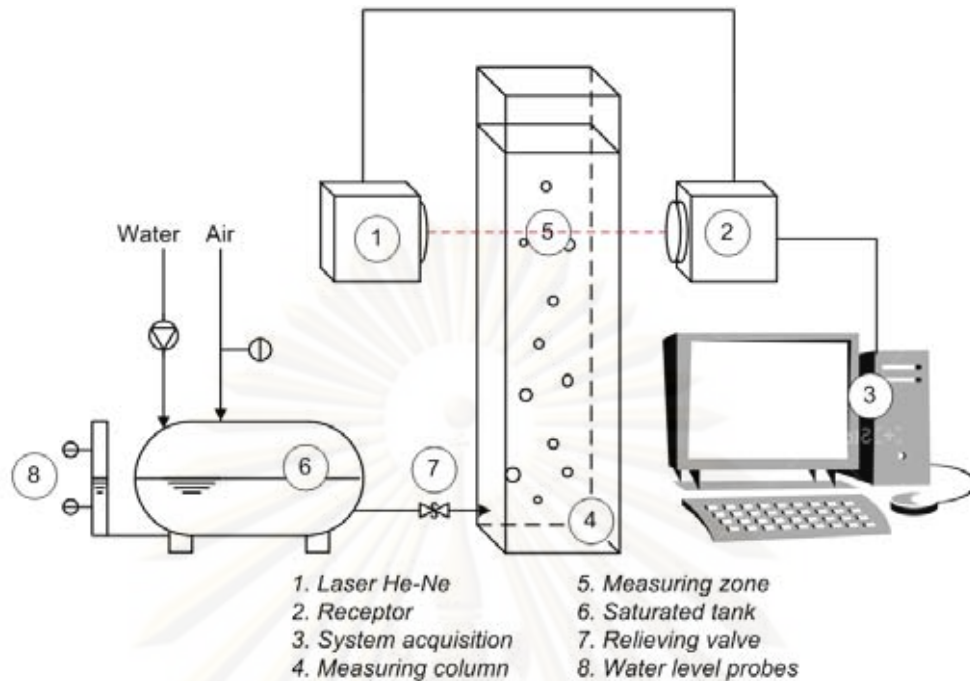
Figure IV-15 Schematic of the installation

4.2.4 The bubble generation system

The micro bubbles are generated by the DAF technique. The saturation pressure range was between 3.4 – 6.2bar limited by the system capacity.   Air is dissolved in the saturated tank during for 10 minutes before the experiment. The water is fed inside the saturated tank. The water level inside the tank is controlled by two electro-valves. The air pressurized water passes through the relieving valve which controls the flow rate and also provides the air bubble precipitation from the air-liquid saturated phase.

4.2.5 The laser diffraction instrument

The micro bubble size from the DAF technique is measured by Spraytec® equipment from *Malvern Instrument Ltd*. It measures the size of particles in a spray. Specifically, it measures the distribution of different sizes within a spray using a He-Ne (Helium-Neon) laser to produce a laser beam that passes through the spray delivered to the measurement zone.   Optical sensors in the Receiver modules detect the light diffraction pattern produced by the bubbles, converting the light detected into electrical signals. The signals are processed by analogue and digital electronics boards, and passed to the analysis software. The light diffraction pattern is analyzed using an appropriate scattering model to calculate the bubble size distribution.

Spraytec software calculates the size by comparing the acquired light scattering pattern to an optical model which predicts how particle scattering changes the particle size. The theories behind the calculations are Fraunhofer approximation and Mie theory. Fraunhofer approximation model predicts the scattering pattern that is created when a solid, opaque disc of a known size is passed through a laser beam. This model is

satisfactory for large particles (over 50μm diameter) but it does not describe the scattering exactly. The accepted theory which accurately predicts the light scattering behavior of all material under all conditions is known as the Mie theory. It was developed to predict the way light is scattered by spherical particles and deals with the way light passes through or is absorbed by the particle. This theory presumes that the particles being measured are perfect spheres. One way to get a single unique number to describe an irregular shaped particle or bubble is to compare some feature of the actual droplet to an imaginary spherical droplet. This technique is known as equivalent spheres. (Malvern, 2005)

4.2.6 The experimental setup

Water and air were pumped into a saturated tank. Under a pressure condition from 3.4 – 6.2bar, the air dissolved into the water after at least 10 minutes contact time. Two probes control the water level inside the saturated tank. When water level is too low, it will pump the water inside the tank. On the other hand, if water level is too high, air will be injected inside the tank. The air saturated water passes the relief valve before getting into the column, decreasing to atmospheric pressure causes the saturated liquid-air to release in the gas phase to be micro bubbles inside the column filled with water higher level than the measuring zone. The laser beam passes through the column which is called the measuring zone. The data will be recorded and sent to the acquisition system by the receptor. Finally, Spraytec software calculates the data and presents the micro bubble size distribution. It is noted that during the laser diffraction measurement, it must comply with a transmission of between 25% and 75%, knowing that at zero percent the laser cannot be measured because there are too many bubbles. On the other hand, with 100% transmission there are no bubbles to measure.

The first part of the experiment works on the accuracy of the results from the laser diffraction technique. It is to find the reproducible micro bubble size distribution to assure the good quality measurement results for the next experiments. The second part is to study the effects of the column height to the size distribution. The measuring zone will change from 9, 13, 21, 29cm from the bottom of the column. The last part studies the pressure influence on the size distribution; it will be varied from 3.4, 4.5, 5.4 and 6.2bars.

4.2.7 Calculations

The software provides a volume distribution of bubbles. But it is important not to rely only this distribution. Indeed, the observation of certain distributions suggests that there is a presence of a few particles of very small size and many of the larger size. However, the distribution in diameter, that is the frequency of bubbles appearance by diameter, shows that the majority of particles have a small diameter. This reflects the fact that these particles represent only a very small volume compared to particles much larger than them, even if they are the majority.

To calculate the relation between the frequency and size in diameter uses the following method of calculating the percentage of bubbles associated with the corresponding diameter. The volume of a bubble for each diameter is determined:

$V_i(\mu m^3) = \pi \times \dfrac{D_i^3}{6}$. Then the total volume is $V_{TOT}(\mu m^3) = \sum x_i V_i$. So, $x_i = \dfrac{n_i V_i}{V_{TOT}}$ and n_i is amount of bubble of volume V_i and volumetric frequency x_i are given by the software. The number of bubbles for each diameter can thus be deduced: $n_i = \dfrac{x_i \times V_{TOT}}{V_i}$ and the total number of bubbles is $n_{TOT} = \sum n_i$. The bubble percentage for each diameter is then $\% = \dfrac{n_i}{n_{TOT}} \times 100$. The average diameter can also be calculated as follows $\bar{d}(\mu m^3) = \dfrac{\sum(n_i \times D_i)}{n_{TOT}}$. For each measurement, the bubble distribution with diameter is plotted. From each set of data, the software can also calculate the different average diameters (D_i) that are included in the database (in μm).

For that, the micro bubble size representative could be mentioned in two ways. The majority diameter is a micro bubble size with the highest frequency. This size can be obtained directly from the size distribution by Spraytec that is the peak on the size distribution curve. On the other hand, the average diameter ($\bar{d}$) is calculated as mentioned above.

4.2.8 Results and discussion

4.2.8.1 The preliminary experiment

The objective was to obtain accurate results to be a good representation of micro bubble size. To measure the micro bubble, the results from Spraytec sometimes presented more than one size distribution. There was a small amount (low %volume frequency) of the larger size which distorts the size analysis as shown in Figure IV-16 which is an example of micro bubbles size distribution from the Spraytec instrument. Thus, the average size is unable to be representative of all bubbles. Therefore, the very small number of the large size was not taken to calculate the average size in order to assure the calculated size represents of the majority size of the bubbles.
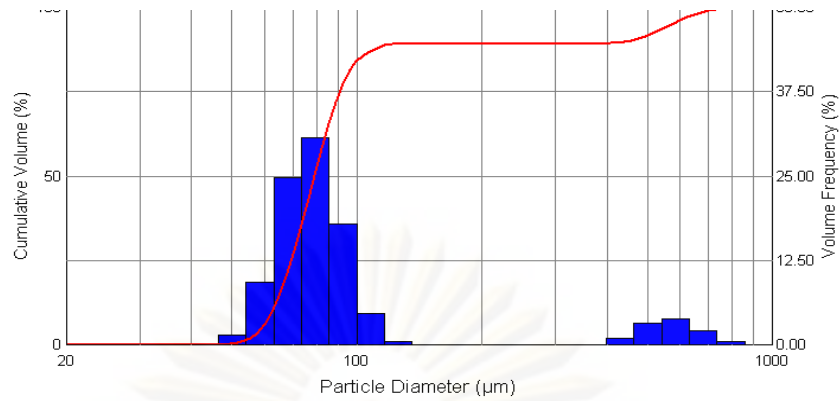
Figure IV-16 An example of the size distribution from Spraytec

The bubble size as a percentage which corresponds to the volume percentage is shown in Figure IV-17. To calculate the average bubble size, it is obvious that a few amounts of large bubbles may show a high volumetric frequency because of their total volume is large compared to the small bubble size. Consequently, when a large bubble sizes appeared, the results calculated with volumetric percentage could be obtained as shown in Figure IV-17. The peak value from volumetric average was 600μm.
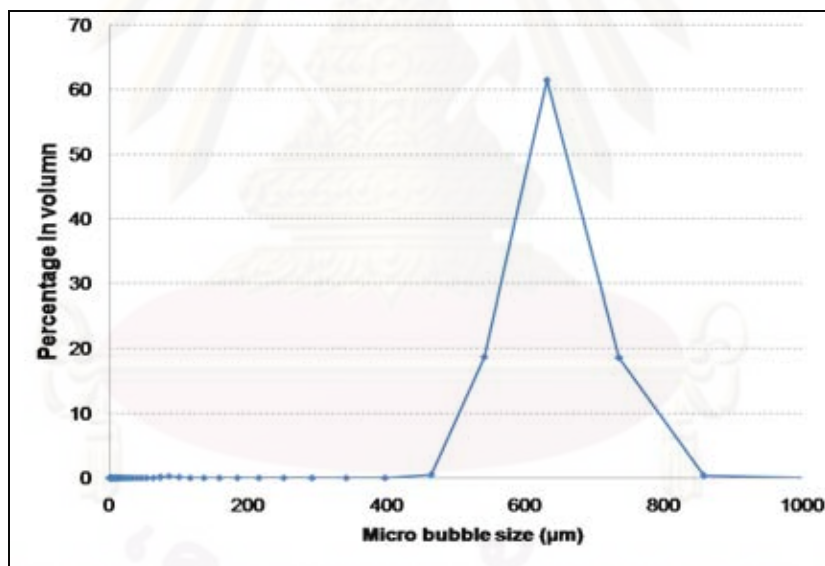
Figure IV-17 Volumetric percentage of bubble size

It was therefore important to convert these volumetric percentages to the quantity in number of bubbles. The amount of bubbles can be calculated from the relation between volumetric percentage and its corresponding diameter of bubble: $n = \dfrac{V_i}{\pi d^3/6}$. From the same data results, the percentage of bubbles in numbers demonstrates as follow.
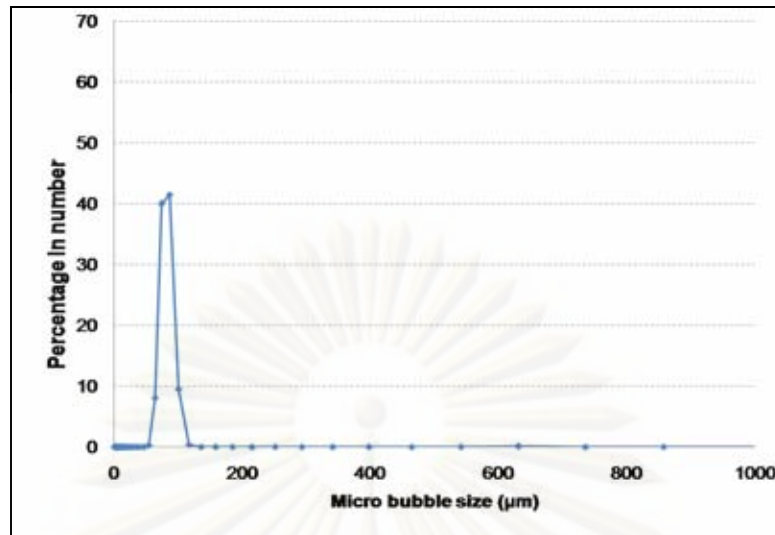
Figure IV-18 Percentage in number of bubble size

After converting the volumetric percentage from the same data, it was able to conclude that the large bubbles were negligible with the low frequency. Thus, the high percentage of micro bubble size was eventually around 90μm.

Analyzing the data to obtain the average bubble diameter provided without considering the effect of a few large bubble sizes, each measurement is performed using the same procedure if there is a more than one size distribution, the results are not taken into account.

The other point concerning the results quality is the reproducibility of the data from Spraytec. The size distribution measurement was performed each time randomly and compared with the size distribution. Besides, each pressure also measured the sizes three times to reassure the accuracy results. The measurement started at 15 minutes in order to assure to have a stable condition. It appears as the Figure IV-19 that the measurement obtains a good reproducibility.
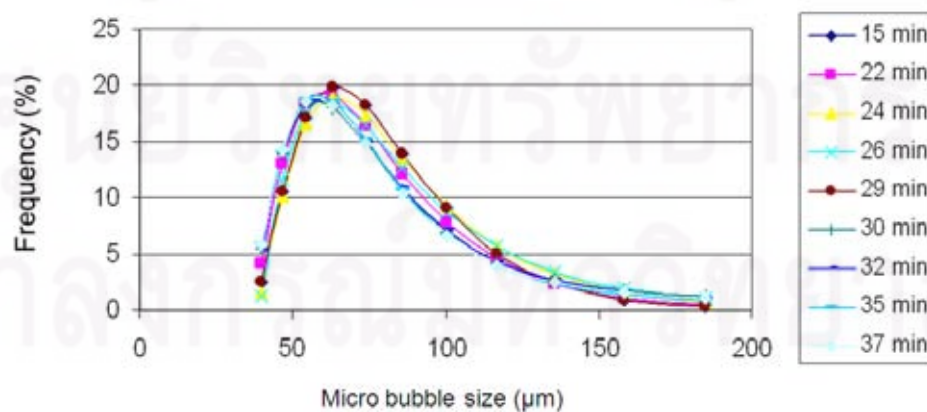
Figure IV-19 Reproducibility measurement experiment
with 3.4bar saturated pressure
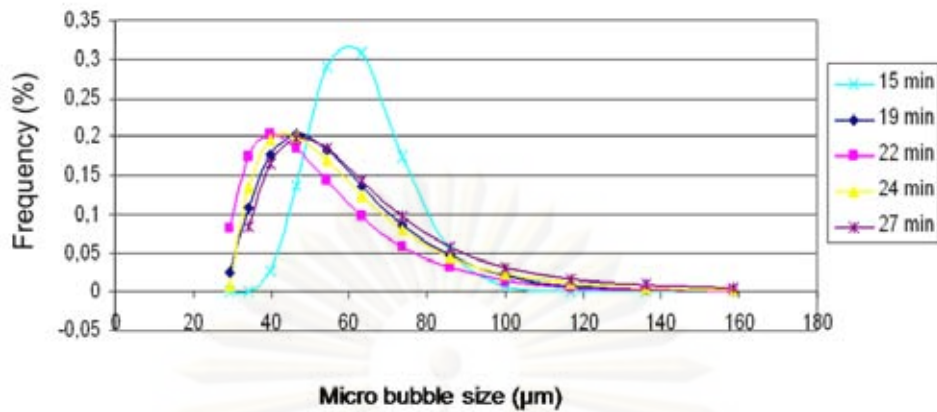
**Figure IV-20 Reproducibility measurement experiment
with 5.4bars saturated pressure**

Figures IV-19 and IV-20 show that the micro bubble size distributions are identical in time differences. The reproducibility of measurement could therefore consider fewer amounts of the following experiments. In case a distribution is very different from the others, such as Figure IV-20 at 15 minutes measurement, it can be discarded as considered a minority.
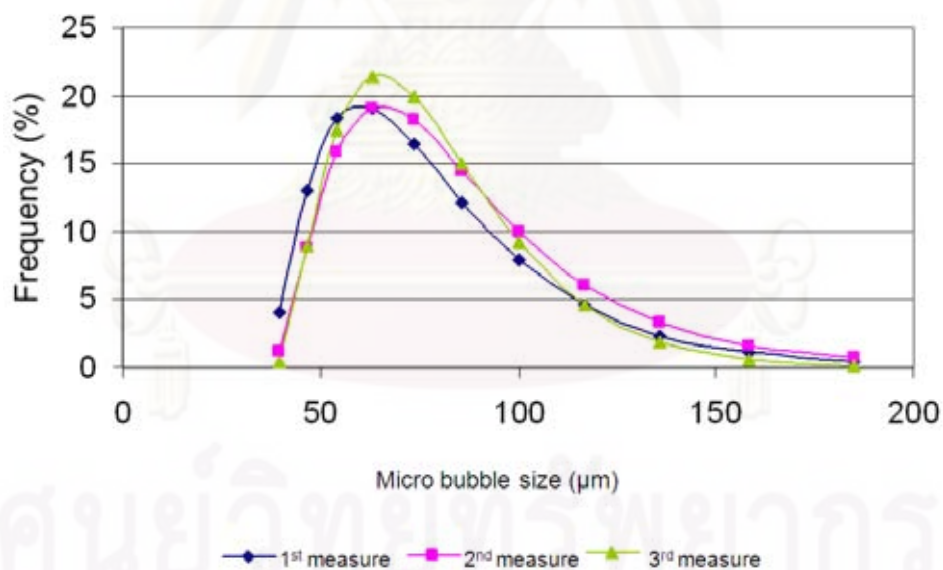
**Figure IV-21 Reproducibility measurement experiment
with 5.4bar saturated pressure**

Figure IV-21 is an example of the experiment with 5.4bar saturated pressure with three testd. The results are clearly reproducible. With all the others, a given pressure overall presented the same trend.

4.2.8.2 The influence of the height on the bubble size

This part was to study the influence of the liquid height on the bubble size. Several measurements at the same height with a constant pressure (3bar) and to compare the size distribution were obtained each time. Each height was done with three measurements with three intervals.
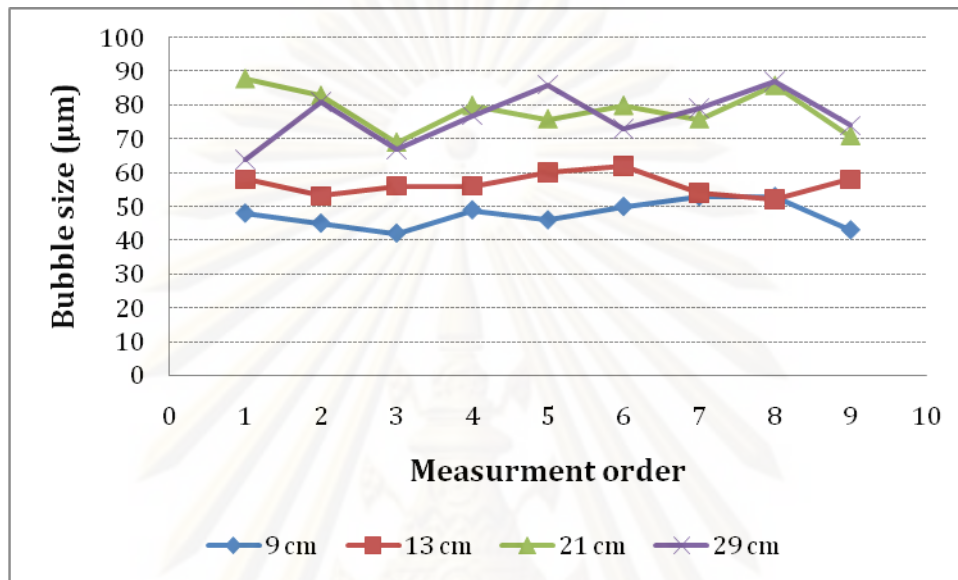
Figure IV-22 Micro bubble size from each height measurement (P=3bars)

Figure IV-22 shows that the reproducibility seems decent. It appears that the bubble size slightly increases with height as shown in the average size value reported in Figure IV-23.
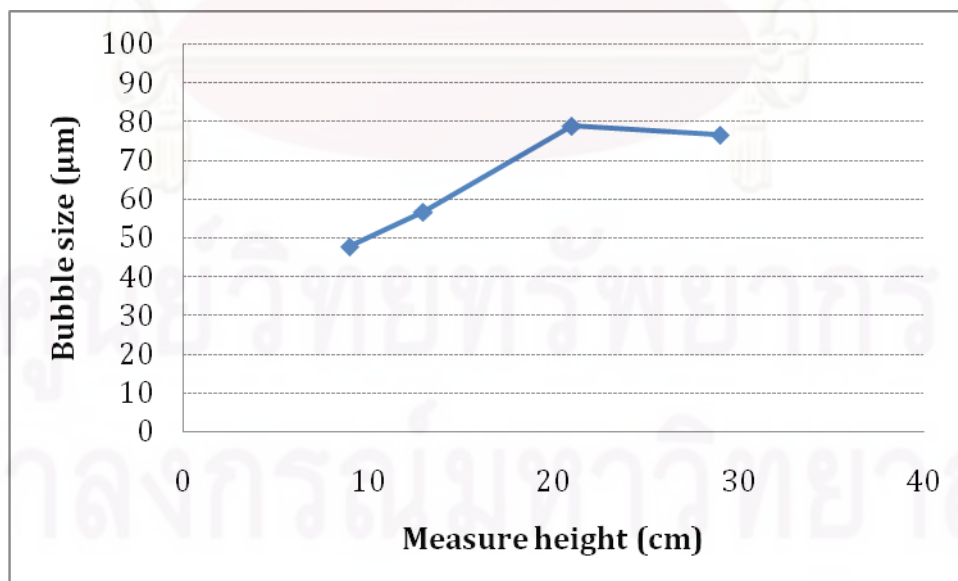
Figure IV-23 Average micro bubbles size from each height measurement

There is a significantly size difference between 9cm and 29cm. The size difference due to the bubble growth which can be explained by the following factors:

- Uptake of the air from the saturated main flow. As the bubble formation is less complete, the main flow remains more supersaturated and the possibility of gas transport into the bubbles will increase (Sander et al., 1994)

- Decrease of the hydrostatic pressure. Additional bubble growth may occur as the bubbles rise in the flotation tank due to a decrease in the hydrostatic pressure (Edzwald, 1995). In the case of this study, this effect on the bubble size is negligible because the difference in measuring height is not enough or significant at the water depth used in practice (Sander et al., 1994 cited in Jedele, 1984)

- Coalescence. In practice it appears that coalescence occurs mostly in the turbulent zone because when the bubbles rise up, they have the possibility to encounter the other bubbles leading to coalescence phenomenon. In this study, the column was filled with water and the air pressurized water was fed continuously. At the top near the water surface, it was observed that the bubbles swirl and it causes an encounter between themselves.

In the new developing water treatment process, combing coagulation, flocculation and flotation in a hydrocyclone reactor, the flocs cover around the micro bubblees and these flocs-bubbles are separated in the upper part of hydrocyclone under the centrifugal force. It is nescessary to get small bubble size in order to improve the process because small bubbles are included into the floc more easily and the possibility of collision and adhesion between a bubble and a particle increases more than proportionally to the number of bubbles and is independent of the bubble size (Flint and Howarth, 1971). The results from this study uses the properties to developing that process. Consequently, the bottom part of the reactor is desirable to work with small bubble size.

However, the four level heights are slightly different between themselves. It would be interesting to perform additional steps or perfect by beating the best possible parameters that influence the effectiveness of the measurement by increasing the column height. Still, the bubble size range from this study is between 48 – 79μm. Compare to many researches, DAF is a well-known solid-liquid or liquid-liquid separation process in water and wastewater treament where most bubbles are lower than 100μm (Féris and Rubio, 1999; Englert et al., 2009; Karagüzel, 2010). Edzwald (1995) mensioned that the size range of bubble for DAF systems is 10 to 100μm and a reasonable estimate of the average bubble diameter is 40μm. It shows that the results from this study is in the DAF regime.

4.2.8.3 The influence of the pressure on micro bubble diameter

Since the pressure can be adjusted, it is questioned which pressure could present the optimum conditions for producing small micro bubble sizes. Consequently, this part worked on the influence of pressure on bubble diameter and the size distribution. The

pressure was adjusted between 3.4, 4.5, 5.4 and 6.2bar. It corresponds to the minimum system pressure and for security reasons the maximum pressure. The experiments were conducted to have the reproducible conditions for a given pressure with a constant measure height 30cm from the bottom. The results are shown in Figure IV-24.
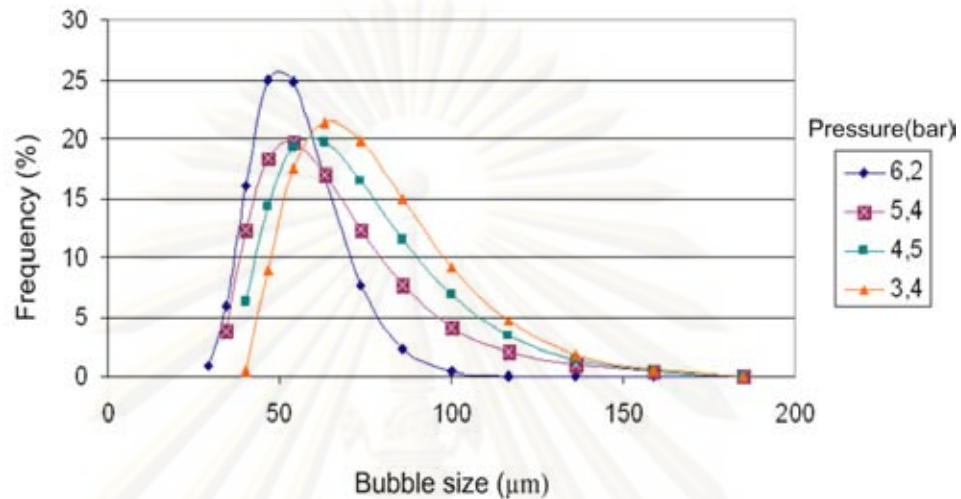
Figure IV-24 Micro bubble size distributions from difference pressures (H=30cm)

From Figure IV-24 considers the peak diameter of bubbles, which varies depending on the pressure. There is a real tendency of bubbles to concentrate around a small size as the pressure increases. The largest peaks (63μm – 73μm) are achieved from pressure 4.5 and 3.4bar respectively. At 6.2bar, 26% of the bubbles range is 46-54μm.
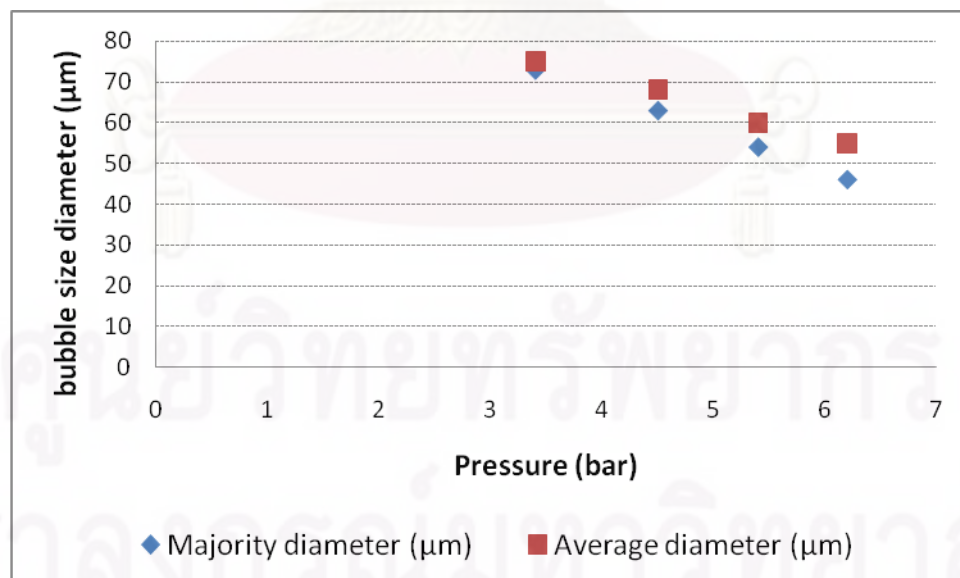
Figure IV-25 Majority and average bubble size as a function of pressure

The quantity of air which can be dissolved in water is based on Henry's law: $C_s = k_H \times P$ where, C_s is saturation concentration of the gas in water (g/m³), k_H is

Henry's coefficient (g/m³·Pa) and P is partial gas pressure (Pa). It shows that the quantity of air is high when the pressure increases. Although, the relation between the higher pressure and the small bubble size is not fully understood. However, Sander et al.(1994) mentioned that with a known quantity of air the bubbles should be as small as possible in order to increase the bubble concentration. The bubble concentration is inversely proportional to the bubble size, so that the relation found for the bubble size also applies to the bubble concentration. Increase in the pressure leads to a higher bubble concentration. Many researches agree that the bubble size decreases as the saturated pressure is increased (Sander et al., 1994; Hudson et al., 2009). However, some researches mension that above 5bar, increasing the saturated pressure has a small effect on bubble size (Heinanen et al., 1992; De Rijk et al., 1994). By the way, to ensure small bubbles, pressure differences (saturated guage pressures) of 4 to 6bar are recommended (Edzwald, 1995).

4.2.9 Conclusions

Reliable and reproducible assay of the bubble size distribution was achieved by laser diffraction. It is a quick technique for the characterization of bubble size. With this study it is also noted that the importance of the preliminary analysis of results to obtain consistent and accurate date. It was verified that the distribution of bubble size obtained for different measures, large bubbles did not influence because their percentage is negligible compared to small bubbles that were the main part of bubble size distribution.

In agreement with results obtained at different heights, the size distribution of bubbles increases progressively as the distance between the output of bubbles and the light beam is extended. The efficiency in the flotation process will not be the same according to the depth at which the bubbles are injected in the case of large basins. Moreover, the bubbles do not collide with the particles with the same efficiency of their height. This result is crucial for the future design of hybrid process. Thus, the air pressurized water injection will be placed in the lower part of the hydrocyclone in order to provide the micro bubbles where coagulation phenomenon will occur.

The pressure influence to the bubbles size, increasing the saturated pressure promotes a behavior: the shift of bubble size distribution to a smaller diameter. Produced bubbles size from this study is between 48 – 79μm. It is believed that this study will be the basic result for research in DAF and the water treatment processes, either theoretically or practically. In order to get very small bubbles in our process, the saturated pressure level will be considered 4.5bar.

CHAPTER V

HYBRID PROCESS EXPERIMENTAL STUDIES

5.1 Part I: The hybrid process on bentonite suspension

5.1.1 Abstract

A new water treatment process which combines coagulation, flocculation and flotation process within a hydrocyclone is developed as a Hybrid process. The experiment is done with a 100mm diameter and 1000mm heigh hydrocyclone cylindrical reactor to study the influence of the parameters to the process such as; inlet flow rate, raw water suspension, coagulant, flocculant concentration and pilot configurations.

The results show a good performance in swirling flow by vortex flow without the micro bubble coalescence (saturated pressure 3.5 – 4.0bar). Since this study is being developed to be applied for the future water treatment work, the raw water has been decreased in concentration from 0.50 to 0.10g/L of bentonite suspension to examine the ability of the process. Aluminum sulfate coagulant was also utilized. However, cationic polymer coagulant FO107 presented a high percent turbidity decreased (>70%) and suspended solid removal (>60%). This work also studied the difference between the coagulation inside the hydrocyclone reactor (by injecting coagulant inside hydrocyclone directly without flocculant) and pre-coagulation by static mixer before getting in the hydrocyclone. It is believed that the results from this study will be the basis of knowledge to develop this hybrid process for a natural water treatment process.

5.1.2 Introduction

A conventional water treatment process consists of coagulation, flocculation and particle separation. There are many techniques in a separation process such as, sedimentation, flotation and filtration (Monod, 1991). Each process requires space and volume for its unit structure. It is interesting to develop a water treatment process which requires a small footprint.

The hydrocyclone is equipment for separation. It is widely used in many fields such as mineral, pulp and paper industries. It is primarily designed to separate two phases with different densities. Simplicity, low cost and ease of operation contribute to its popularity. Recently, many studies have applied the hydrocyclone for water treatment process to remove particles. Menezes et al. (1996) combined coagulation and flocculation process to separate the solid particle in a dynamic separator. Rosa and Rubio (2004) developed flocculators with a flotation technique to produce aerated floc and separate by a centrifuge cell to remove very fine emulsions.

This study aims to combine three water treatment processes compacted in one reactor; coagulation, flocculation and separation by a hydrocyclone mechanism, using a vortex flow to separate colloidal particle which is a bentonite suspension. Raw water is

injected tangentially inside hydrocyclone causing the centrifugal force and gradient velocity. Very fine bentonite particles are coagulated by coagulant and under this present gradient velocity to be micro floc. Spontaneously, micro bubbles produced from the dissolved air flotation technique is injected at the bottom of reactor, and then trapped by the micro floc to become *aerated floc*. The volumetric mass of these flocs are very low because they contain the micro bubbles inside. There are separated by the vortex flow provided from the inlet tangentially raw flow rate.

Various researchers have studied this process. Chaiyaporn Puprasert et al. (2004) studied the feasibility of the process with a 5-cm diameter and 50cm height hydrocyclone. This work achieved in producing the aerated floc but it was not possible to separate in the continuous operation. Vorasiri Siangsanun (2006) studied the parameters effecting the process and also hydrocyclone geometries between cylindrical and conical hydrocyclones. The cylindrical one could be used for the separation process in the batch operation. In a conical hydrocyclone, a vortex flow occurred along the cyclone axis but there was micro bubble coalescence. It decreased the possibility of aerated floc production because the floc was not able to cover the large bubble. Moreover, the important parameters that affect hybrid process were the air fraction and the coagulant concentration. Thus, Pradipat Bumrungsri et al. (2008) studied the hydrodynamic characteristic developed inside three hydrocyclone geometries by a new simple method, called the oil droplet method. The results showed that the axial velocity inside hydrocyclone flowed downward along the hydrocyclone axis. It explained the micro bubble coalescence phenomenon occurring at the bottom part of cyclone. Besides, this study found the optimum operating conditions for the hybrid process. Cylindrical hydrocyclone geometry was recommended. All researches show the potential and approach a novel separation concept and devices. This study constitutes an advance within this line of research and development. The hydrocyclone reactor is modified with a cylindrical larger diameter for a better separation and be able to treat higher uptake. The air pressurized water inlet position is installed vertically close to the wall in order to avoid the micro bubble coalescence and to be able to attach with the coagulated particle. Furthermore, in study is aimed to develop the hybrid process to operate in continue. Previous hydrodynamics results are taken into account to define the best operating conditions. The parameters such as; coagulant, flocculant and air fraction will be studied to find out the optimum conditions and validate the process for natural water treatment.

5.1.3 Materials

There are three main parts in this pilot, the preparation tanks for raw water and coagulant solution, the hydrocyclone reactor and micro bubble generation system. The pilot plant installation is shown in Figure V-1. Each part will be explained clearly as follows.
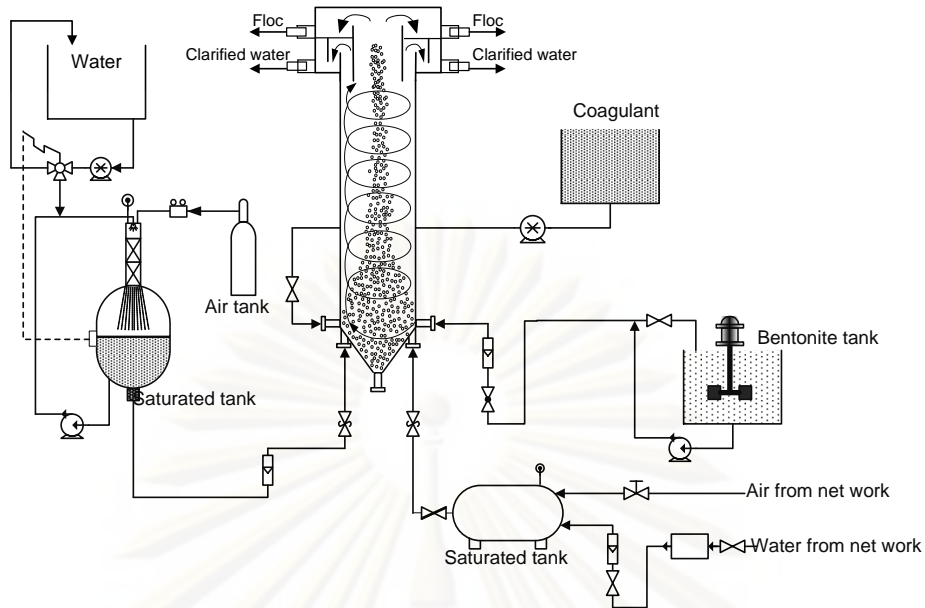
Figure V-1   The pilot schematic

5.1.3.1   Synthetic water

To study the effect of this parameter, it was decided to use synthetic raw water in order to control its characteristics. In this study, bentonite (BENTONIL CV15T) in powder from SUD-CHIMIE (France) with an average size of 4-5µm and a specific surface of $3.5 \times 10^6 m^2/m^3$ was used to mix with tap water to represent the colloid suspended in water. It was mixed with an agitator in a 500L tank for 24 hours to assure adequate particle dispersion. The maximum flow rate was 1000L/hr by the pump. This synthetic raw water was analyzed by suspended solid analysis and turbidity meter.

5.1.3.2   Coagulation and flocculation

An involved process in this study was coagulation with a sweep coagulation mechanism. As mentioned above this hybrid process that is being studied for the different water treatment possibilities. Consequently, the first part of this study used a cationic polymer commercial name FO107 in order to have suitable conditions for the process. The dosage and the type had been considered by the Jar test method. The experiment is done in a flocculator (FLOCULATEUR 11196, BIOBLOCK SCIENTIFIC). The second part involved the hydrocyclone with coagulation and flocculation. The coagulant in this part was Aluminum sulfate manufactured by Prolabo (France) in crystal form with a purity of >99.5%. The flocculant in the second part was cationic polymer FO107. The both solution were prepared and stored in a tank with peristaltic pump to feed inside the hydrocyclone.

5.1.3.3   Air pressurized water system

From Figure V-1, there are two pressurized water systems. Both of them used the Dissolved Air Flotation (DAF) technique. The first one provided air from the fluid-air

tank. Tap water was pumped inside the saturated tank passing through the media which gave the encounter between air and water. Inside the saturated tank, the water level was controlled by an electrical valve. If the water level is too low, the water pump will feed water inside the tank. Pressure in the saturated tank was controlled to 3-4bar while the maximum pressure of this system is 6.5bar. The retention time before being used in the experiment was around 15minutes to assure the air dissolves into the water. To inject into the hydrocyclone, pressurized water passed through the relieve valve, the saturated air precipitated as micro bubbles because the pressure decreased to atmospheric pressure.

A second air pressurized water system was added because of the flow and pressure limit from the first system. The air and tap water were generated inside the second saturated tank having the same retention time inside to dissolve the air. To inject into hydrocyclone, the air pressurized water passes the valves and then the saturated air becomes micro bubbles as well as the previous system. This system used a butterfly valve to open the saturated tank and a gate valve at the entrance to hydrocyclone. The flow rate was not measure directly by this second system.

With both methods, micro bubbles were expected to encounter the floc inside the hydrocyclone and be separated by the vortex flow.

5.1.3.4 The hydrocyclone reactor

The hydrocyclone mechanism separates the particles by a physical process. The flow enters tangentially into the hydrocyclone which induces a swirling motion which causes an apparent centrifugal force on the fluid and particles. In this study, with the DAF technique, the floc contains micro bubbles inside its structure. These aerated flocs exert a smaller force than the fluid due to their lesser density and migrate to the axis of cyclone. The exit of the aerated-floc is on the top part of reactor. See Figure V-2.
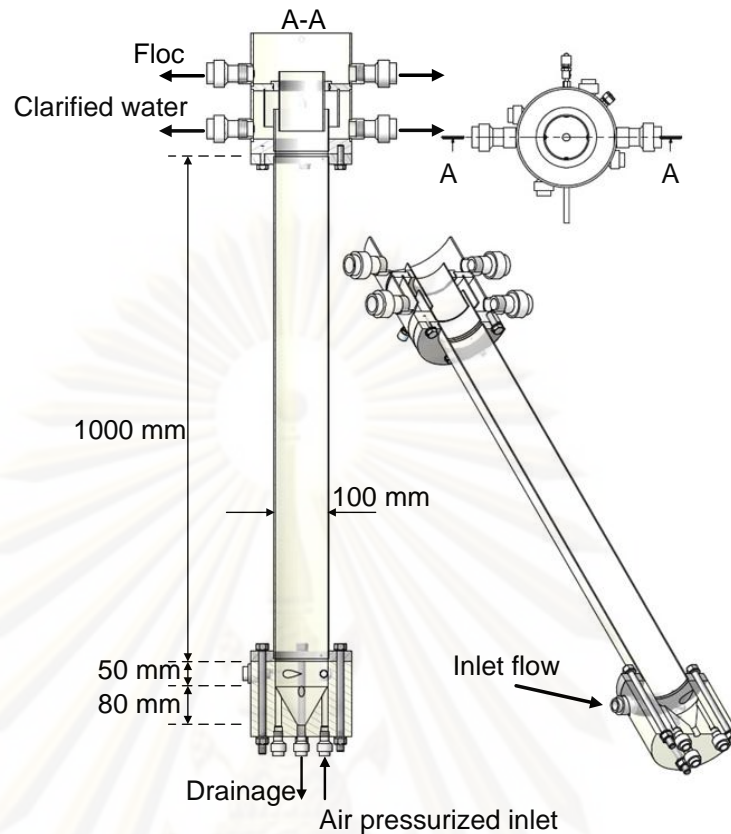
Figure V-2   Hydrocyclone reactor dimensions

Due to the migration of aerated-flocs to the axis of the reactor, the fluid on the wall zone is relatively devoid of flocs. Hence, clear fluid is extracted to the wall and exits to the effluent tube.

The hydrocyclone is a cylindrical 1000mm high and 100mm in diameter (see Figure V-2).   It was built from transparent acrylic resin so the phenomenon inside the reactor can be seen.   The inlet zone is on the bottom part (the conical part).   There are four tangential inlets of 10mm diameter for raw water and coagulant injection.   On the other hand, there are four vertical inlets which were designed for the air pressurized water injection as shown in Figure V-2. The central vertical tube is for fluid draining in case of cleaning inside. The sample collection is on the top part. The centre zone water effluent or floc sludge swirl and drain out at the two upper horizontal tubes while the clarified water drains out at the two horizontal tubes which are underneath the floc effluent.

5.1.4   Experimental analysis

5.1.4.1   Jar test

The preliminary coagulant and flocculant concentration influence had been done to determined the maximum turbidity decreased by a Jar test method experiment. The jar test trials were conducted to determine the conditions of coagulation most appropriate for

the application. The water treatment jar test can separate the supernatant of flocs formed during coagulation tests are conducted using a flocculator (Floculateur 111196) with 6 beakers of 1L equipped with stirring blades with a flat dimension of 2×7.5cm. The rotation speed is adjustable. The coagulant is injected into each beaker. Immediately, a rapid agitation at 200rpm is carried out for 1minute to fully connect the coagulant and the solution. Then, a slow stirring is performed for 5minutes, the rate being maintained at 60rpm. The blades are then gently removed from the water to allow the floc to settle for 10 minutes. After settling, the supernatants were collected and the turbidity and the suspended solids are analyzed.

5.1.4.2 Water Sampling

Samples from the experiment will be collected from the effluent tubes as shown in Figure V-3. The process operates in continuous operation during sampling with 500L of bentonite suspension in the storage tank. The outlet flow rates are measured by timing the amount of water and calculated by Equation V-1.

$$Outlet\ flow\ rate = \frac{water\ weight(kg)}{Time(s)} \times \frac{1}{\rho_{water}(kg/m^3)} \qquad \text{Equation V-1}$$
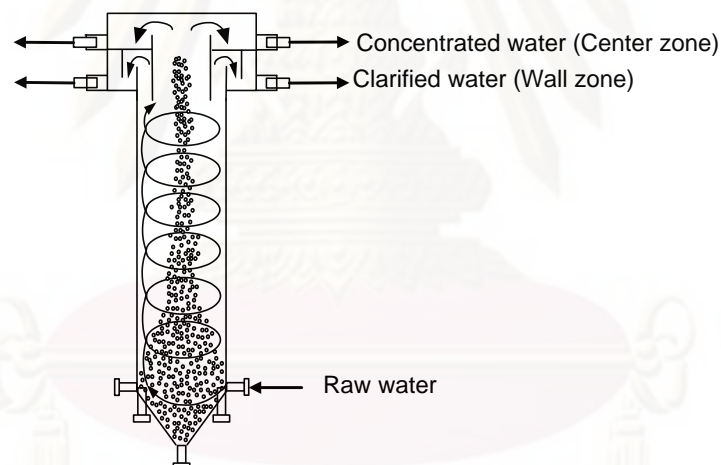
Figure V-3   Water zone for sampling for result analyzing

5.1.4.3 Turbidity and Suspended solid (SS) measurement

The clarified water at the wall zone and concentrated water at the centre zone are determined by turbidity measurement and suspended solids. In the sense of water treatment, the coagulation process will be indentified with the % of turbidity decreased and % of suspended solid (SS) removal compare to the raw water. On the other hand, in the sense of separation phenomenon, treated water will be analyzed with % separation efficiency that is compared between the centre zone (concentrated water) to the wall zone water (clarified water).

Turbidity determination will be measured by a turbidity meter (HACH 2100N IS TURBIDIMETER). Suspended solid is analyzed with a drying method at 103º - 105ºC with a dry oven and balancing instrument (SARTORIUS, MA145).

The removal percentages are calculated by the Equation V-2 and V-3. The separation efficiency is calculated by the Equation V-5 and V-6. The matter flux recovery fraction to illustrate the hydrocyclone separation ability to eliminate the floc through the centre zone is calculated by the Equation V-7. Vortex performance and floc floating are observed by a digital video camera (CANON, POWERSHOT S3 IS).

<u>The Equation for water treatment analysis</u>

$$\%Turbidity\,decreased = \frac{(T_{Raw\,water} - T_{Wall\,zone})}{T_{Raw\,water}} \times 100\% \qquad \text{Equation V-2}$$

$$\%Suspended\,solid(SS)\,removal = \frac{(SS_{Raw\,water} - SS_{Wall\,zone})}{SS_{Raw\,water}} \times 100\% \qquad \text{Equation V-3}$$

$$\%Flow\,Recover = \frac{Q_{Wall\,zone}}{Q_{Raw\,water}} \times 100 \qquad \text{Equation V-4}$$

<u>The Equation for hydrocyclone separation efficiency</u>

$$\%Separation\,Efficiency\,in\,Turbidity = \frac{(T_{Center\,zone} - T_{Wall\,zone})}{T_{Center\,zone}} \times 100\% \qquad \text{Equation V-5}$$

$$\%Separation\,Efficiency\,in\,Suspended\,solid = \frac{(SS_{Center\,zone} - SS_{Wall\,zone})}{SS_{Center\,zone}} \times 100\%$$

$$\text{Equation V-6}$$

$$\%Matter\,Flux\,Recovery = \frac{(SS_{Center\,zone} \times Q_{Center\,zone})}{(SS_{Raw\,water} \times Q_{Raw\,water})} \times 100 \qquad \text{Equation V-7}$$

5.1.4.4 Air fraction

Since there was no flow meter to measure the air pressurized water flow rate, the air fraction will be calculated from the total outlet flow minus the raw water inlet flow rate as Equation V-8. Thus, the amount of air dissolved in water and the corresponding air fraction will be calculated by Henry"s law. The calculation is clearly shown in Appendix B. To compare the hybrid process in the sense of flotation process with the conventional DAF, it is noted that the DAF technique has the criteria of air flow of 15-50% of air to water inlet flow rate or 0.1500-0.5000 of air fraction (Monod, 1991). It is noted that the raw water inlet flow is the bentonite suspension flow rate.

$$Air\ pressurized\ water\ flow\ rate = Total\ outlet\ flow - Raw\ water\ inlet\ flow$$

<div align="right">Equation V-8</div>

The floc floating is identified with a batch operation (after stopping all the inlet flow rates). During the operation, the aerated floc is not able to be observed. It is necessary to stop the operation and then observe the floc floating up to the top of reactor which implies the aerated floc is being produced.

5.1.5 The experimental Setup

This study worked on the parameters that affect the hybrid process and compared the results to find the optimum operating conditions in order to develop this hybrid process. Since there are three main processes that are encountered in this study. Thus, there are many varied parameters to study in order to determine their effects on the hybrid process. The studies had been provided as followed.

Table V-1   Experimental plan of hybrid process on Bentonite suspension

Subject	Varied parameter
1. Characterization of the vortex flow and micro bubbles at different heights of the hybrid reactor	10, 30, 50 and 80cm level height
2. Influence of the bentonite suspension	0.25 and 0.50g/L
3. and inlet flow rate	800, 900 and 1000L/hr
4. Influence of the coagulant type	FO107 (cationic polymer) and Aluminum sulfate
5. The coagulation inside hydrocyclone	Coagulation inside hydrocyclone (without static mixer)
6. The pre-coagulation before getting in the hydrocyclone	Coagulation at static mixer

5.1.6 Characterization of the vortex flow and micro bubbles at different heights of the hybrid reactor

5.1.6.1 The experimental method

To observe the vortex performance in the hybrid process, the inlet flow rate with only tap water was maintained at 1000L/h and entered tangentially through a single, circular inlet aperture. Air pressurized water from two systems was fed vertically into the

reactor. The main objective of this experiment is to identify the hybrid process configurations and to avoid the micro bubble coalescence phenomenon in the reactor. The operating conditions used in this part are shown in Table V-2.

Table V-2 vortex performance experimental condition

Varied parameter	Operating condition
Observation level height of the hydrocyclone	10, 30, 50 and 80cm
Control parameter	**Operating condition**
- Saturated pressure	3.5 – 4.0bar
- Inlet tap water flow rate	1000L/hr
Method of analysis	Video recorder

The expected phenomenon from the vortex and micro bubble behavior is that the micro bubbles did not coalesce in the bottom part in order to maintain their micro size and to be covered by micro floc from the coagulation process easily. Afterwards, the micro bubble is separated to the reactor axis by hydrocyclone mechanism as it is less dense than water. The objective of these experiments will be to identify the operating conditions to avoid the collapsing and coalescence phenomenon inside hydrocyclone.
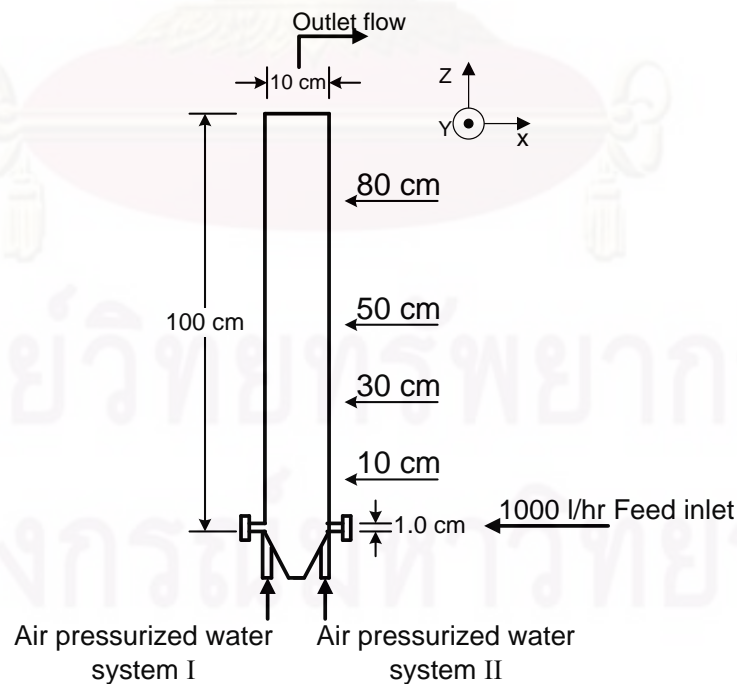
Figure V-4   Observation level heights

The operation was run in continuous operation. The results were observed and recorded by digital camera. The phenomenon was observed at four different levels as shown in Figure V-4.

5.1.6.2 Results and discussions

The different level heights inside hybrid reactor were supposed to present different phenomenon. The coalescence of micro air bubbles from the air pressurized water inlet zone at the bottom part was not desirable. Bubble coalescence is an important parameter to control the aerated floc forming. The large bubble size has less free surface area to attach and be covered by the floc. The observation results are shown in Figure V-5.
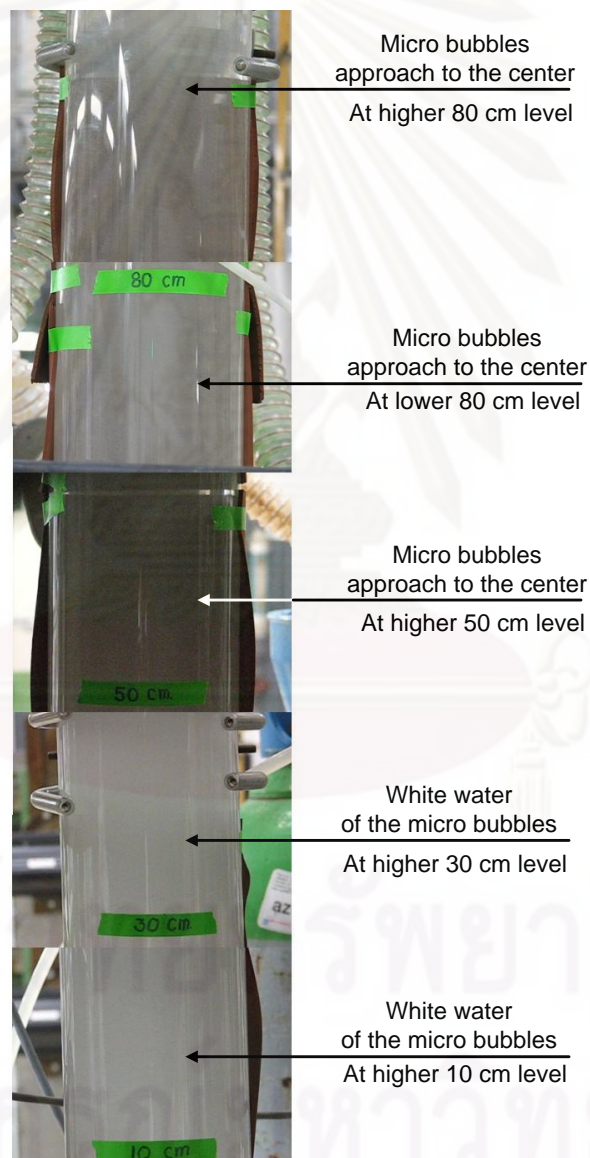
Figure V-5   Vortex observation results

At the 10cm height level from the bottom of hydrocyclone the white water was observed because of the micro bubbles entering into the reactor from the injector close to

the wall without coalescence. Above the 50cm level, it can be observed that the micro bubbles started to approach the cyclone axis. At the 80cm level, the micro bubbles are clearly grouped at the axis. The micro bubble performance results in this part of study appear as the expected phenomenon as shown in Figure V-6. The micro bubbles are created by the DAF technique and passed through the relieve valves. There are two air pressurized water injectors which are installed close to the wall.   The centrifugal force from the tangential inlet water separates the micro bubbles to the cyclone axis. The vortex flow spins along the cyclone axis until the top and drives the micro bubbles at the centre.
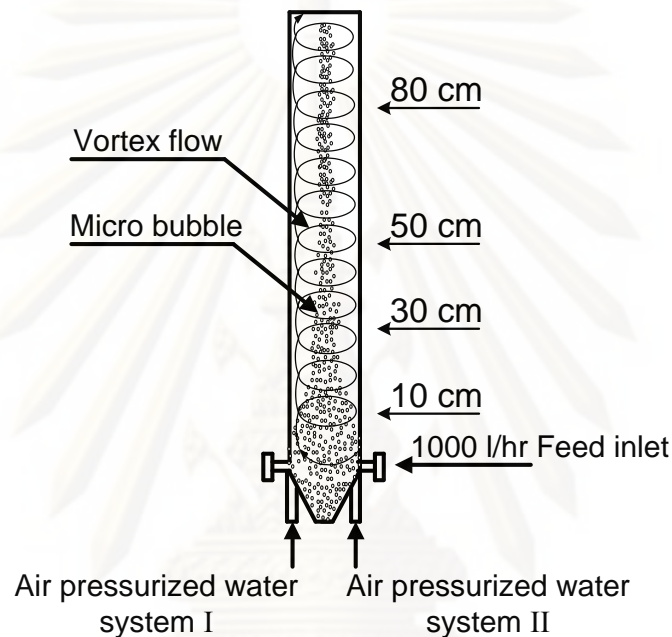
Figure V-6   expected phenomenon of micro bubble and vortex flow

The centrifugal force from the tangential feed inlet created separation between the water and the micro bubbles which can be explained with Equation V-8.

$$\vec{F}_{centifuge} = (\rho_p - \rho_m)\frac{v_y^2}{R} \cdot \frac{\pi d_p^2}{6}$$
    Equation V-8

Where, ρ_p is the density of the solid particle and ρ_m is density of the dispersion phase. In the hybrid process, the dispersion phase is water while the particle is the micro bubble which has a lower density than water. Thus, the term $(\rho_p - \rho_m)$ is negative. Instead of being separated and moved to the cyclone wall, the micro bubbles are separated and moved to the cyclone's axis.

The results from the previous chapter; the numerical simulation method by FLUENT® had done the calculation on the magnitude of the velocity at different heights of the cyclone which is shown in Figure V-7. Reynolds Stress Model was used to simulate the velocity profile from 1000L/hr inlet flow rate which created 1.58m/s inlet velocity.
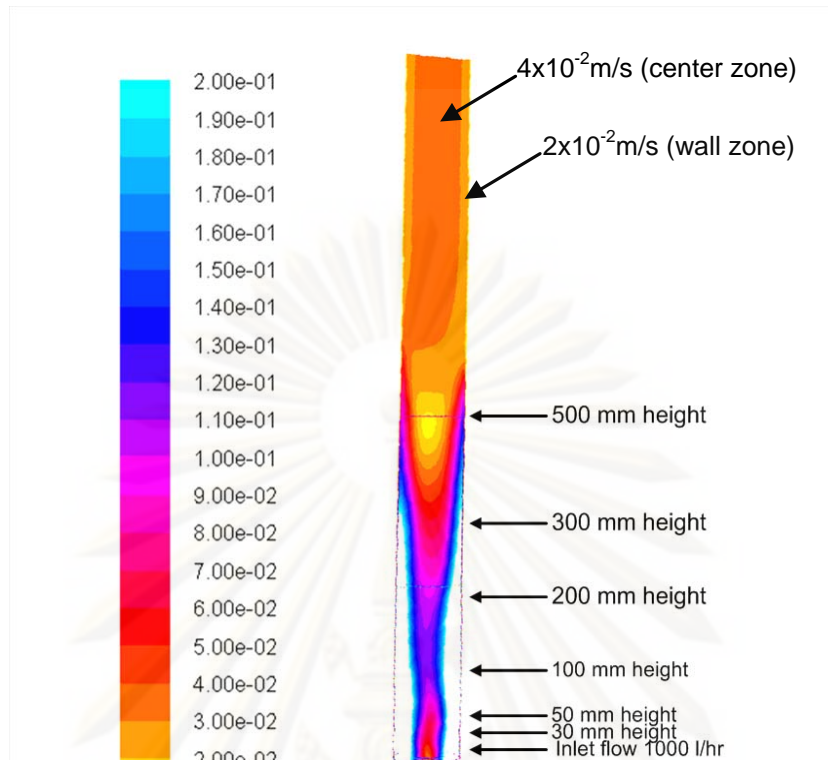
Figure V-7 the magnitude velocities in hydrocyclone from numerical simulation (1000L/hr inlet flow rate, 1.58m/s inlet velocity)

It can be seen in Figure V-7 that at the lower part (0 – 500mm height) the velocity is high, especially near the cyclone wall. This part of the cyclone has a high velocity gradient which means high turbulence. Thus, the micro bubbles enter close to the cyclone wall and are mixed with the optimum turbulent condition which does not cause micro bubble coalescence. The micro bubble size remains in the range of 48 – 79μm from the results of laser diffraction measurement in Chapter IV. The upper part (500mm to the top) remains the velocity value as shown in Figure V-7. The wall zone velocity was about 2×10^{-2}m/s while at the center zone remained at 4×10^{-2}m/s to the top of cyclone. Even thought the velocity values are low it is suitable for the separation phenomenon between micro bubbles and water at the top of the cyclone.

On the other points, considering the velocity gradient from the numerical simulation by FLUENT with Reynolds Stress Model as shown in Figure V-8, it can be seen that at the 30mm level from the injection level the tangential velocity gradient is approximately in the $100s^{-1}$ range and the maximum is close to the wall reaching $700s^{-1}$. The theoretical range of velocity gradient for the flocculation process is $30\text{-}100s^{-1}$ (Monod, 1991). It shows that velocity gradient inside this hydrocyclone is suitable for both the coagulation process (close to the wall) and the flocculation process (along the hydrocyclone height).
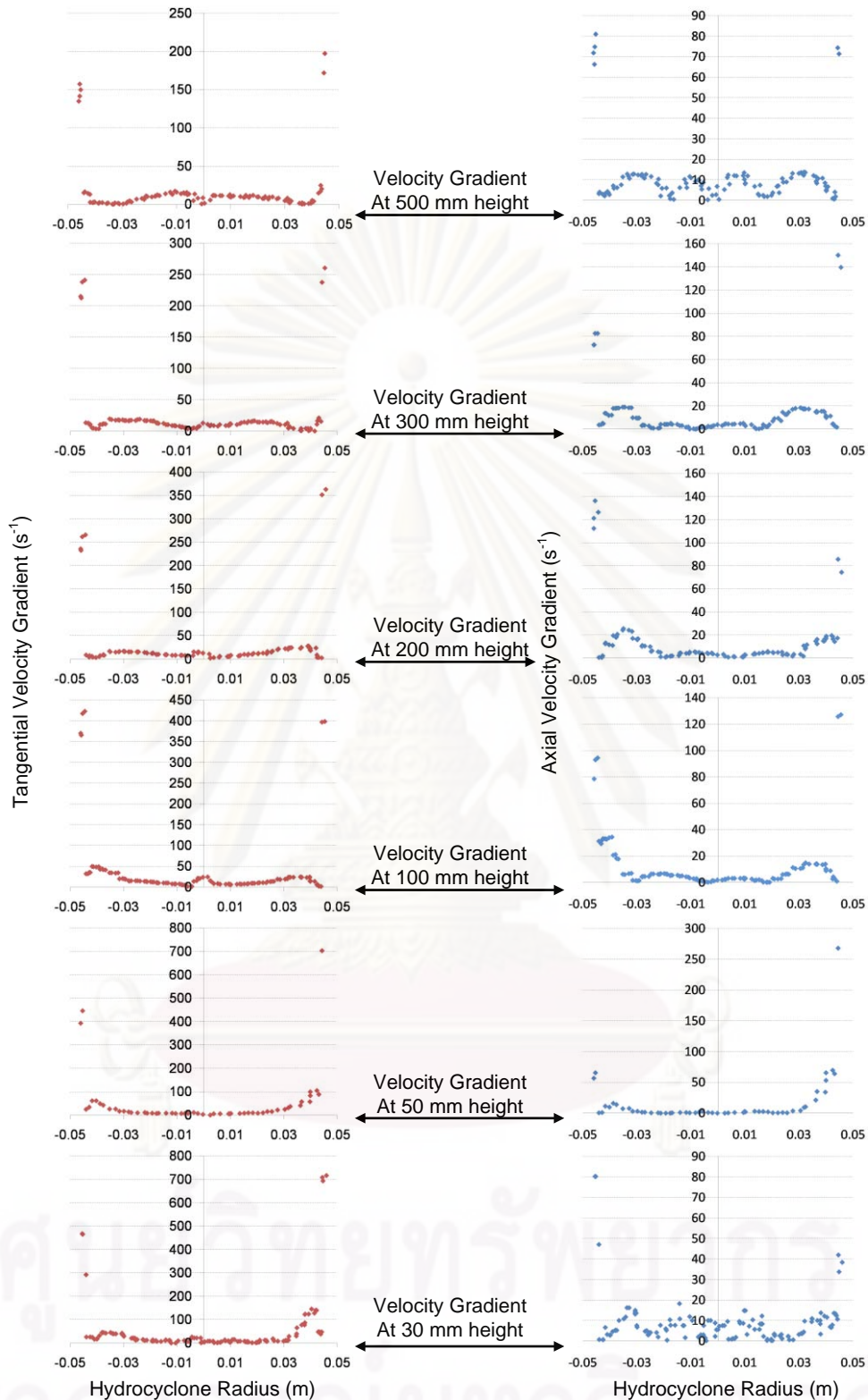
**Figure V-8   Tangential and axial velocity gradients from
Reynolds Stress Model numerical simulation at different level height
(1000L/hr inlet flow rate, 1.572m/s inlet velocity)**

The hydrocyclone in this hybrid process is different from the conventional one. The inlet apertures are all in the bottom part while the exit is on the top part. Thus, there

is no Locus of Zero Vertical Velocity line (LZVV) which distinguishes the external vortex (downward flow) and the internal vortex (upward flow) to explain the separation between wall zone and centre zone.
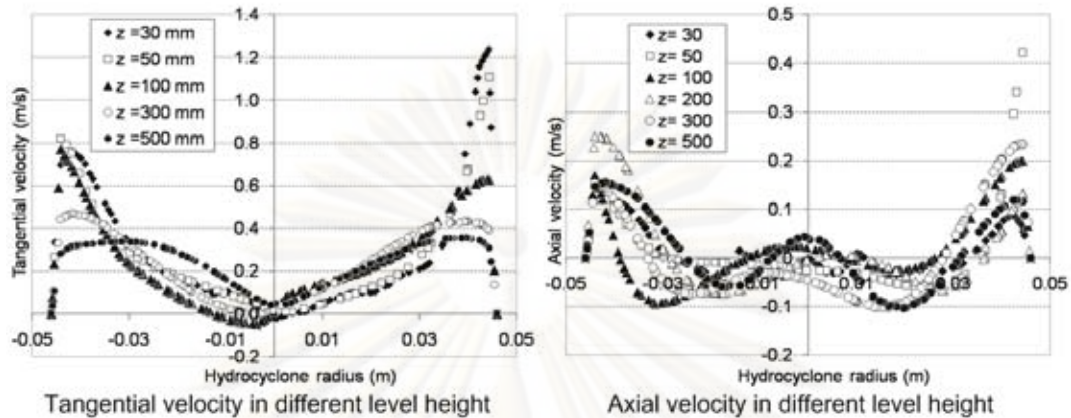
Figure V-9   tangential and axial velocities inside hydrocyclone at different height levels

However, considering the velocity profile inside hydrocyclone at different heights from Figure V-9, it can be seen with the tangential velocity profile that the velocities slightly increase apart from the centre axis until 0.03m radius and sharply increase to the hydrocyclone close to the wall.   Additionally, with the axial velocity profile, the velocities at the centre are nearly zero and are negative apart from the centre that implies the downward direction of the water movement. Afterwards, the axial velocity increases apart from 0.03m radius that indicates an upward motion of the water inside the hydrocyclone.   Therefore, the difference of the water movement direction from the velocity profile is able to explain the separation zone between the water and micro bubble.   The heavier phase as water is driven to the wall zone (radius > 0.03m approximately) by a higher velocity gradient and also velocity.   On the other hand the lighter phase is as the micro bubbles are driven to the centre zone (radius < 0.03m approximately).   It can be seen that the upper part shows a very low velocity and velocity gradient but it could create the separation phenomenon between the water and micro bubbles.

This phenomenon met the separation mechanism by hydrocyclone.   The lighter phase is separated in the hydrocyclone core. The results were satisfactory in the sense of separation by a hybrid process.   It was supposed to separate the aerated-floc in the cyclone axis without bubble coalescence.   Since 1000L/hr presented the separation phenomenon between water and micro bubble. The next part of the study will remain with this flow rate to work on the other parameters.

5.1.7 The influence of the bentonite suspension concentration and inlet flow rate on the hybrid process performance observed

5.1.7.1 Experimental method

The presence of the higher turbidity in the water affects the coagulation process due to the formation of the larger flocs (Ho and Newcombe, 2005). The effect of the turbidity on the separation phenomenon in the hybrid process has been demonstrated using synthetic water containing the 0.25 and 0.50mg/L bentonite in tap water. The operating conditions are shown in the Table V-3.

Table V-3 Experimental conditions used to study the influence of bentonite suspension concentration under experimental conditions

Varied parameter	Operating condition
Bentonite suspension	0.10, 0.25 and 0.50g/L
Inlet flow rate	800, 900 and 1000L/hr
Control parameter	**Operating condition**
- Coagulant type	Cationic polymer FO107
- Coagulant concentration	0.50mg/L
Method of analysis	
- Vortex performance	Video recorder
- Separation	Observation
- Floc floating	Observation

For all conditions, the cationic polymer FO107 was used as the coagulant with 0.50mg/L concentration. The optimum conditions in the hybrid process should present the optimum velocity gradient that creates the coagulation process. Moreover, the presence of vortex flow is necessary for the separation phenomenon. Consequently, the inlet flow rate was also varied to be 800, 900 and 1000L/hr in order to observe the vortex flow phenomenon. The results were mainly observed by VDO recorder.

5.1.7.2 Result and discussion

Three different raw water characteristics were 0.10, 0.25 and 0.50g/L bentonite suspension. It presented 22, 73 and 120NTU respectively. The observation results are shown in Table V-4. It can be seen that there was no difference in each condition. The vortex presence to the top of the hydrocyclone occurred with all conditions. The floc

floating was observed by batch operation, after stopping the experiment, the floc settled to the bottom. Thus, it can be assumed that the coagulation process is achieved but the mechanism of floc cover or attach to the micro bubbles did not succeed; there was no aerated-floc. Since the raw water turbidity affects the floc size, higher turbidity presents larger floc. Beside, the floc size by video observation from the different raw water turbidity found that 0.50g/L bentonite suspension presented a larger floc size than 0.25g/L. It corresponds to Monod (1991) that the flocculation depends on the particle concentration in the reactor; higher turbidity presents high efficiency for flocculation.

However, in the sense of floated floc, the results did not show any difference from these three bentonite concentrations. That means there was no floating floc. It can be assumed with two reasons. First, the aerated-floc did not occurr because the floc and micro bubble interaction mechanism was not achieved. Second, assuming the aerated-floc occurred but the created flocs were large and heavy, thus the micro bubble inside the structure could not decrease the aerated-floc density enough to be lower than the water density. Consequently, there was no separation process by vortex flow.

Table V-4   Result of the bentonite suspension concentration influence

Flow rate (l/hr)	800	900	1000	1000	1000
Bentonite concentration (g/l)	0.50	0.50	0.50	0.25	0.10
Vortex presence	Yes	Yes	Yes	Yes	Yes
Micro bubble coalescence	no	no	no	no	No
Floc formation	Yes	Yes	Yes larger floc	Yes smaller floc	Yes small floc
Floc floating	no	no	no	no	no
Separation phenomenon	no	no	no	no	no

Decreasing the bentonite suspension concentration reduced the weight of the floc while the different inlet flow rate from 800 – 1000L/hr did not show any difference in the vortex performance and floc formation. Consequently, it is interesting to study on the varied coagulant concentration and type. Moreover, the different inlet flow rates such as 300L/hr are also appealing to study the influence to the hybrid process.

5.1.8 The influence of the coagulant type (Cationic polymer and Aluminum sulfate) to hybrid process observed

5.1.8.1 Experimental method

Since the hybrid process has been developed from several researches such as Chaiyaporn Puprasert (2004a), Vorasiri Siangsanun (2006) and Pradipat Bumrungsri (2008), the method to choose the coagulant type was a Jar test experiment. Cationic polymer FO107 was chosen to use in this study. Realizing the optimum conditions by decreasing the cost, it was questioned whether it was possible to use aluminum sulfate as a coagulant resembling the conventional coagulation process. This part of the study, changing the coagulant type was considered to compare between cationic polymer FO107 and Aluminum sulfate $(Al_2(SO_4)_3)$. Moreover, 300L/hr inlet flow rate is considered to represent a low inlet flow in producing the aerated floc (floc floating) and the vortex performance to compare with 1000L/hr. The results are mainly observed by the performance to be the experimental basis for the next part. Coagulant concentration was resolved by jar test experimental and chosen 0.50mg/L FO107 cationic polymer and 15.0mg/L Aluminum sulfate.

Table V-5 Operating conditions used to work on the effects of coagulant concentration to hybrid process

Varied parameter	Operating condition
Coagulant type	
- Cationic polymer FO107	- 0.50mg/L
- Aluminum sulfate	- 15.0mg/L
Inlet flow rate	300 and 1000L/hr
Control parameter	**Operating condition**
Bentonite suspension	0.50g/L
Saturated pressure	3 – 4bars
Method of analysis	
- Vortex performance	Video recorder
- Separation	Observation
- Floc floating	Observation

5.1.8.2   Result and discussion

There are two changing parameters in this part; coagulant type and the raw water inlet flow rate. The observation results are shown in Table V-6.

Table V-6   the results of the coagulant type and flow rate affect to hybrid process observed

Coagulant type	Alum 15mg/L	Alum 15mg/L	FO107 0.5mg/L
Inlet flow rate (l/hr)	300	1000	1000
Bentonite concentration (g/l)	0.5	0.5	0.5
Vortex presence	no	yes	yes
Micro bubble coalescence	no	no	no
Floc formation	yes	no	yes
Floc floating	no	no	no
Separation phenomenon	no	no	no

The effect of the inlet flow rate range was between 300 and 1000L/hr, the higher flow rate presented the vortex flow up to the top part of reactor but there was no floc formation by Aluminum sulfate. 1000L/hr inlet flow rate logically creates a higher velocity gradient inside the hydrocyclone. Coagulation by this flow rate should be more obvious than 300L/hr. Moreover, the retention time is too short to observe the flocs. Thus, the results allow concluding that it is necessary to find the compromise between high velocity gradient and high retention time. Comparing between 15mg/L Aluminum sulfate and 0.5mg/L FO107 with the same flow rate 1000L/hr, the floc formation occurred by using FO107. This can be discussed that the condition of 15mg/L Aluminum sulfate and 1000L/hr, inlet flow rate actually created the micro floc from the coagulation process but the micro flocs might not be able to form larger size because the aluminum sulfate was less efficient than the polymer to gather the micro floc. Otherwise, Aluminum sulfate requires a higher retention time to create the floc since 300L/hr presented a higher retention time inside the reactor and it produced floc but no vortex flow, or the float floc.

The micro bubble formation was very satisfactory as there was no micro bubble coalescence under any conditions of hybrid process with coagulant involved. From the previous work, Pradipat Bumrungsri (2008) studied many parameters effecting coalescence; the inlet flow rate, saturate pressure and the air fraction. It was mentioned that the high flow rate (higher than 250L/hr) with high air fraction (higher than 0.0070), coalescence occurred. On the other hand, with a low flow rate, the coalescence did not appear. The effect of the inlet velocity was not clearly mentioned. Thus, considering the

flow rate in this study, it was 1000L/hr and it presented 3.54m/s inlet velocity (with inlet diameter 10mm). This could be discussed by inlet velocity from the previous work. Even though 1000L/hr flow rate is higher than 250L/hr from previous work the inlet velocity is equal since inlet diameter of Pradipat Bumrungsri's work was 5mm. It resulted 3.54m/s inlet velocity. That could be explained with this inlet velocity which was not too high to cause micro bubble coalescence.

Optimizing the hybrid process, vortex flow is necessary for the separation process. 1000L/hr inlet flow rate is considered to maintain and so does FO107 coagulant for the coagulation in hybrid process because the floc formation by FO107 was presented in the observation results.

5.1.9 The study of the difference between coagulation inside the hydrocyclone and pre-coagulation before getting in the hydrocyclone

To develop the hybrid process, it is interesting to separate the process in order to indicate how the influence of coagulation or flocculation could improve the development of the hybrid process. In order to increase the resident time without decrease of velocity gradient, the experiment is divided into two main parts; the coagulation stage inside the hydrocyclone and coagulation stage before getting into hydrocyclone. The second part used the coil wire mesh as the static mixer. This part of the study will explain both methods and then discuss the results all together.

5.1.9.1 The method of coagulation inside the hydrocyclone

This part of study is the coagulation inside the hydrocyclone. It is exactly the same Pilot plant description as the previous parts where the coagulant solution is injected directly into the hydrocyclone reactor. The coagulation process will occur at the bottom part from the injection of raw water while the flocculation process will occur at the higher level along the hydrocyclone height by the vortex flow. The Pilot plant was setup as shown in Figure V-10.
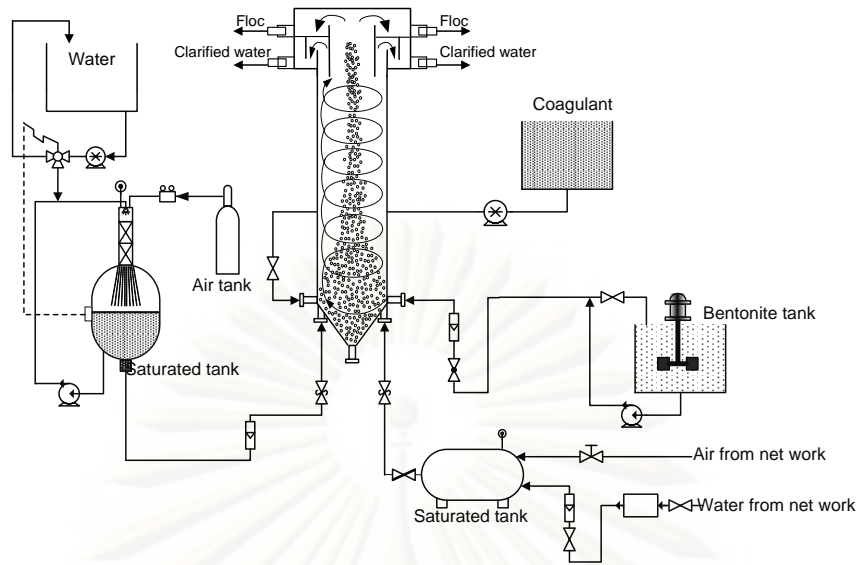
**Figure V-10 The pilot schematic diagrams of coagulation inside the reactor
(without static mixer)**

To operate the hybrid process, the bentonite suspension is pumped into hydrocyclone via the tangential inlet aperture with 1000L/hr flow rate. Even though there are four raw water inlet apertures; it is fed through only one inlet. Coagulant is fed tangentially in the opposite direction to the raw water.   The raw water inlet creates a suitable velocity gradient for the coagulation process. Meanwhile, air pressurized water from the DAF technique is injected close to the wall via the vertical inlet apertures. The micro bubbles from DAF technique are produced spontaneously in the hydrocyclone with the coagulation process. The produced floc includes micro bubbles inside its structure to be separated by the vortex flow. The coagulant concentration is controlled by the injection flow rate. Two parameters were varied to find out the optimum conditions. Table V-7 shows the experimental conditions used.

Table V-7 Experimental conditions to study the coagulation inside hydrocyclone

Varied Parameter	Value for experiment
Bentonite suspension	0.10 and 0.25g/L
Coagulant type	
1. Polymer FO107	0.1 and 0.5mg/L
2. Aluminum sulfate	15.0mg/L
Control parameter	**Value for experiment**
Bentonite suspension flow rate	1000L/hr
Saturated pressure (two systems)	4bar

5.1.9.2   Method of Pre-coagulation before hydrocyclone

In this part of the study a static mixer was added which was made from coiled wire meshed. The coagulant tank was additionally installed with a peristaltic pump to inject the coagulant solution into the raw water line at the position to get in a static mixer. The coagulation process by aluminum sulfate coagulant is supposed to occur at the static mixer and the flocculation process by cationic polymer flocculant occurs inside the hydrocyclone reactor. The operating conditions are shown in Table V-8 and the pilot installation is shown in Figure V-11 with a static mixer.
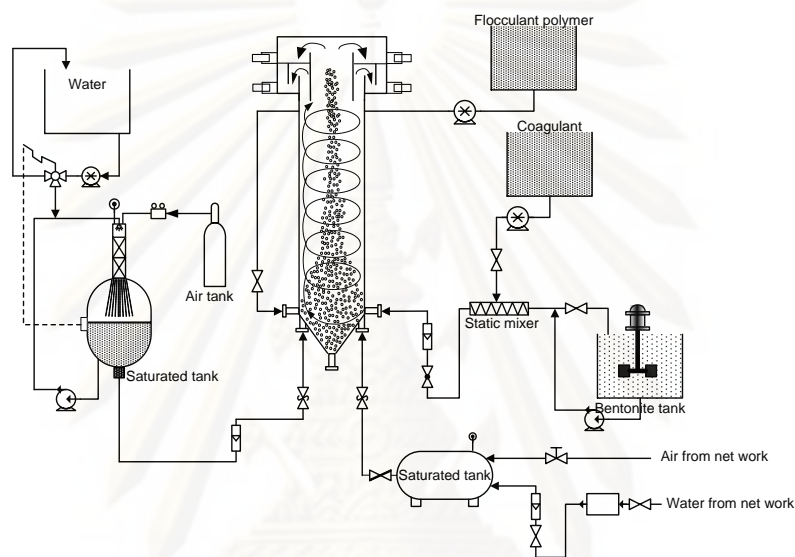
Figure V-11   Pilot schematic diagrams with static mixer

Table V-8   Pre-coagulation before hydrocyclone experimental conditions

Parameter	Value for experiment
Bentonite suspension	0.50g/L
Coagulant type	
Aluminum sulfate	5.0 and 15.0mg/L
Flocculant type	
Polymer cationic FO107	0, 0.1, 0.5mg/L
Control parameter	**Value for experiment**
Bentonite suspension flow rate	1000L/hr
Saturated pressure	4bars

To determine the results, which will be considered in terms of the water treatment with turbidity decreased and suspended solid removal percentage that compares between the clarified water from the wall zone to the bentonite suspension raw water. In addition, the separation efficiency of hydrocyclone that compares between the floc concentrated from the centre zone to the clarified water from the wall zone. Moreover, the matter recovery is also considered from the matter flux effluence from the centre zone compare to the raw water inlet.

5.1.10 Result and discussion

To discuss the result from hybrid process, it should illustrate the optimum conditions from the previous work because many parameters are developed from the results of Pradipat Bumrungsri (2008). The optimum conditions are as follow.

Hydrocyclone geometry	50-mm diameter and 1000mm height
Raw water flow rate	200L/hr (=2.83m/s with 5.0mm inlet diameter)
Bentonite suspension	0.5g/L
Raw water inlet	5.0mm
Coagulant concentration	3.0 – 4.0mg/L cationic polymer
Saturated pressure	3.5bars
Air fraction	0.0082 – 0.0100

These conditions are shown to realize that the hybrid reactor is not the same configurations. However, this study is developed from the previous results. It should be shown to distingue whether the hybrid process is developed positively. Moreover, there are some parameters that should be compared such as; the inlet velocity, the air fraction and coagulant concentration.

The results of this hybrid process are presented and mainly rely on the bentonite suspension concentration and the difference of coagulation process position.

- 0.10g/L bentonite suspension with coagulation inside hydrocyclone

- 0.25g/L bentonite suspension with coagulation inside hydrocyclone

- 0.50g/L bentonite suspension with pre-coagulation at static mixer

These three conditions will be discussed on the turbidity decreased, suspended solid removal, separation efficiency, the matter recovery and air fraction. All the experimental results are shown in Appendix C. It should be noted that the air fraction is calculated from the total outlet flow. For that, it is not shown in the experimental conditions table but in the results part.

5.1.10.1 The results of coagulation efficiency and air fraction in the hybrid process

The results in this part imply the hybrid process's ability in water treatment. Clarified water is compared with raw water inlet characteristics (turbidity). Figure V-12, V-13 and V-14 show the results of the turbidity decrease and air fraction under all conditions.
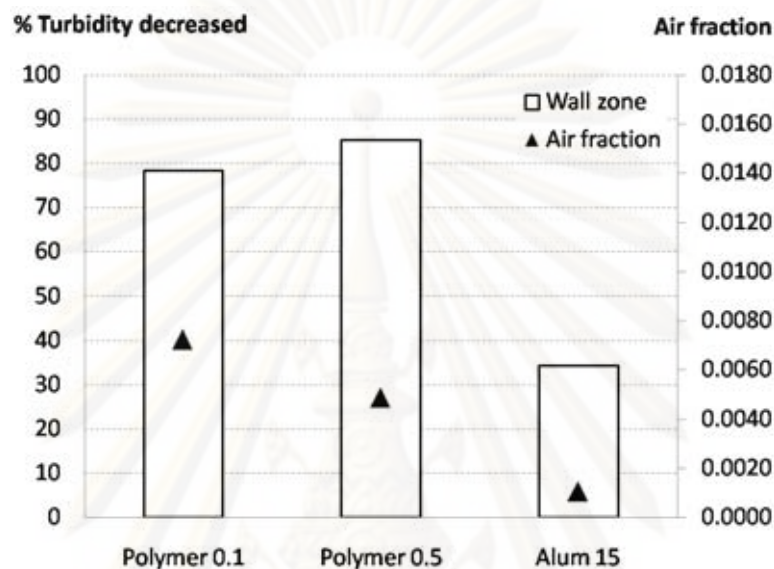
Figure V-12   %turbidity decreased and air fraction of *0.10g/L* bentonite suspension with varied coagulant concentration without a static mixer

Figure V-12 illustrates that there was a %turbidity decrease in all conditions. It indicates that the coagulation process occurred with those conditions. The coagulant concentration which presents the high turbidity decreased is 0.5mg/L polymer even the air fraction is low (0.0049) compared to 0.1mg/L polymer's one. However, the condition with 15mg/L aluminum sulfate shows very poor results but it can be discussed that because the air fraction is very low (0.0011) it was not able to create the aerated floc.
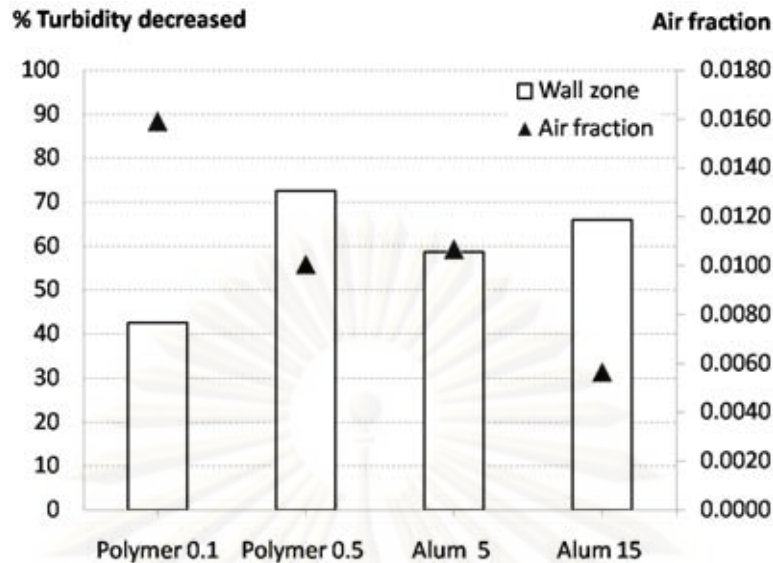
Figure V-13 **%turbidity decreased and air fraction of *0.25g/L* bentonite suspension with varied coagulant concentration without a static mixer**

Figure V-13 illustrates the results by increasing the bentonite suspension (0.25g/L) and a trail with 5mg/L Aluminum sulfate concentration. It can be seen that 0.5mg/L polymer presented a good result. On the other hand, the air fraction difference does not affect to the percent removal. It can be discussed that the coagulation process occurred in these conditions. Although, the interaction between micro bubbles and flocs did not achieve since the high air fraction did not present the differences in the %turbidity decreased.
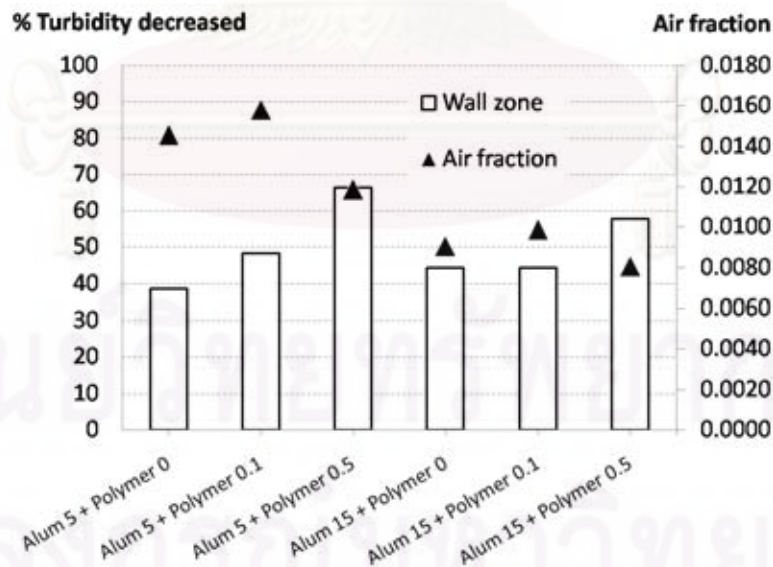
Figure V-14 **%turbidity decreased and air fraction of *0.50g/L* bentonite suspension with varied coagulant, flocculant concentrations with a static mixer (Pre coagulation)**

The removal percentages in the hybrid process with pre-coagulation by a static mixer are shown in Figure V-14. Considering the condition without adding flocculant

polymer, it can be declared that the coagulation process was achieved by a static mixer. The %turbidity decreased were 39% without polymer. Considering the consitions between without flocculant (Alum 5 + Polymer 0) and 0.5mg/L polymer, the % of turbidity removal increased from 39% to 47%. It implied that the idea of pre-coagulation at a static mixer before getting in hydrocyclone could improve the process. On the other hand, increasing the alum concentration with low air fraction could present the same % turbidity removal. It points out that the important parameters are coagulant concentration and air fraction. For both methods, coagulation inside the hydrocyclone and pre-coagulation by a static mixer could produce the coagulation process. In condition of 5mg/L coagulant aluminum sulfate and 0.5mg/L flocculant polymer presented 66.4% turbidity decreased. Thus, 0.5mg/L polymer is satisfied in the sense of economic compared to the previous work that used 3.0- 4.0mg/L polymer.

Besides, this part of study show that an important parameter that effects to the removal percentages is the coagulant and the flocculant concentrations while the air fraction is not able to play its role to the process.

However, the weak point of this result is that the flocculation process or the aerated floc production. To consider the difference between centre zone and wall zone water, the separation efficiency is determined which will be explained in the next part.

5.1.10.2 The results of separation efficiency and the %matter recovery fraction of the hybrid process

Separation efficiency and matter recovery fraction are considered in the hydrocyclone performance of this study. Separation efficiency determines the difference of wall zone water (clarified water) to the centre zone water (floc concentrated). Besides, the matter recovery fraction is to consider the matter flux exit in the centre zone compared with raw water.
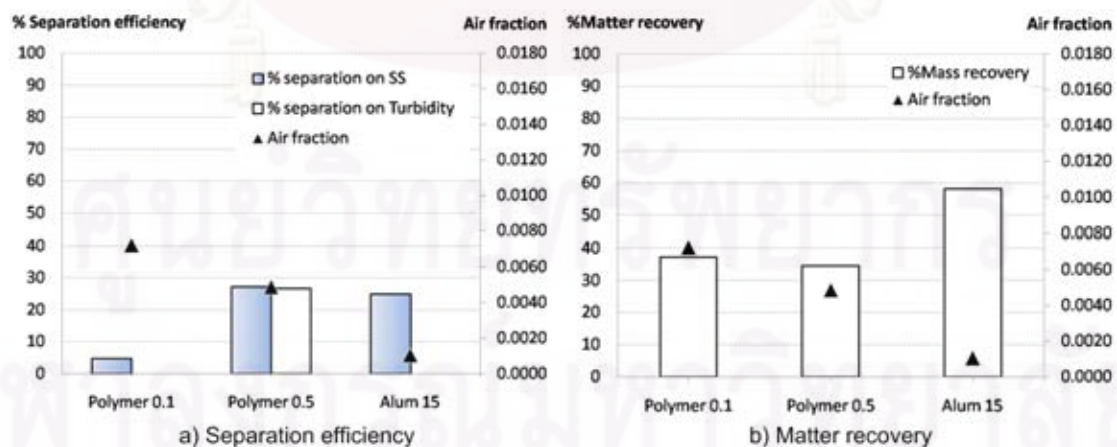
Figure V-15   Separation efficiency and %matter recovery fraction of *0.10g/L* bentonite suspension with varied coagulant concentrations without static mixer

The separation efficiency in Figure V-15 a) shows that with 0.5mg/L polymer could present the separation process but low percentage (27%) with low air fraction (0.0049). There was no separation with 0.1mg/L polymer even the air fraction was higher (0.0072). However, air fractions of these conditions are lower than the optimum condition by the previous work (air fraction 0.0082).
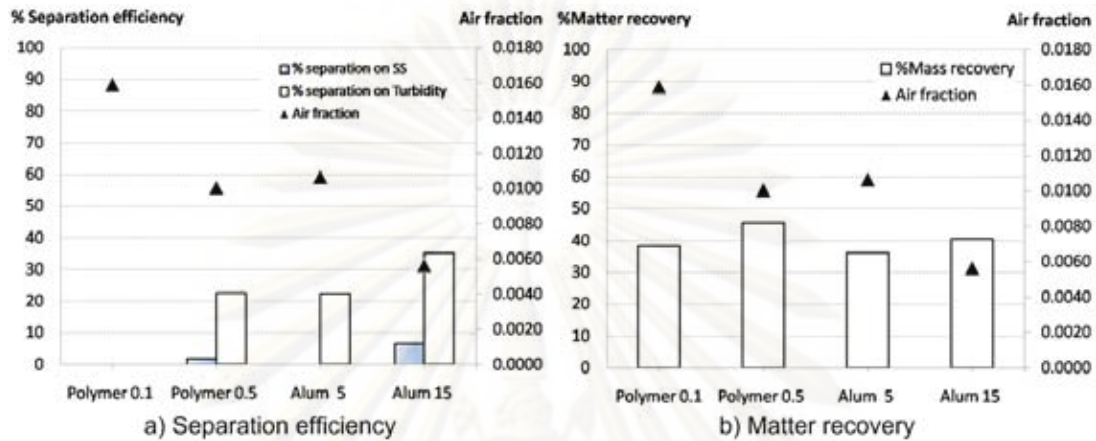
Figure V-16   separation efficiency and matter recovery fraction of 0.25g/L bentonite suspension with varied coagulant concentration without a static mixer

Considering the separation efficiency in Figure V-16, the air fractions of all conditions are higher than 0.0071. The separation phenomenon occurred with 0.5mg/L polymer, 5mg/L and 15mg/L aluminum sulfate in turbidity but they do not relate to the air fraction.
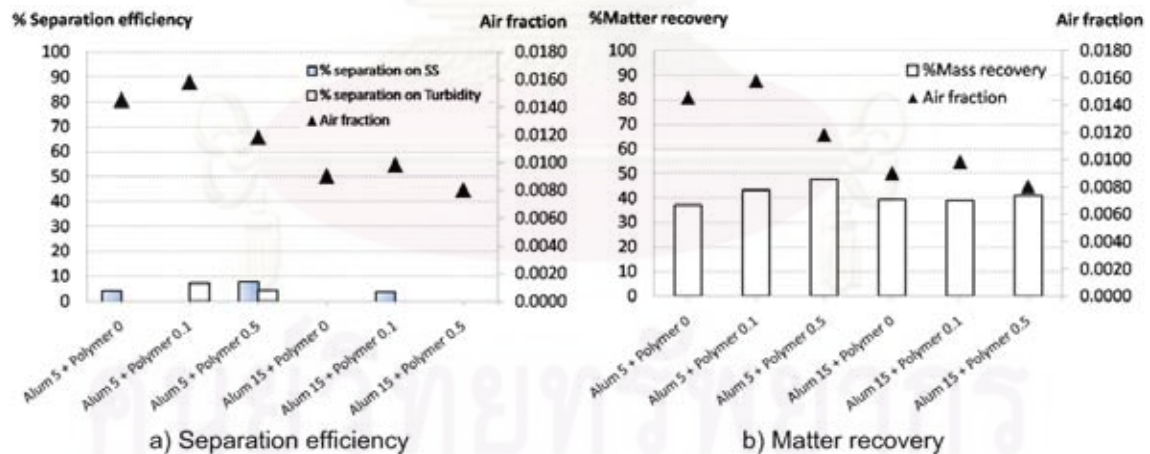
Figure V-17   separation efficiency and matter recovery fraction of 0.50g/L bentonite suspension with varied coagulant, flocculant concentrations with a static mixer (Pre coagulation)

Figure V-17 a) presents the very poor separation efficiencies even when the air fraction under all conditions was higher than the optimum conditions of the previous worked. In this pre coagulation experimental part, the coagulation process occurred at a static mixer. The coagulation mechanism was sweep coagulation because this step, pH had not been taken into account (as an adsorption and charge neutralization mechanism).

When alum is added to water, it reacts with the water and results in positively charged ions and aggregate with particle in the water. With sweep coagulation, alum had been added to excess. Consequently, colloid-coagulant charges remained positively charged by this step. Therefore, adding the cationic polymer caused the difficulty for the flocculation process. Consequently, a suitable flocculant polymer is anionic polymer. This study used cationic polymer to aggregate the cationic floc from the coagulation process. Even when it was the flocculation polymer bridging mechanism however using the opposite charge would be more effective.

While in the experimental work of coagulation inside the hydrocyclone, cationic was used as coagulant. It was suitable since the bentonite particle has a negative charge on its surface. Adding cationic polymer neutralizes the particle charge. Then the flocculation process could occur by the polymer bridging mechanism from a high polymer molecular weight.

In further hybrid process research, it is therefore recommended to use anionic polymer as the flocculant.

In the matter of recovery fraction under all conditions (Figure V-15b) V-16b) and V-17b)), the fractions are between 35 – 60%. It shows the possibility of the hybrid process to recover the particle or floc to the centre. However, the results do not correspond to the air fraction.

5.1.10.3 The flow recovery from hybrid process with bentonite suspension

Since the hybrid process is willing to be developed for water treatment process, it is important to verify the process's ability to recover the treated water. Table V-9 shows the %flow recovery which considers the wall zone outlet flow (clarified water) compare to raw water inlet as Equation V-4.

$$Flow\ \operatorname{Re}cover\ Fraction = \frac{Q_{Wall\ zone}}{Q_{Raw\ water}}$$

Equation V-4

Table V-9 Treated water recovery by hybrid process with bentonite suspension

Bentonite suspension 0.10g/L (without static mixer)	
Condition	**Treated water flow recovery (%)**
Polymer 0.10mg/L	47
Polymer 0.50mg/L	41
Aluminum sulfate 15mg/L	44

Bentonite suspension 0.25g/L (without static mixer)

Condition	Treated water flow recovery (%)
Polymer 0.10mg/L	55
Polymer 0.50mg/L	42
Aluminum sulfate 5mg/L	51
Aluminum sulfate 15mg/L	44

Bentonite suspension 0.50g/L (with static mixer)

Condition	Treated water flow recovery (%)
Alum 5mg/L without polymer	43
Alum 5mg/L with 0.10mg/L polymer	42
Alum 5mg/L with 0.50mg/L polymer	25
Alum 15mg/L without polymer	47
Alum 15mg/L with 0.10mg/L polymer	47
Alum 15mg/L with 0.50mg/L polymer	28

Table V-9, the %flow recovery from hybrid process is in the range of 25-55% of inlet flow. It is very low to present as a water treatment process. This can be improved by decreasing the center zone outlet diameter. However, the priority of hybrid process is the separation between concentrated floc and clarified water. Consequently, the separation phenomenon should be improved, and then it can be considered to increase the clarified water partition.

5.1.10.4 The effect of the bentonite suspension concentration

Since the bentonite suspension concentration was also varied, the results are rearranged in order to see the effect of the raw water turbidity. The results are shown in FigureV-18.
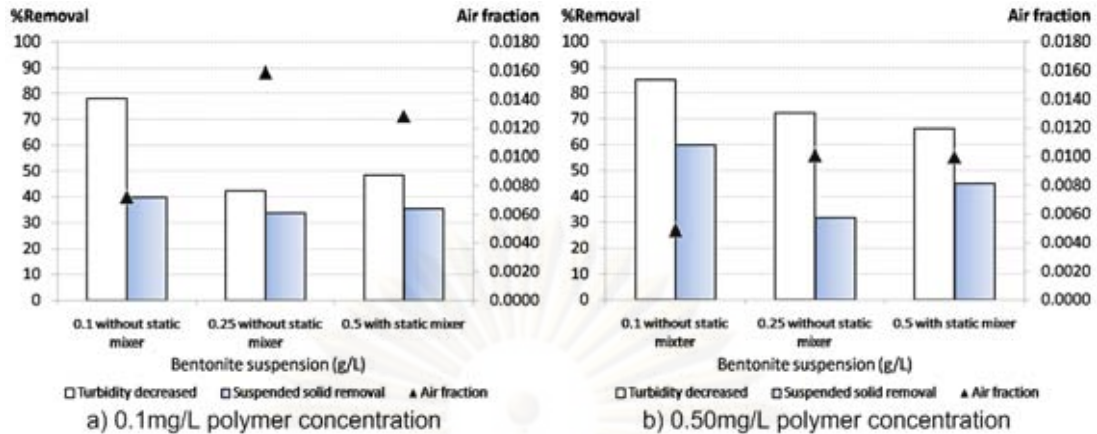
Figure V-18 removal percentages with varied bentonite suspension concentration

Bentonite suspension 0.1g/L shows the highest percentage in turbidity decrease and suspended solid removal compared to higher bentonite suspension (0.25 and 0.50g/L). This result is in contrast to previous studies; higher turbidity could support for the coagulation process. Since low turbidity has a greater distance between particles so the possibility of particle collision and aggregation is reduced (Kathy et al., 2003). Higher turbidity should present the higher turbidity decreased and suspended solid removal. However, the previous study focused on the coagulation and the flocculation process. Whereas, the hybrid process has the effect of vortex flow and flotation process which are another factor influencing the results.

However, low raw water turbidity with good results was satisfactory since the hybrid process is being developed for application in the treatment of natural water such as river water that has very low turbidity.

From all the results as shown above, it can be concluded that the hybrid process working on bentonite suspension achieved the coagulation process from the percentage of removal. On the other hand, there was no separation between wall zone and centre zone. This weak point can be discussed with the following reasons.

The bentonite suspension storage tank was 500L working with 1000L/hr flow rate. An experiment could run continuously for a maximum of 30 minutes. The operation might not be in the stable condition during the sampling. It is recommended to enlarge the storage tank in order to operate the process for a longer time and sampling at the different times to assure stable operation.

Moreover, as discussed above that there was no separation process occurring by the hybrid process with bentonite suspension even though the vortex performance and micro bubble formation had very good result (Part 5.1.11, characterization of the vortex flow and micro bubble at the different height of the hybrid reactor). The coagulation process occurred in this process and also the excess air fraction. It can be explained that the interaction mechanism between the micro bubble and micro floc was not successful enough to produce the aerated floc to be separated by vortex flow. It is strongly

recommended to use anionic polymer in the flocculation process and also extend the retention time to be adequate for micro bubble-floc interaction.

5.1.11 Conclusions

The hybrid process with synthetic raw water has been studied with many parameters. The main conclusions are as follows.

- The vortex performance inside the hybrid reactor presented as the expected phenomenon. There was no bubble coalescence which is the most important factor for the hybrid process. At higher levels inside reactor, micro bubble swirled and flowed along the cyclone axis. Saturated pressure was 3.5 – 4.0bars and inlet flow rate was 1000L/hr.

- The influence of the bentonite suspension concentration is reasonable that the low turbidity produced smaller floc while the higher turbidity created larger floc.

- The study of the influence of the coagulant type showed that FO107 polymer (0.5mg/L) was more efficient than aluminum sulfate with the same flow rate (1000L/hr)

- The difference between coagulation inside the hydrocyclone and pre-coagulation before getting in the hydrocyclone

    o **Coagulation inside the hydrocyclone**

    Since there was no flow meter for the air pressurized water, it was difficult to control the air fraction inside hydrocyclone. However, the coagulant type and dose which presented the best results was 0.5mg/L polymer. The effect of raw water turbidity found that 0.10g/L bentonite suspension had been the most success in percentage of turbidity decreased and suspended solid removal, at 85.2% and 60.0% respectively.

    o **Pre-coagulation before getting in the hydrocyclone**

    The coagulation process succeeds in the percentage of removal. The conditions which presented the best results were; 0.50g/L bentonite suspension, 5mg/L coagulant aluminum sulfate and 0.50mg/L flocculant polymer. The percent removals were 66.4 % turbidity decreased and 45.2% suspended solid removal.

The hybrid process is being developed to apply for treating natural water. It is recommended to use an anionic polymer for the flocculation stage. The air pressurized water flow rate should be fixed in order to control the air fraction. The next chapter will modify the parameters according to this study to work on river water that will be present in Part II of the hybrid process with natural water.

5.2 Part II: Hybrid process with natural water

5.2.1 Abstract

This study deals with a new hybrid process which allows in one step the coagulation of particles and/or natural organic matter flocculation attached to micro bubbles and the separation of flocs inside a hydrocyclone (Hebrard et al., 2008). This process can be an alternative to the classical coagulation/flocculation/settling or flotation in drinking water treatment plants. Indeed, the development of new methods for water treatment is a perpetual challenge. It requires a development process that is reliable, economical, compact and efficient. The developed hybrid process aims to reach those objectives with a significant reduction of the plant's footprint. The separation of a dispersed phase from a continuous one (e.g. particles from water) is frequently used in the mineral industry for solid separation and classification or in the sand industry for particle removal. The separation is induced by centrifugal force. The lighter phase goes along the centre of the hydrocyclone and the heavier at the wall. This hybrid process is developed for natural water in a water treatment process. It innovates the lighter phase by producing the aerated floc by coagulation, flocculation and micro bubble from dissolved air flotation technique simultaneously. Thus, this aerated floc is separated from the water by the centrifugal force of the hydrocyclone mechanism. For this case study system, clarified water had an efficiency of 61%, the turbidity decreased and 66% of suspended solids were removed. The process achieved continuous operation with 1000L/hr inlet flow. The hybrid process shows a strong potential to be able to be developed for industrial work.

5.2.2 Introduction

In the water treatment field, there are several studies which applied the separation by centrifugal force in the water treatment process. Menezes F.M. et al. (1996) worked on coagulation and flocculation in a dynamic separator to remove silica (500mg/L) and clay particles (50mg/L). This study achieved, using a coagulation process in conjunction with a dynamic separator, separation of the solid phase (silica and clay) from the water phase. Rubio J. and Rosa J. (2004) used a flocculation and flotation process to produce aerated polymeric floc of emulsified oil dispersion then separation by a centrifuge cell. However, most of those studies utilized only synthetic raw water but never with real raw water with very low turbidity. There has been no completed water treatment process in one hydrocyclone unit yet. Consequently, this hybrid process is being developed.

Chaiyaporn Puprasert et al. (2004a) studied the feasibility of a hybrid process with a 5cm diameter and 50cm high hydrocyclone. The aerated flocs which contained the micro bubble inside the structure were a success. Vorasiri Siangsanun (2006) studied on the parameters effecting to the process and also hydrocyclone geometries. The conical geometry hydrocyclone achieved a vortex flow performance through the hydrocyclone axis but there was still no separation phenomenon. On the other hand, the 5cm diameter cylindrical hydrocyclone had micro bubble coalescence that reduced the aerated floc

production. Besides, coagulant, flocculant concentration and also the air fraction influenced the process. The work continued to be studied, Pradipat Bamrungsri (2008) studied the hydrodynamic characteristics inside three hydrocyclone geometries and found the optimum operating conditions for the hybrid process. The velocity profiles explained how the water spins downward on the cyclone axis that caused the micro bubble coalescence. Moreover, the hydrocyclone diameter was recommended to be increased from 5cm to 10cm in order to allow an easier distinction of the hydrodynamic phenomenon. The optimum conditions found are: 0.0082 – 0.0100 air fraction, 3-4mg/L flocculant polymer and 250L/hr inlet flow rate. Besides, the modified 10cm diameter hybrid process and reactor are being developed as in the previous chapter for the synthetic raw water to find the optimum conditions and the influencing parameters. All research shows the potential and approaches the novel separation concepts and devices. Consequently, this study is aimed at operating the hybrid process with natural water. The operation should run continuously for at least 1 hour to assure stable operation. A jar test experiment is integrated to find the optimum coagulant and flocculant concentration assuming equal retention time.

5.2.3 Material and method

5.2.3.1 Pilot plant description
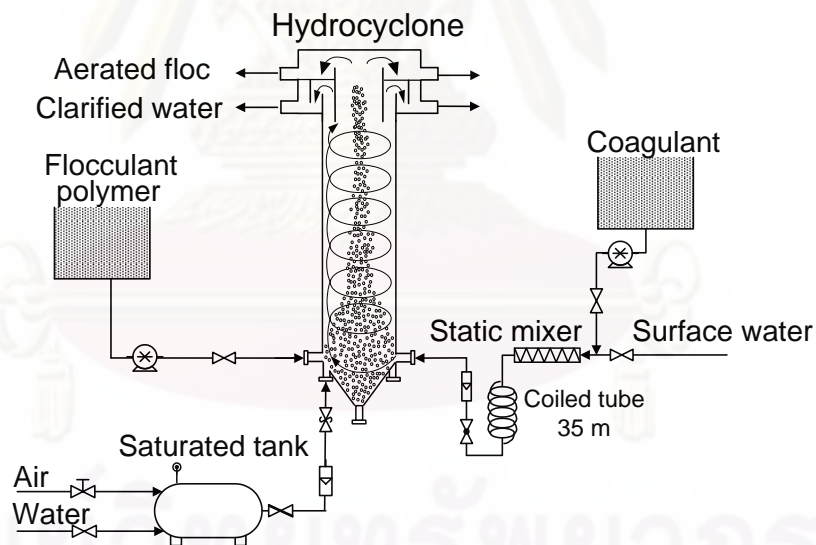
Figure V-19 Pilot plant schematic

The pilot plant was modified for treating the natural water from La Marne River in France. There were four parts which contributed to this process.

5.2.3.2 Coagulant solution

The prepared coagulant is Aluminum sulfate WAC HB which is served in the required concentration depending on the flow rate from the pump. The static mixer was installed to produce the coagulation process. The raw water was pumped and passed

through a static mixer at 1000L/hr. Meanwhile, the coagulant solution was injected into the system before the raw water passed the static mixer. Then, there was the 35m tube with 2.54cm diameter. This tube allows 1 minute of retention time before entering the hydrocyclone reactor.

5.2.3.3 Flocculant solution

The flocculation tank has been prepared with AN905 anionic polymer which is injected at a flow rate to present the required concentration. It is injected directly into the hydrocyclone reactor. This step is expected to present the flocculation process and the retention time inside the hydrocyclone was 30 seconds (with 1000L/hr).

5.2.3.4 Micro bubble generation

The air pressurized water or bubble generation system functioned in a saturated tank with the air and the water at 4-5bar and 4.3bar pressure respectively. It is the Dissolved Air Flotation technique (DAF) which is one of the flotation processes in water treatment. It is exactly the same air pressurized water system from Chapter V, Part I. The retention time to assure that the air would dissolve in the water was set at around 10 minutes. The inlet was installed vertically underneath the hydrocyclone and close to the wall. The relief valve allows decreasing pressure and the saturated air in the water to precipitate to be micro bubbles and get into hydrocyclone. The micro flocs, then from the coagulation and flocculation process are produced and cover the micro bubbles in their structure. The special floc which contains the micro bubbles inside is called „aerated floc". The flow meter is installed to measure the air pressurized water flow rate in order to compare the flow ratio of the conventional flotation process to this hybrid process.

5.2.3.5 Hydrocyclone reactor

During all these experiments, only one hydrocyclone reactor was used. Its characteristics are 1000mm high and 100mm diameter. It is expected to present the separation process inside the reactor. 1000L/hr flow rate is injected tangentially to the hydrocyclone wall, causeing the vortex flow. It was fabricated in transparent acrylic resin in order to observe the phenomenon inside the reactor. The inlet zone is on the bottom part (the conical part). There are four tangential inlets with 10 mm diameter for raw water and coagulant injection. On the other hand, there are four vertical inlets which were designed for the air pressurized water injection as shown in Figure V-20. The central vertical tube is for fluid draining in case of cleaning inside. All the inlet apertures are designed to easily adjust the experiment. However, in this study, the inlet raw flow rate used only one tangential inlet aperture and also only one air pressurized water inlet. The sample collecting is designed on the top part. The centre zone water effluent or floc sludge swirls and drains out at the two upper horizontal tubes while the clarified water drains out at two horizontal tubes which are underneath the floc effluent.
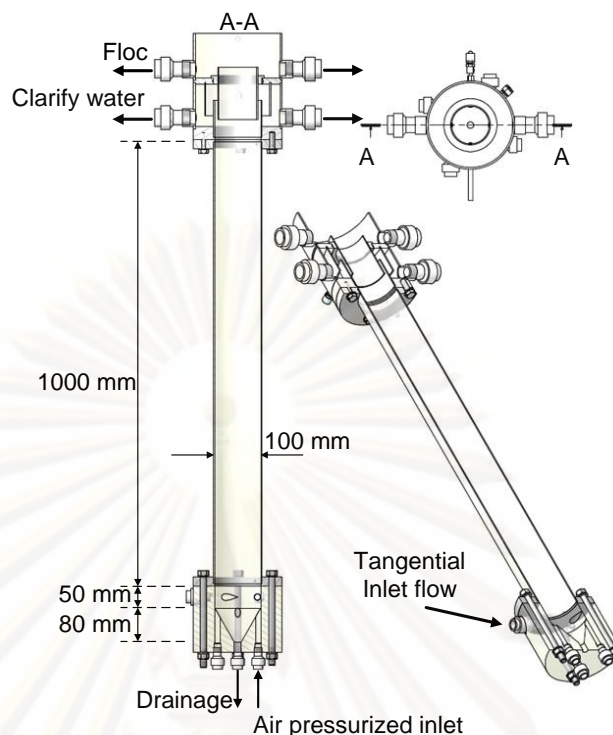
Figure V-20   Hydrocyclone reactor, front, upper and lateral view

5.2.4   Experimental analysis

5.2.4.1   The jar test method

The jar test method is considered to find out the optimum coagulation and flocculation concentration and to test the effect of coagulation and flocculation time. The tests are conducted using a flocculator (FLOCUMATIC P, SELECTA) with 6 beakers of 1L. The rapid mixing time for the coagulation process is 1 minute, the rate being maintained at 160rpm. While the slow mixing time for the flocculation process is varied as the experimental set up and the rate is maintained at 45rpm. The sedimentation time is 10 minutes, the supernatants are then collected for analysis.

5.2.4.2   Turbidity and Suspended solid (SS) measurement

The turbidity measurement used in this study is a turbidity meter (HACH 2100N IS TURBIDIMETER). The suspended solid is analyzed by the method dried at 103° - 105°C. The filter paper used is 0.45μm pore (PALL LIFE SCIENCES, LE TUFFRYN 47mm diameter). 100mL of sample is filtrated by the filter paper and then dried in the oven for 2 hours.

5.2.4.3   UV-254nm absorbance (Filtrated Optical density)

The determination of organic matter in a solution by measuring the absorbance of ultraviolet UV radiation by water is an indirect method based on the property of certain organic molecules to adsorb these radiations. The absorbing molecules are molecules with

carbon atoms bound by conjugated double bonds such as those contained in the constituent aromatic rings such as aromatic hydrocarbons and humic acids (hence the term aromaticity of organic matter is sometimes given to the measurement of UV absorbance) The intensity of the UV absorbance of a water sample is proportional to the number of molecules containing conjugated double bonds in the sample, and that number is even proportional to the concentration of organic material of the same sample and measuring the UV absorbance can then determine (or estimate) the organic content of water through prior determination of the proportional relationship between these two quantities. Two wavelengths that commonly used are 254nm and 280nm.

For that, the UV-254nm absorbance is used to indicate the dissolved organic matter which is reduced by the coagulation process in the hybrid process. The samples will be filtrated by the filter paper 0.45μm in order to analyze the dissolved organic matter. The filtrated water will be put into a 5cm cube to measure the UV-254nm absorbance with a Spectrometer UV-254nm (HACH LANGE DR5000).

5.2.4.4 Water sampling in hybrid process operation

In each experiment there were three samples that were taken during the hybrid process operation. As the operation was run for one hour continuously, the effluence water was sampled at 15 minutes, 30 minutes and 50 minutes after the start of the operation in order to represent the whole operation. The clarified water from the wall zone was sampled through the small tube which was installed to provide a small flow rate which was open it continuously during 1 hour of the operation. The water from centre zone with the floc was sampled with a small tube as well. These small tubes with opening valve solved the problem of the floc stuck at the exit which could disturb the representative of water sample. Each sample was analyzed with three measurements; turbidity by the turbidity meter, suspended solid and UV 254nm absorbance which presents the organic matter in water.
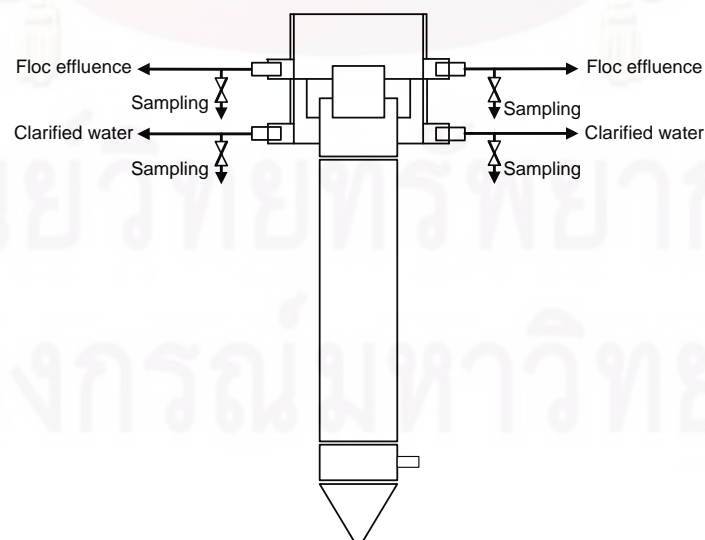
Figure V-21 Sampling positions in hybrid process with La Marne River water

The results will be considered in two senses of efficiency; water treatment process and separation process. The water treatment process will identify the coagulation process with % of UV absorbance reduced, the flocculation process with the % of turbidity decreased and % of suspended solid removal by comparing between clarified water from wall zone to raw water. On the other hand, the separation phenomenon will be identified by the % of separation efficiency which compares between the clarified water from wall zone and the concentrated water from the centre zone.

The Equation for water treatment analysis

$$\%\,Turbidity\,decreased = \frac{(T_{Raw\,water} - T_{Wall\,zone})}{T_{Raw\,water}} \times 100\% \qquad \text{Equation V-2}$$

$$\%\,Suspended\,solid(SS)\,removal = \frac{(SS_{Raw\,water} - SS_{Wall\,zone})}{SS_{Raw\,water}} \times 100\% \qquad \text{Equation V-3}$$

$$UV\,absorbance(abs/m) = UV\,abs/5cm \times 20 \qquad \text{Equation V-9}$$

$$\%\,UV\,absorbance\,reduced = \frac{UVabs_{Raw\,water} - UVabs_{Treated\,water}}{UVabs_{Raw\,water}} \times 100\%$$

$$\text{Equation V-10}$$

The Equation for hydrocyclone separation efficiency

$$\%\,Separation\,Efficiency\,in\,Turbidity = \frac{(T_{Center\,zone} - T_{Wall\,zone})}{T_{Center\,zone}} \times 100\% \qquad \text{Equation V-5}$$

$$\%\,Separation\,Efficiency\,in\,Suspended\,solid = \frac{(SS_{Center\,zone} - SS_{Wall\,zone})}{SS_{Center\,zone}} \times 100\%$$

$$\text{Equation V-6}$$

5.2.5 Experimental setup

This study is mainly working with natural water from La Marne River. There are many variable parameters to study in order to see their effects on the hybrid process. The studies had been provided as shown in Table V-10. The experiment will present each part followed by its results and discussion.

Table V-10 Experimental plan of hybrid process on La Marne River water

Subject	Studied parameters
1. Jar test experiment	- Raw water turbidity - Coagulant concentration - Flocculant concentration - Flocculation time
2. The flow performance by the hybrid process	- Vortex flow and micro bubble performance - Flow partition between centre and wall zone
3. The hybrid process on La Marne River water	- Coagulant concentration - Flocculant concentration - Air pressurized water flow rate

5.2.6   Jar test experiment with varied raw water turbidity

Determining the coagulant and flocculant dose was done by Jar test experiments by Flocculator (FLOCUMATIC P, SELECTA, maximum mixing speed 210rpm) which there were two main parts. This experiment was considered in order to assume the conditions which will be happen in the hydrocyclone and also to choose the coagulant and flocculant concentration. From the characteristics of the hybrid pilot, the coagulation process which occurs in a static mixer from Fluidcontrol® (PMS15-4-316L-DIN2576, IMP 3419) and the retention time for this step is 1 minute from 35m length of coiled tube before being injected into the hydrocyclone.

The flocculant polymer is injected directly at the hydrocyclone inlet. The retention time inside the reactor is 30 seconds (1000L/hr inlet flow rate) which is the retention time for flocculation process. Table V-10 illustrates the experimental plan for the coagulant concentration and the influence of the flocculation time. The different slow mixing time was chosen at 30 seconds because the hydrocyclone reactor presents 30 seconds of retention time. Then, 1 minute, was to distinguish the influence of the slow mixing time difference. 15 minutes was the conventional flocculation contact time.

The objective of these experiments is to characterize the water quality of La Marne River from the coagulation and flocculation point of view.

Table V-11 Jar test experimental conditions with varied raw water turbidity

Varied parameter	Experimental value
Raw water turbidity	5.68, 6.13, 6.17, 10.05, 15.60NTU
Coagulant concentration	28, 30, 40, 50, 60mg/L
Flocculant concentration	0.1, 0.5mg/L
Flocculation stage time	30 seconds, 1 minute, 15 minutes (45rpm)
Controlled parameter	**Experimental value**
Raw water flow rate	1000L/hr
Coagulation stage time	1 minute (160 rpm)
Sedimentation time	10 minutes

5.2.6.1 The influence of the flocculation time to the removal percentage

The results from this study are to show the possibility of flocculation in the hybrid process. Since the flocculation time in a hybrid process with a 1000L/hr is 30 seconds (hydrocyclone volume 9.08L). Therefore, the results compare between the variations of flocculation time in this jar test experiment.
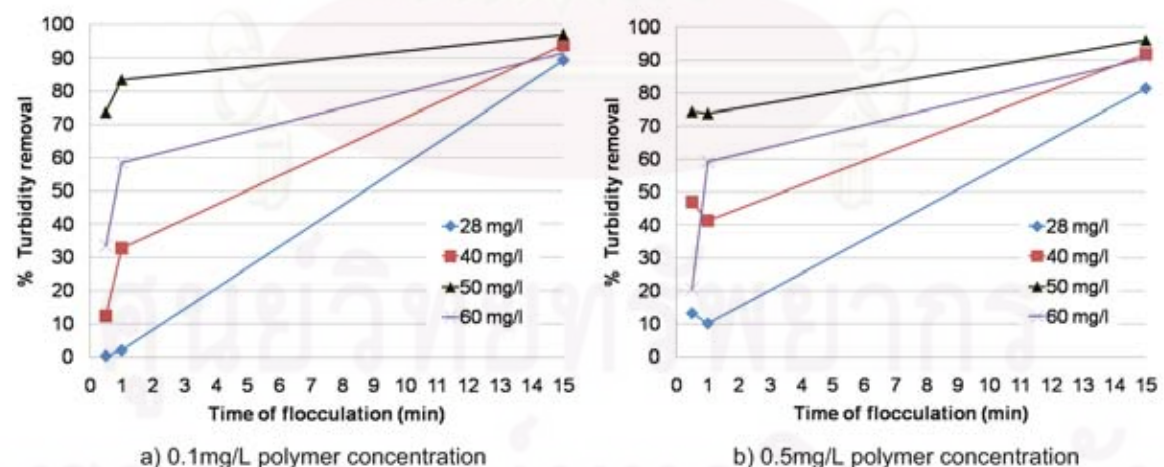
Figure V-22 The flocculation time and coagulant concentration affect on the % of turbidity removal

Figure V-22 shows the flocculation time effect to the turbidity removal with different polymer concentrations. Increasing the coagulant concentration presented the higher turbidity removal. 50mg/L coagulant dose gave the most satisfactory result. It

was questioned whether 60mg/L coagulant concentration could present a better result. It can be explained that each coagulant concentration test used different raw water (tested on a different day). The experimental data can be seen in Appendix D-I. It is important to underline that during the experiments conducted on the water quality of La Marne River, the inlet raw water turbidity is naturally changing. For example, the raw water turbidity of 50mg/L coagulant concentration condition was 15.6NTU while the 60mg/L's condition was 5.7NTU. Consequently, the lower raw water turbidity was more difficult to agglomerate and form the floc even though the coagulant concentration was higher (Monod, 1991). For that, it is necessary to test the influence of the coagulant concentration using the same initial raw water turbidity.

Considering the 30 second flocculation time, 50mg/L alum concentration in Figure V-23 a) and V-23b), the highest turbidity removal is 73.7% by 0.1mg/L polymer concentration and 74.4% by 0.5mg/L polymer concentration (These two conditions were the same raw water turbidity: 15.6NTU). Moreover, it can be seen that the coagulant concentration has a small effect on the turbidity removal percentage if the flocculation time is high enough since all concentrations show a similar % of turbidity removal at 15 min of flocculation time. On the other hand, considering the polymer concentrations, there was no difference between 0.1 and 0.5mg/L polymer concentration in turbidity removal.

a) 0.1mg/L polymer concentration   b) 0.5mg/L polymer concentration
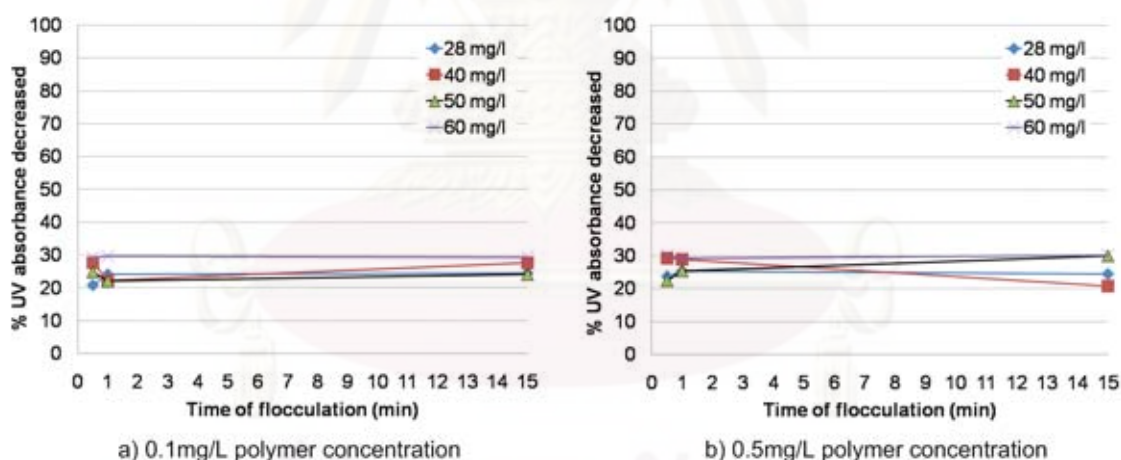
**Figure V-23   The flocculation time and coagulant concentration
effect on the dissolved organic matter removal**

The percent of optical density removal was done with a 0.45μm filter pore size and 254nm UV absorbance analysis, to determine the dissolved organic matter in the water. It is also an indicator for the coagulation process. If the UV absorbance is decreased, it implies that the coagulation process is achieved because the dissolved organic matter has been removed. From Figure V-23 a) and b), it can be seen that the coagulant concentration differences present identical results in % of UV absorbance decrease in each condition. It means that the coagulation process is independent of the flocculation time. It can be understood that with those coagulant concentrations could produce

coagulation. On the other hand, it implies that the important effect to the Jar test experiment is the flocculation process which depends on the flocculation time.

However it was shown that with only 1 minute coagulation mixing for all condition and 30 seconds flocculation stage condition, the coagulation was occurred as a conventional method (15 minutes flocculation). For that it is believed that the coagulation process in the hybrid process could be occurring.

5.2.6.2 The influence of raw water turbidity to percentage of turbidity decreased

Since the hybrid process is being developed for natural water from the La Marne river water, the water treatment depends on the raw water characteristics such as turbidity. It is interesting to study the influence of the raw water turbidity on the coagulation process efficiency. Raw water has randomly presented different turbidity depending on the climate (such as a rainy day), and it has been tested with different coagulant concentrations. The flocculation time considered was 30 seconds with 0.1mg/L and 0.5mg/L polymer concentrations. The results of turbidity removal are shown in Figure V-24.
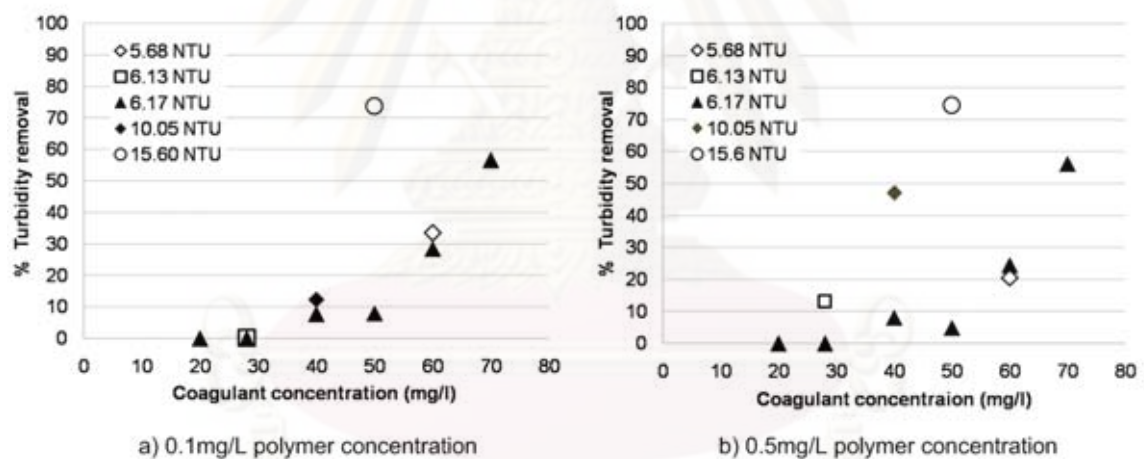
Figure V-24   The effect of raw water turbidity and turbidity removal percentages

Figure V-24, considering 6.17NTU raw water turbidity, the turbidity removal increased when the coagulant concentration increased. Moreover, it can be observed that 15.6NTU raw water could present higher turbidity removal than 6.17NTU raw water even if it used the same coagulant concentration (50mg/L). Moreover, it is very clear that the raw water which presented the highest turbidity removal was 15.6NTU even if the coagulant concentration was not the highest (50mg/L). Furthermore, focusing the same coagulant concentration and the similar raw water turbidity, at 60mg/L coagulant concentration, it is found that 5.18NTU and 6.17NTU raw water turbidity have the same % of turbidity removal (30 % by 0.1mg/L polymer in Figure V-24 a) and 20% by 0.5mg/L polymer in Figure V-24 b)).

Consequently, the coagulation process from this study shows the influence of two parameters; the raw water characteristic and the coagulant concentration. The higher the turbidity the easier it is to achieve the coagulation process because the particles have more possibility to interact each other. As a result, higher coagulant concentration presented higher turbidity removal.

Anyway, there was no clearly difference between 0.1 and 0.5mg/L flocculant concentration on the turbidity removal efficiency. It can be assumed that 30 seconds of at the flocculation stage was not sufficient for the polymer to work to their potential.

5.2.7 Jar test experiment with constant raw water turbidity

The second jar test experiment is to vary the coagulant and flocculant concentration with the same flocculation time 30 seconds which is equal to the retention time in the hydrocyclone. The experimental conditions are shown in Table V-12. In this part of the study, the results were analyzed by the turbidity and the organic matter in the water by 254nm UV absorbance.

Table V-12 Jar test experimental conditions to study the influence of coagulant and flocculant concentration with a constant raw water turbidity

Varied parameter	Experimental value
Coagulant concentration	20, 30, 40, 50, 60, 70mg/L
Flocculant concentration	0.1, 0.5mg/L
Controlled parameter	**Experimental value**
Raw water turbidity	6.17 NTU
Coagulation stage time	1 minute (165 rpm)
Flocculation stage time	30 seconds (45 rpm)
Sedimentation time	10 minutes

5.2.7.1 The influence of coagulant concentration

To verify the coagulant concentration influence on the turbidity removal and the dissolved organic matter, this experiment was set up on a Jar test with 6 different coagulant dosages tested with the same raw water. The coagulant concentrations were 20, 30, 40, 50, 60 and 70mg/L and the raw water turbidity was 6.17NTU. The coagulation mixing was 1 minute at 165rpm with the slow mixing for30 seconds to have the same flocculation stage as in the hybrid reactor at 45rpm. The sedimentation time was 10 minutes for each sample. The polymer concentrations were 0.1 and 0.5mg/L. The result are shown in Figure V-25 and V-26.
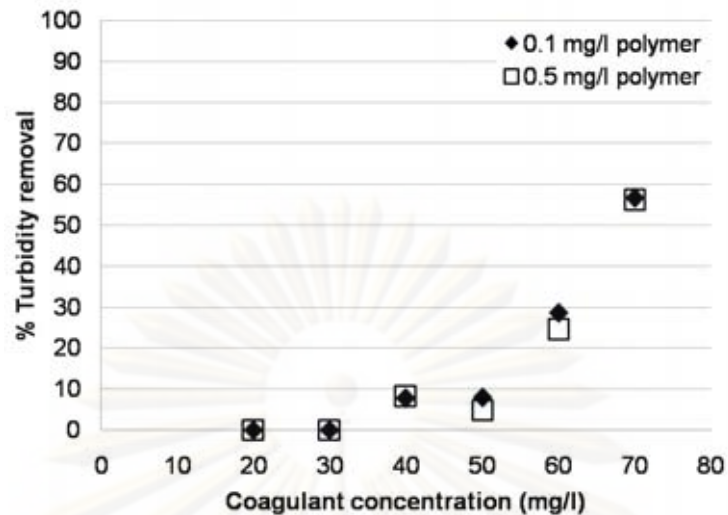
Figure V-25 Coagulant concentrations effect to turbidity removal percentage

From Figure V-25, increasing the coagulant concentration showed that the clarified water turbidity logically decreased. The highest % of turbidity removal is 70mg/L coagulant concentration. There was no difference between 0.1 and 0.5mg/L of polymer. It confirms the previous experiment, which 30 seconds at the flocculation stage was not sufficient for the polymer to work to their potential. It is interesting to work with the hybrid process and see the difference of the results.
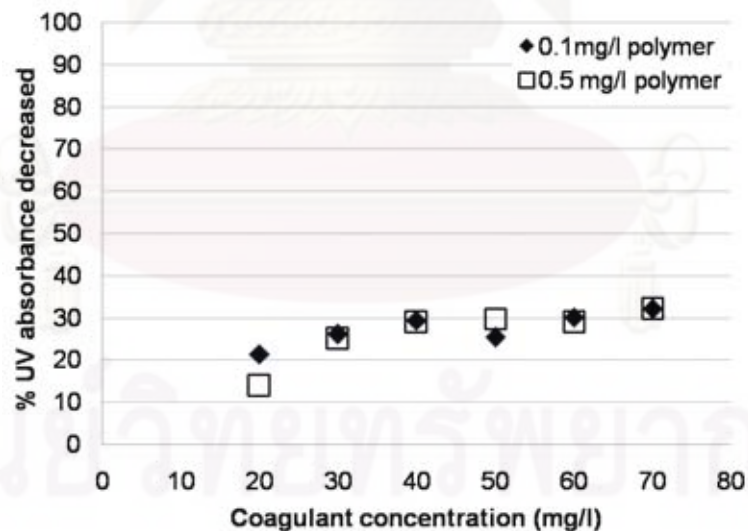
Figure V-26 Coagulant concentrations effect on dissolved organic matter

Figure V-26 illustrates that increasing the coagulant concentration has the slightly trend of increasing the percent of optical density with the filtrated sample analyzed which indicates that the dissolved organic matter is decreased when the coagulant is increased.

This experiment showed the weak point in a lack of flocculation time for the hybrid process (30 seconds). The coagulant concentrations were varied with many different

concentrations but it presented little difference in the results. The flocculant polymer concentration effect had similar results when 0.1 and 0.5mg/L concentrations are used. It can be explained that 30 seconds for the flocculation stage mixing time was not enough for the polymer to function efficiently in the process. It means if the flocculation contact time could be increased, the floc size would be larger and the turbidity removal could be more efficient.

However, the floc size from 30 seconds flocculation stage time was around 0.5mm by observation (See observation data in Appendix D-I). It was acceptable as the hybrid process requires light floc which could agglomerate with the micro bubbles and be separated by the vortex. In addition, the centrifugal force which is proportional to the drag force depends on the project surface of the floc which is greater when the floc size is greater. For that, the large size floc was not desirable because it could be difficult to create the aerated floc and it could be easily broken.

This is a preliminary experiment for the hybrid process to predict the coagulation and flocculation which could occur in a hydrocyclone. But in a jar test experiment, the micro bubbles are not taken into account. The phenomenon would not be exactly the same. However, it is believed that this study is efficient to determine the suitable coagulant and flocculant concentration for the hybrid process.

5.2.8 The flow performance by hybrid process

This part of study is also a preliminary experiment on the Hybrid process in terms of flow performance. The experiment worked with raw water from La Marne River and air pressurized water. The first part is to observe the vortex flow and micro bubble phenomenon. The objective is to assure that this hybrid process could function continuously. The second part is to verify the flow partition between centre zone and wall zone compared with conventional water treatment processes. Each part will explain the method, results and discussion as follows.

5.2.8.1 The vortex flow and micro bubble performance

This experiment is to operate and verify the air pressurized water system. It is operated for 1 hour continuously to observe the micro bubbles performance and the vortex flow inside the hydrocyclone. The air from the net work at 4-5 bar and the water at 4.3 bar, are stored in the saturated tank. There are two electro valves to control the water level inside the saturated tank. If water level rises up to the high position, the electro valve will let the air inside the tank. On the other hand, if water level decreases to the low position, the electro valve will let water in. The flow meter measures the air pressurized water flow rate controlled by the relief valve. Then, the flow rate was varied from 50, 100, 150 and 200L/hr witht 5, 10, 15 and 20% of air pressurized water to the 1000 l/h raw water or 0.0030, 0.0058, 0.0083 and 0.0106 air fraction respectively. The performance will be observed and recorded by a digital camera (CASIO EXILIM, EX-Z 40).

Table V-13 vortex flow and micro bubble performance

Varied parameter	Experimental value
Air pressurized water flow rate	50, 100, 150, 200L/hr
(Air fraction)	(0.0030, 0.0058, 0.0083, 0.0106)
Controlled parameter	**Experimental value**
Raw water flow rate	1000L/hr

5.2.8.2 Result and discussion of the vortex flow and micro bubble performance

The objective of this part is to test the effect of air pressurized water flow rate on hydrodynamic condition; particular attention will be focused on the bubble coalescence phenomenon.

a. *50L/hr air pressurized water flow rate*

The micro bubbles were present in the hydrocyclone. There was no coalescence of the bubbles. The vortex could be seen along the cyclone axis to the top. The system could operate 1 hour continuously.

b. *100L/hr air pressurized water flow rate*

With this flow rate it could be seen clearly that the water became white because of the micro bubbles. The vortex flow spun up to the top with micro bubbles condensed along the cyclone axis.

c. *150L/hr air pressurized water flow rate*

The result was similar to 100L/hr flow rate. The water inside the hydrocyclone became white. The micro bubbles were populated along the cyclone axis with the vortex flow spin up to the top. With the higher air pressurized inlet flow rate, the water level inside the saturate tank decreased rapidly and the electro valve should have controlled the water into the tank. During the operation, when the water level decreased the pressure inside the saturate tank stayed at 4.5bar which was higher than the water pressure (4.3bar). Water could not get inside the saturated tank. A valve was needed to decrease the pressure to allow the water to get inside the tank. While decreasing the pressure, it could be observed that the quality of the micro bubbles decreased in the sense that the water was less white. It was assumed that the micro bubble populations were decreased.

d. 200L/hr air pressurized water flow rate

This flow rate presented the good micro bubbles inside the hydrocyclone. However, there was the same problem as 150L/hr flow rate that the water level inside the tank decreased rapidly which required it to decrease the pressure in the tank in order to operate the system 1 hour continuously. If water level decreased until the saturated tank was empty, the flow that went into the hydrocyclone would be only air.

The air pressurized water from the pilot system could function continuously during 1 hour operation. All the flow rates presented the micro bubble inside the hydrocyclone and there was no micro bubble coalescence. The vortex flow appeared to the top of the reactor as it depends on the raw water inlet flow rate (1000L/hr). From this observation, to choose the air pressurized water flow rate, 100L/hr is considered. It is because this flow rate presented a large amount of micro bubbles more than 50L/hr by observing that water was whiter. While the 150L/hr and 200L/hr had the problem of decreasing the water level inside the tank even though they presented the same quality as 100L/hr.

5.2.8.3 The flow partition between centre and wall zone

Before working with the hybrid process, the flow component between the centre zone and the wall zone has to be considered. With a hybrid process, the centre zone is working as the thickener in which the aerated floc should be separated and exists here while the wall zone is working as the clarifier. For that, to develop the hybrid process and perform in industrial working conditions, it is desired to provide 90% of the clear water from the inlet flow rate and 10% the floc or the sludge from the inlet flow rate.

In the hybrid process, there are two parts that affect the liquid flow component. First, it is the distance between the wall zone effluents which are installed at the same height to the centre zone. If the tubes for the wall zone are higher, the centre zone effluent would be increased. The second part is the weir height of the centre zone effluent as shown in the Figure V-27. If the weir height is high, the centre flow effluent is decreased. For that, this pre-experiment was done to find the maximum possibility to have the flow component close to 90:10 of clear water flow to sludge flow.

The centre zone out let flow rate and wall zone out let flow rate are measured by timing the amount of water and calculated by Equation V-1.

$$Flow\,rate = \frac{water\,weight(kg)}{Time(s)} \times \frac{1}{\rho_{water}\,(kg/m^3)} \qquad \text{Equation V-1}$$
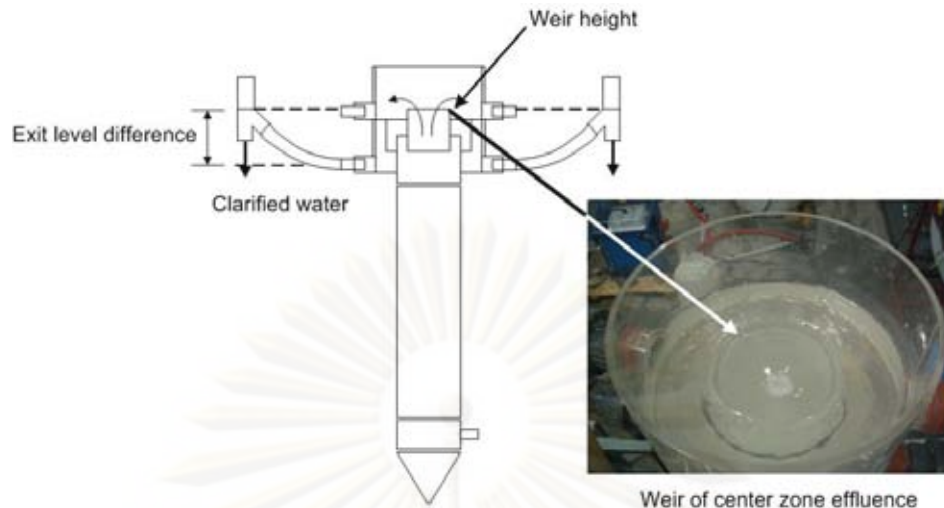
Figure V-27   Weir and the exit level difference

The result of this pre-experiment found out that with 2.5cm of the wall zone (clarified) water tube levels decreased (from the installed position) and the 2.5cm weir height corresponds to a ratio of 70:30 of wall zone to centre zone flow rate is attended. It is the maximum wall zone to centre zone flow rate ratio that the hybrid process could achieve. This flow ratio will remain to work on the hybrid process experiment which will be presented in the next part.

5.2.9   Hybrid process experiment with La Marne River water

This part of study is the most important part of the hybrid process. The pilot was modified and developed from the results of the previous parts. The main objective is to performance water treatment process and separation phenomenon in a continuous operation.

5.2.9.1   Method for the experiment of the hybrid process La Marne River

From the Jar test experiment, the coagulant concentration has chosen 2 values. The lower concentration is 30mg/L because it could achieve the coagulation process in Jar test experiment. The higher value is 70mg/L because it presents the highest % of reduction and has a large difference to distinguish the effect of its concentration. The flocculant polymer concentration remained at 0.1mg/L and 0.5mg/L as in the Jar test experiment.

Each operating condition is run for one hour continuously and is sampled 3 times at; 15 minutes, 30 minutes and 50 minutes from the wall zone and centre zone. The results will be analyzed for turbidity, suspended solids, UV absorbance and separation. The value of each sample was measured three times in order to assure each parameter and to get good accuracy. The operating conditions are shown in the following table.

Table V-14 The operating conditions in hybrid process

Varied parameter	Experimental value
Coagulant concentration	30, 70mg/L
Flocculant concentration	0.1, 0.5mg/L
Air pressurized water flow rate	50, 100, 200L/hr
(Air fraction)	(0.0030, 0.0058, 0.0106)
Controlled parameter	**Experimental value**
Raw water flow rate	1000 l/h
Operating time	1 hour

The results will be discussed as

- Influence of the coagulant concentration to the hybrid process

- Influence of the flocculant concentration to the hybrid process

- Influence of the differences in air pressurized water flow rates to the hybrid process

5.2.9.2 Influence of the coagulant concentration to the hybrid process

This experiment has been done with many conditions to compare certain parameter effects. The first one is to compare the influence of the coagulant concentration. The experimental conditions and results are shown in Table V-14.

Table V-15 Experiment conditions for the influence of coagulant concentration

Varied parameter	Experimental value
Coagulant concentration	30, 70mg/L
Controlled parameter	**Experimental value**
Raw water flow rate	1000 l/h
Flocculation concentration	0.1mg/L
Air pressurized water flow rate	100L/hr
Operating time	1 hour

Table V-16 Results of the experiment for the study the influence of coagulant concentration

Analyzed parameter	Coagulant 30mg/L			Coagulant 70mg/L		
	Raw water	Centre zone	Wall zone	Raw water	Centre zone	Wall zone
Turbidity (NTU)	6.31	7.64	5.58	8.46	8.54	3.30
Suspended solid (mg/l)	3.50	9.70	8.30	3.00	13.70	1.00
% UV absorbance	-	24.27	25.88	-	32.24	35.37
% Turbidity removal	-	-	11.57	-	-	60.70
% Suspended solid removal	-	-	error	-	-	66.67
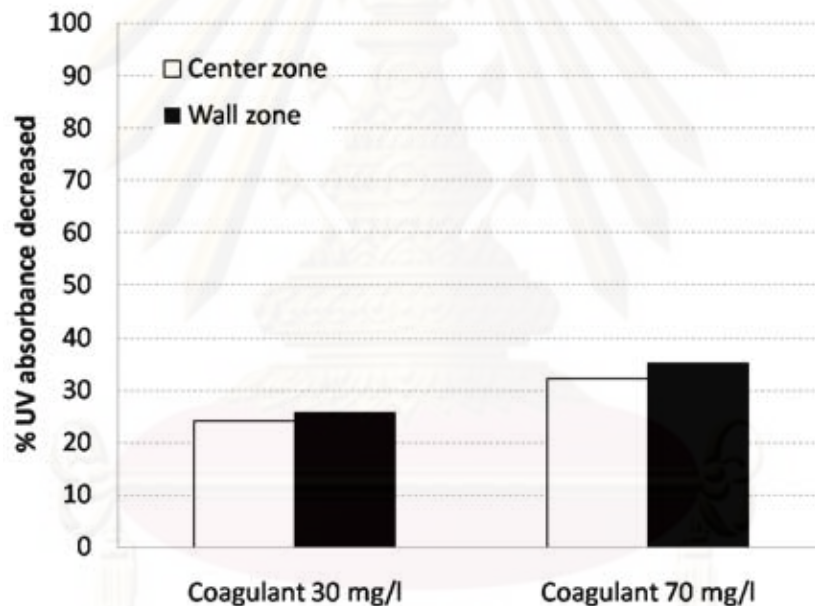
Figure V-28   % of UV absorbance compared between 30 and 70mg/L coagulant concentration

The results from Table V-15 are rearranged to distinguish the parameter¨s effect. In Figure V-28 which shows the % of UV-254nm absorbance decreased which implies that the coagulation process occurred inside the hybrid process and is able to reduce the dissolved organic matter in the water. Increasing the coagulant concentration slightly increased the coagulation process in terms of the UV absorbance. The % of UV-254nm absorbance in this study is between 25- 35% that corresponds to the results from the Jar test experiment. It could be concluded that these two coagulant concentrations achieve produce the coagulation process by the hybrid process.

The % of reduction in Figure V-29 considered the water treatment process by comparing between clarified water and the raw water inlet. It can be seen that 70mg/L coagulant concentration presents high % of turbidity decrease and suspended solid removal (61% and 67% respectively). Note that the error value in suspended solid analyze happened from an experimental error. The raw water inlet had a low turbidity (less than 10 NTU). To analyze suspended solids in this study a 100ml of sample was used which was not enough for low turbidity water. It is recommended for future work to increase the volume of the sample to be more accurate about the amount of mass in the water.
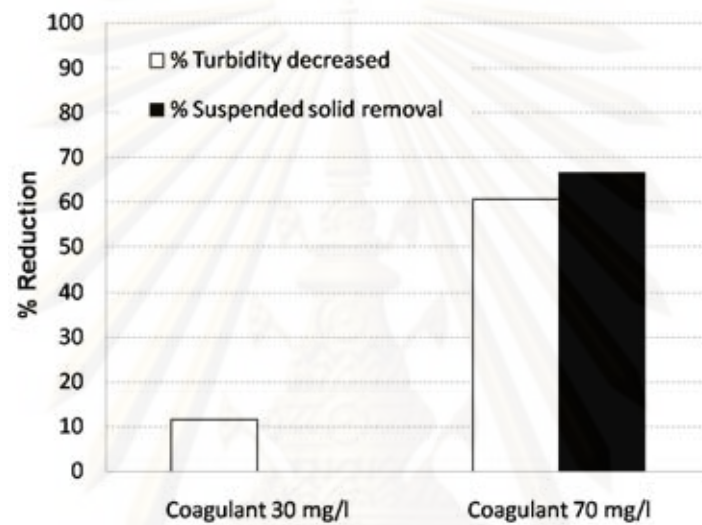
Figure V-29   % of reduction comparing between 30 and 70mg/L coagulant concentration
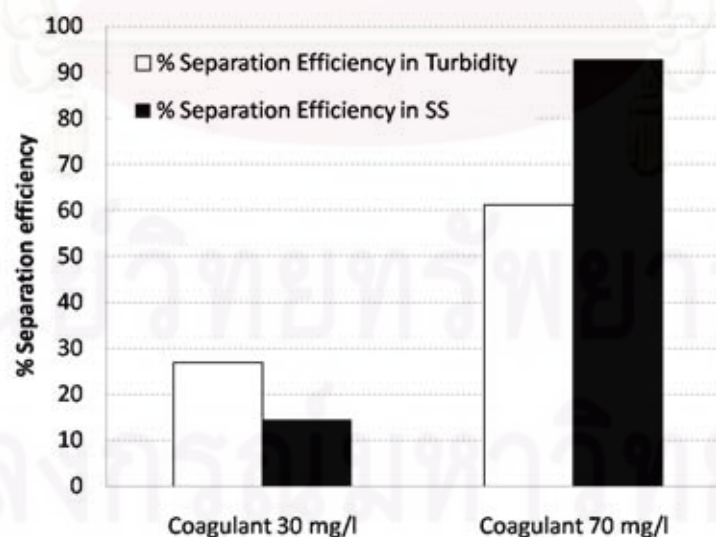
Figure V-30   % of separation efficiency comparing between 30 and 70mg/L coagulant concentration

Considering in the separation phenomenon by the hybrid process in Figures V-30, the floc concentration from the centre zone is compared to the clarified water from the wall zone. It can be seen from the turbidity that the separation phenomena happened with these two coagulant concentrations. With 70mg/l coagulant concentration is obviously presents good separation, 93% separation efficiency in Suspended solid and 61% separation efficiency in turbidity.

This result is very satisfactory in the separation phenomenon with the continuous operation. The hybrid process achieves in creating the aerated floc which is separated to the hydrocyclone axis. The clarified water from 70mg/L coagulant condition presented a constant turbidity effluence (3.30NTU) since the sample had been collected at three different times (15 minutes, 30 minutes and 55 minutes). It also indicated that this hybrid process is able to operate continuously which is a very important point to develop this process for further work.

5.2.9.3 The influence of the flocculant concentration on the hybrid process

In this part the presented results are concerned with the influence of flocculant concentration on the turbidity decreased of the hybrid process. The experimental conditions are shown in Table V-17.

Table V-17 Experimental condition for influence of flocculant concentration

Varied parameter	Experimental value
Flocculant concentration	0.1, 0.2 and 0.5mg/L
Controlled parameter	**Experimental value**
Raw water flow rate	1000 l/h
Coagulant concentration	70mg/L
Air pressurized water flow rate	100L/hr
Operating time	1 hour
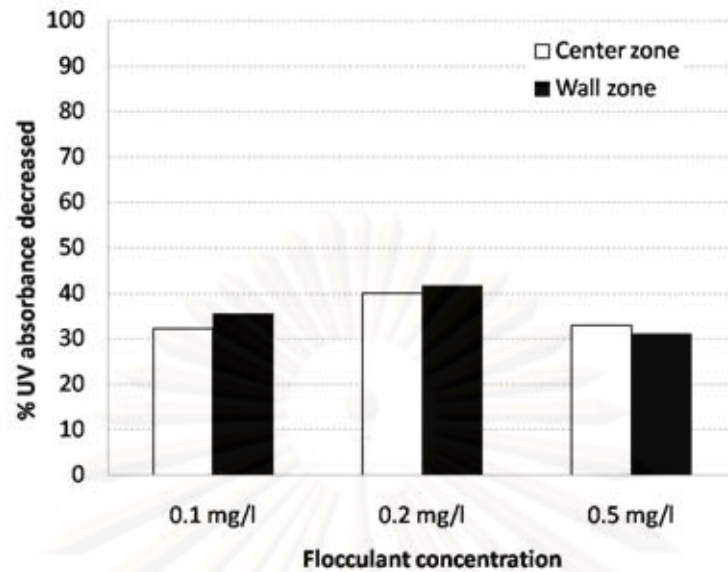
Figure V-31 %UV absorbance decreased with varied flocculant concentration

Figure V-31 illustrates the decrease of dissolved organic matter in water. This experiment uses a constant coagulant concentration (70mg/L), it can be noted that dissolved organic matter had been removed from the water indicated by the % of UV absorbance decrease. It proves that the hybrid process could coagulate the particles. Moreover, the UV absorbance percentage is in the same range as from Jar test experiment (with the same 70mg/L coagulant concentration) which was 32% while the hybrid process presented between 30- 50% UV absorbance removal.
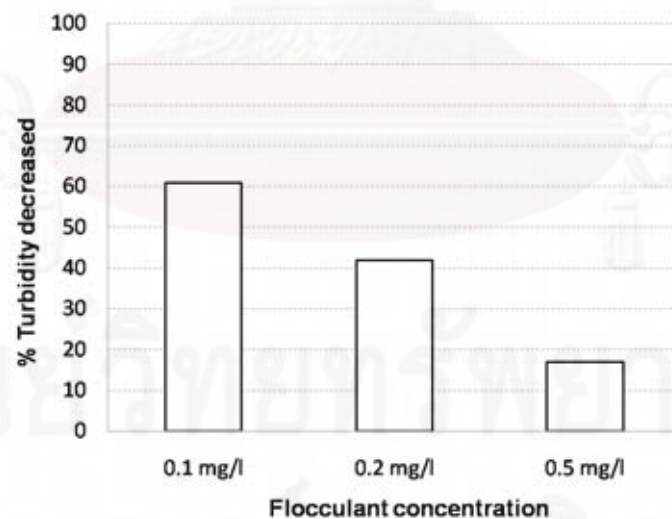
Figure V-32 turbidity removal percentages with varied flocculant concentration

From Figure V-32, it clearly appears that polymer flocculant concentration plays an important role on the water treatment process. The % turbidity decreased is highest with 0.1mg/L polymer (61%). the polymer concentration which had been used in this experiment was 0.1, 0.2 and 0.5mg/L. It was a very high concentration compared to

conventional water treatment processes. From the results, it could be seen that with 0.1mg/L flocculant presents the better results in the hybrid process than the other concentrations. Even though it was expect that the 0.2 and 0.5mg/L should perform a better result. This phenomenon can be explained with two reasons.
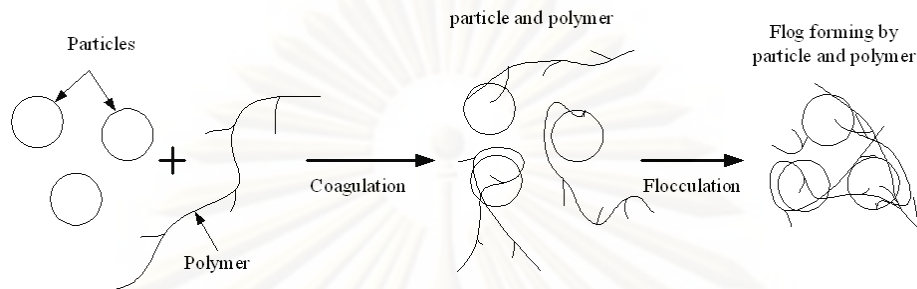
Figure V-33   polymer bridging mechanism

First, there is a limit in adding the polymer flocculant. The synthetic organic polymer which is used as the coagulant to destabilize the colloid has a large molecular weight. Figure V-33 shows the polymer bridging mechanism and how the polymers link with the colloid on its surface. The adsorption is from the different ion of the polymer and colloid or the chemical reaction between the same ion of the polymer and colloid. The connected colloid-polymer which still has a free bond to connect with another colloid is a *destabilized colloid*. This colloid is able to connect to other particles with the polymer as the bridge. This linkage occurs whenever the polymer and the colloid surface are available. Using an over dose of polymer can cause the *restabilization* because many polymer molecules link with the same colloid particle (Metcalf and Eddy, 2004). The polymer has lost its surface for another colloid-polymer and the micro bubble to link. The colloid stabilization is not neutralized and the aerated floc production is not efficient.

Second, 30 seconds of flocculation mixing time in the hybrid process was not enough to achieve polymer performance. There was no significant difference from increasing the polymer flocculant dosage. Therefore, there is an experimental to increase the contact time between the coagulated water and polymer. This will be shown later.
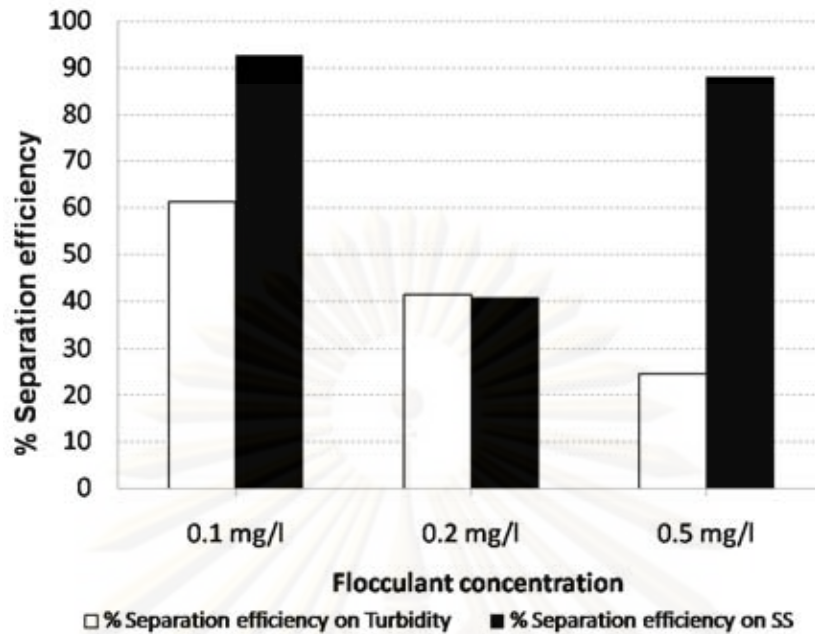
Figure V-34 Separation efficiency with a varied flocculant concentration

The polymer flocculant concentration difference had a separation phenomenon as shown in Figure V-34. The separation efficiency on suspended solids are very high (90%) with 0.1mg/L and 0.5 mg/L. By the way, %separation efficiency on suspended solid at 0.5mg/L polymer has a contrary result to %turbidity removal. It can be discussed that there was some experimental error. However, it is very satisfactory that the separation phenomenon occurred in the hybrid process during continuous operation.

Since from the previous condition result (70mg/L coagulant concentration, 0.1mg/L polymer concentration and 100 air pressurized water flow rate), it was remarkable that there was separation and it presents a satisfactory results better than the other conditions. Consequently, it was interesting to vary the effect of the air pressurized water flow rate to the hybrid process.

5.2.9.4 The influence of the different air pressurized water flow rates to the hybrid process

This part of the study is to vary the air pressurized water (air fraction) in the hybrid process. The vortex flow and micro bubbles performance have been previously studied in part 5.2.8. Consequently, the air pressurized water flow rate is chosen at three values, 50, 100 and 200L/hr that are 0.0030, 0.0058 and 0.0106 air fraction respectively.

Table V-18 Experimental conditions for influence of air pressurized water flow rate

Varied parameter	Experimental value
Air pressurized water flow rate (Air fraction)	50, 100, 200L/hr (0.0030, 0,0058, 0.0106)
Controlled parameter	**Experimental value**
Raw water flow rate	1000 l/h
Coagulant concentration	70mg/L
Flocculant concentration	0.1mg/L
Operating time	1 hour
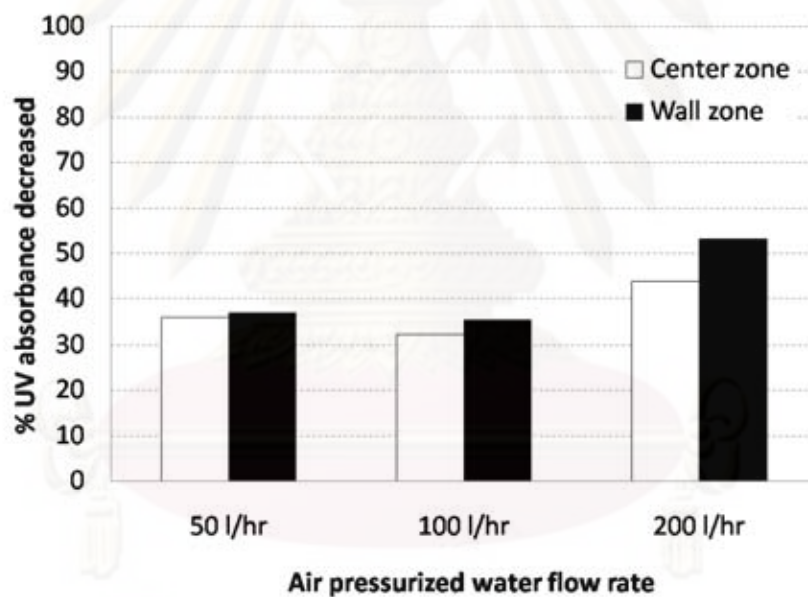
**Figure V-35 The percentage of UV absorbance decreased
with varied air pressurized water flow rates**

Considering the coagulation process by the % of UV-254nm absorbance as shown in Figure V-35, it can be noted that all these three air pressurized flow rates produced the coagulation process. 200L/hr air pressurized water flow rate presented the highest %UV absorbance decreased. It implies that with this flow rate, the dissolved organic matter had been removed better than the other flow rates. However, it is insignificantly different in the % of UV absorbance decrease. All the conditions present a similar range to the results in the Jar test experiment (> 30% UV-254nm absorbance decrease).
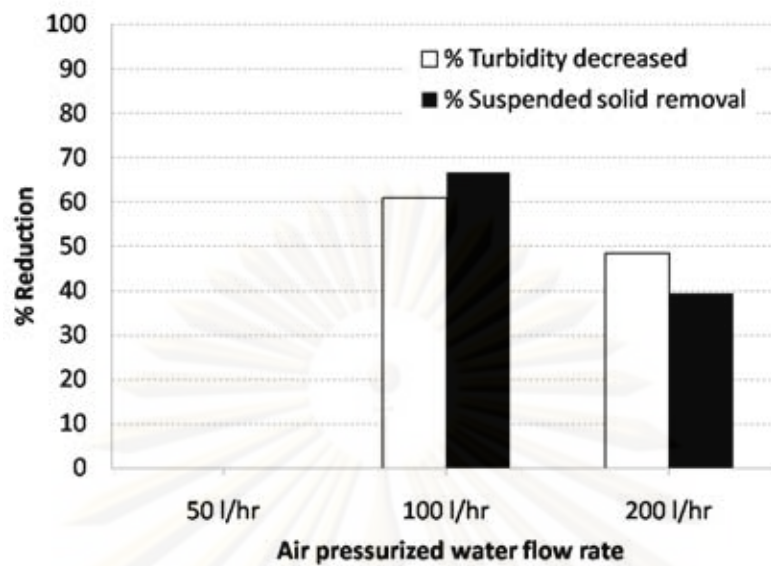
Figure V-36   % of reduction with varied air pressurized water flow rates

In view of % of reduction by the hybrid process with varied air pressurized water flow rate, 50L/hr air pressurized water flow rate (0.0030 air fraction) could not present any %reduction. It means there was no difference in turbidity and suspended solid from the wall zone water to the inlet water. All these three operating conditions used the same flocculant polymer (0.1mg/L), this can be distinguished that not only did the flocculant polymer play an important role on the flocculation process, but also the air pressurized water flow rate. 50L/hr air pressurized water flow rate could not produce the aerated floc to be separated by the vortex flow.

100L/hr air pressurized water presents an excellent % of reduction with turbidity decreased and suspended solid removal (61% and 67% respectively). While with 200L/hr presents 48% and 40% of turbidity decrease and suspended solid removal respectively. This illustrates that the hybrid process achieved water treatment process and is able to remove the floc particle in the water. However, to discuss the difference between the 100L/hr and 200L/hr of air pressurized water flow rates, it is also necessary to consider the % of separation efficiency which will be shown as follows.
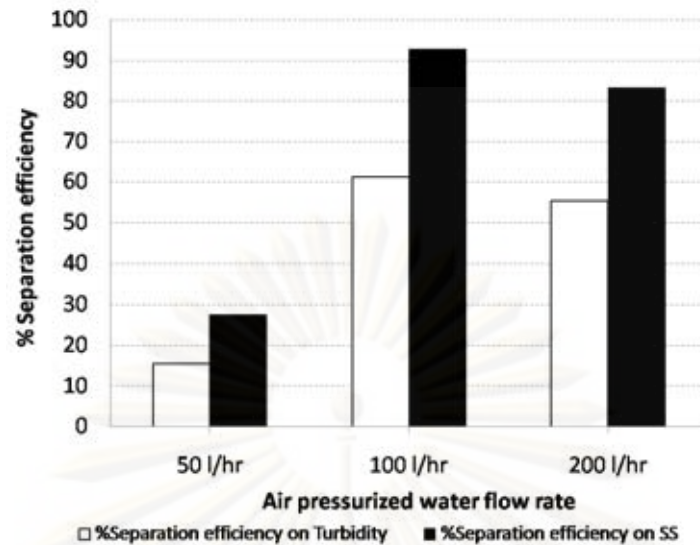
Figure V-37   % of separation efficiency with varied air pressurized water flow rates

Varying the air pressurized flow rate affected the separation in the hybrid process. All these conditions showed in the turbidity and suspended solid results that there was separation between the wall zone and the centre zone. It means that the idea of creating aerated floc that can be separated by the vortex flow inside the hydrocyclone is successful. With turbidity analysis it showed that the operation was stable because the turbidity values were stable as the samples were taken at different times during one hour operation.

The 50L/hr of air pressurized water flow rate presents 15% and 27% of separation efficiency on turbidity and suspended solids while there was no % of reduction by this flow rate. It can be discussed that, with this air pressurized water flow rate could not reduce the floc at the wall zone water (clarified water) as show in Figure V-37 but it could present the separation between wall zone and centre zone water. Except that it presents low % of separation efficiency because there was not enough micro bubbles to support the separation process in the sense of creating the aerated floc.

Whereas the 200L/hr air pressurized water flow rate which is 20% to the raw water flow rate presented the proper conditions both thickening in the centre zone and also clarifying in the wall zone. It presents 55% separation efficiency on turbidity and 83% separation efficiency on suspended solids.

100L/hr air pressurized water flow rate presents 61% separation on turbidity and 93% separation on suspended solids. It is conversely found that higher air pressurized water flow rate (200L/hr) presents poorer results than 100 L/hr. It shows that there is a certain optimum air pressurized flow rate which presents a good entrapment mechanism between the micro bubble and the floc.

Additionally, the ratio of 1000L/hr of treated water and 100L/hr of air pressurized water flow rate was satisfactory because this value, 10% air pressurized water to raw

water flow rate, does not exceed the ratio corresponding to the classical flotation process. In conventional DAF, the typically ratio is 15-50% of pressurized water to treated water (0.1500-0.5000 air fraction) and operating pressures can vary in the range 3-7 bars (Monod, 1991; Kiuru and Vahala, 2009). It is an advantage in the hybrid process from the economical point of view.

In addition, considering the air fraction in the hybrid process from all conditions which are shown in the air fraction table following.

Table V-19 The air fraction in each hybrid experimental condition

Condition	Inlet flow (l/hr)	Coagulant concentration (mg/L)	Flocculant concentration (mg/L)	Air pressurized water flow rate (l/hr)	Air fraction
1	1000	30	0.1	100	0.0057
2	1000	70	0.1	100	0.0057
3	1000	30	0.5	100	0.0056
4	1000	70	0.5	100	0.0055
5	1000	70	0.1	50	0.0030
6	1000	70	0.1	200	0.0104
7	1000	70	0.2	100	0.0056

Compared to the optimum condition in previous study by Pradipat Bumrungsri (2008), the required air fraction range was 0.0082 – 0.0100. The results from the hybrid process with natural water in this study shows that there was aerated floc and separation phenomenon occurring even when the air fraction is less than the required range. As shown in the Table V-19, the air fraction which presented the separation range was 0.0055 – 0.0104 which are less than the air fraction in the conventional DAF.

This hybrid process has many parameters that affect to the optimum conditions. The important difference between the hybrid process with bentonite suspension and with natural water is observed. One parameter that created this different result was the flocculant polymer type. The hybrid process with natural water, using an anionic polymer AN905, was able to create the special floc. Whereas, the bentonite suspension with the hybrid process used cationic polymer FO107 which presented the poorer results in the sense of producing aerated floc and separation. It can be explained that the coagulation process occurred at static mixer. The coagulation mechanism was sweep

coagulation because at this step, pH had not been taken into account (as adsorption and a charge neutralization mechanism). When alum is added to water, it reacts with the water and results in positively charged ions aggregated with particles in the water. With sweep coagulation, alum had been added to excess. Consequently, colloid-coagulant charges had remained positive charged by this step. Therefore, the suitable flocculant polymer is an anionic polymer. Thus, the hybrid process with La Marne River water has been achieved in choosing an anionic coagulant polymer AN905.

The advantage of hybrid process is retention time, 1 minute and 30 seconds. It shows a very compact process comparing to conventional water treatment, coagulation, flocculation and separation which is at least 30 minutes.

Overall the experiments which had done with natural water from the La Marne River, had been successful in the idea of the hybrid process: coagulation, flocculation and flotation in one hydrocyclone reactor. There was aerated floc occurring in the process and it could be separated by the hydrocyclone mechanism. The minimum outlet turbidity removal from hybrid process reached 3.30 NTU. It was satisfactory in the sense of the hybrid process but still not adequate to present to the water industry.

The difficulty of this process is to find the optimum coagulant, flocculant concentration, air fraction and also the hydrodynamics inside. The required optimum floc size is necessary to produce the aerated floc. Then, the aerated floc should be able to rise and be separated by the vortex flow inside the hydrocyclone. For that, the large or heavy floc is not desirable. The flocculant polymer used in this study was high concentration (0.1 to 0.5mg/L). It was because of the lack of retention time for the flocculation process. To develop the hybrid process using less polymer concentration hydrocyclone geometry should be considered in order to increase the retention time for the flocculation stage.

5.2.10 Conclusions

1. The hybrid process development had been successful in terms of creating aerated floc and separation

2. The effluence flow component between wall zone to centre zone (clarified water to concentrated floc) was 70:30

3. The optimum condition in this study was

    -   1000L/hr raw water inlet flow rate

    -   70mg/L coagulant WAC HB

    -   0.1 – 0.2mg/L flocculant polymer AN905

    -   100 – 200L/hr air pressurized water flow rate (10 – 20% to the raw water)

    -   0.0055 – 0.0104 air fraction

4.   The optimum conditions presented

-   3.30 NTU outlet turbidity (from 8.46 NTU raw water) which is 61% turbidity removal

-   66 % Suspended solid decreased

-   91% Separation efficiency

GENERAL CONCLUSIONS

The original principle of this study is to integrate coagulation and flocculation in a hydrocyclone reactor. The tangential water velocity creates the vortex flows which drive the coagulation and flocculation process. The micro bubbles from dissolved air flotation technique are injected simultaneously with raw water and coagulant/flocculant to commence floc formation covers the micro bubbles. Afterwards, these aerated flocs were driven to the hydrocyclone axis by the vortex flows because of their lower density of containing micro bubble inside. The clarified water was separated to the wall zone.

According to four main parts of the study, it can be conclude in each part as follow.

1. **The velocity measurement in the hydrocyclone by oil droplet, Doppler ultrasound velocimetry and CFD modeling.**

The objective of this part was to characterize the hydrodynamic conditions inside the hydrocyclone in terms of the velocity profile by a numerical method, Computational Fluid Dynamics and an experimental method, Doppler Ultrasound Velocimetry technique. These techniques performed the rapid, effective methods due to excellent repeatable results. The hydrodynamics inside hydrocyclone; velocity profiles and velocity gradients explained the phenomena. The results were used as the guide to improve the hybrid process in the experimental step.

2. **The micro bubbles size measurement from the dissolved air flotation by a laser diffraction technique.**

An important parameter of this study was the micro bubble size from dissolved air flotation process. To verify the micro bubble size generated by hybrid process and compare to the conventional DAF, a Laser diffraction technique was considered. The studies worked on influence of saturated pressure and the height level to the micro bubble size. The results proved that the produced micro bubble size from hybrid process was in the range of conventional DAF.

These two parts were the important acknowledge base for the experimental work to further develop for the synthetic raw water and the natural water. Pilot was modified base on the results of these two parts; air pressurized water inlet was installed vertically close to the wall in order to attach directly to the coagulated particle and also avoid the bubble coalescence.

3. **The hybrid process on bentonite suspension**

Coagulation and flocculation process were successful by hybrid process on bentonite suspension. It pointed out the important parameters to be improved for operating with natural water. The experimental works perform the suitable coagulant and flocculant dose and type. Vortex flow performed as in the expected phenomenon that

was the swirl flow movement presented along the cyclone height and the micro bubbles were driven to the cyclone axis without coalescence.

4. The hybrid process on natural river water

From three parts of study as mentioned above, hybrid process was improved with many parameters to operate with natural water from La Marne River, France. The results met the expected phenomena. The coagulation and the flocculation process presented the effective removal percentages. The air fraction was in the suitable range which is lower than the conventional dissolved air flotation process. Aerated floc production was achieved with an important phenomenon that was the separation process. The vortex flow was able to separate the aerated floc to the cyclone axis and the clarified water to the wall zone. The process presented the stable conditions within a continuously operation. The list of the hybrid process characteristic and the optimum condition present in Table V-20

The hybrid process is successful for the first time in the continuous operation with the separation phenomenon. Moreover, it is also the first time the hybrid process has achieved treating the natural water with a new technique in producing the aerated floc which is separated by the vortex flow. This is a very excellent step in water treatment field. It points that the hybrid process is truly possible and it can be further developed to industrial scales with its advantage as a compact water treatment system and small footprint.

Table V-20 The hybrid process characteristic and optimum condition

Parameter	Recommended value
Hydrocyclone geometry	1000mm height and 100mm diameter
Raw water inlet aperture	10mm diameter
Air pressurized water inlet position	Vertically close to the wall
Coagulant position	In a static mixer
Raw water flow rate	1000L/hr
Retention time	90second
Saturated pressure	4.5bars
Coagulant concentration	70mg/L aluminum sulfate WAC HB
Flocculant concentration	0.1 - 0.2mg/L anionic polymer AN905
Air pressurized water flow rate	100 - 200L/hr
Air fraction	0.0055 – 0.0104
Flow partition	Clarified water : Concentrated floc 70:30

PERSPECTIVE OF THIS STUDY

Hybrid process is developing and shows the possibility to perform in the industrial scale. To improve the process, there are some recommends as follow.

1. The separation between clarified water and floc concentration should be improved by enlarge the reactor diameter in order to have clearly zone between center and wall zone. On the other hand, the flow rate is necessary to increase to maintain the same inlet velocity inside hydrocyclone to have the same hydrodynamic condition.

2. Using CFD to improve the process is interesting by simulating two phases; water liquid and solid particle in order to be able to distinguish the particle phenomenon or to be able to indicate the separation position in hydrocyclone.

3. It is interesting to improve the vortex flow on the top section of cyclone by adding the tangential injection of the clarified water as shown in Figure V-38. Moreover, using the CFD to predict the phenomenon that will happen in this hybrid configuration.
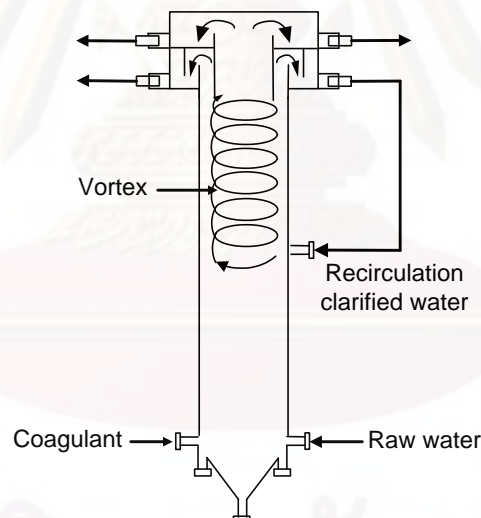
Figure V-38   The perspective sketch of hybrid reactor

REFERENCES

Bai, Z., Wang, H. Tu, S., 2008. Experimental study of flow patterns in deoiling hydrocyclone. **Minerals Engineering**, doi10.1016/j.mineng.2008.09.003.

Bamrungsri, P. et al., 2008. Development of a simple experimental method for the determination of the liquid field velocity in conical and cylindrical hydrocyclones. **Chemical Engineering Research and Design**, 86, 1263-1270.

Bardow, A. et al., 2008. Sensitivity-based analysis of the k-ε model for the turbulent flow between two plates. **Chemical Engineering Science**, 63, 4763-4775.

Chaiyaporn Puprasert. 2004a. **Contribution a la mise au point d'application specifique des hydrocyclones en traitement des eaux**. French thesis (Ph.D. Eng), Génie des Procédés de l'Environnement. Institut National des Sciences Appliquées de Toulouse.

Chesters, A.K. and Hofman, G. 1982. Bubble coalescence in pure liquids. **Applied Scientific Research** 38 : 353-361.

Chiné, B., Concha, F., 2000. Flow patterns in conical and cylindrical hydrocyclone. **Chemical Engineering Journal**, 80, 267-273.

De Rijk, S.E., Van der Graaf, J.H.J.M and Den Blanken, J.G. 1994. Bubble size in flotation thickening. **Water Research.** 28, 465 – 473.

Degrémont, SA. 2005. **Mémento technique de l'eau/Degrémont**. 2 Vol. 10th ed. France.

Dyakowski, T. Williams, R.A., 1996. Prediction of high solids concentration Region within a hydrocyclone. **Poder technology,** 87, 43-47.

Edzwald, J.K. 1995. Principles and applications of dissolved air flotation. **Water Science Technology**. 31, No. 3-4, 1-23

Englert, A.H., Rodrigues, R.T. and Rubio, J. 2009. Dissolved air flotation (DAF) of fine quartz particles using an amine as collector. **Mineral Processing**. 90, 27-34.

Féris, L. A. and Rubio, J. 1999. Dissolved Air Flotation (DAF) performance at low saturation pressure. **Filtration & Separation.** 61-65.

Flint, L.R. and Howarth, W.J. 1971. The collision efficiency of small particles with spherical air bubbles. **Chemical Engineering and Sciences**. 26, 1155-1168.

Hebrard, G. et al. 2008. Patent submitted 25 April 2008, Procédé de traitement de fluide par hydrocyclone, French patent ref. 085783.

Heinanen, J., Jokela, P. and Peltokangas, J. 1992. **Experimental studies on the kinetics of flotation.** Chemical Water and Wastewaer Treatment II, R. Klute and H.H. Hahn (Eds.). Springer-Verlag, New York, USA, pp. 247-262.

Ho. L and Newcombe, G. 2005. Effect of NOM, turbidity and floc size on the PAC adsorption of MIB during alum coagulation. **Water Research** 39: 3668-3674

Hudson, J.B. et al. 2009. Micro-bubble size distribution measurements by laser diffraction technique. **Minerals Engineering**. 22, 330-335.

Jonas, B. Hannes, V., 2007. Review Experimental hydrocyclone flow field studies. **Separation and Purification Technology**, 53, 8-20.

Karagüzel, C. 2010. Selective separation of fine albite from feldspathic slime containing colored minerals (Fe=Min) by batch scale dissolved air flotation (DAF). **Minerals Engineering**. 23, 17-24.

Kathy, A. N., Ian, S., Michael, A.C. and Geoffrey, W.S. 2003. Wter treatment design for site remediation at Casey Station. **Cold Regions Science and technology** 37 : 169 - 185

Kelsall, D.F., 1952. A study of the motion of solid particles in a hydrocyclone. **Trans Institut Chem Eng**, 30, 87-108.

Kiuru, H and Vahala, R. 2009. Dissolved Air Flotation in Water and Waste Water Treatment. **Wat. Sci. Tech**, 43**:** 8.

Kraipech, W., Suksangpanomrung, A., Nowakowski, A.F., 2007. The simulation of the flow within a hydrocyclone operating with an air core and with an inserted metal rod. **Chemical Engineering Journal**, 143, 51-61.

Launder, B.E. and Sharma, B.I., 1974. **Application of the energy-dissipation model of turbulence to the calculation of flow near a spinning disc**. Letters in Heat and Mass Transfer, 1, 131-137.

Li, H.Z. et al. 2001. Towards the understanding of bubble interactions and coalescence in non-Newtonian fluid:a cognitive approach. **Chemical Engineering Science** 56 : 6419-6425.

Malvern. **Malvern Instrument Spraytec User Manual**. MAN0368 Issue 1. Nov. 2005.

Menezes, F.M., Amal, R., Luketina, D. 1996. Removal of particles using coagulation and flocculation in a dynamic separator. **Powder Technology** 88 : 27-31.

Metcalf & Eddy. 2004. **Wastewater Engineering Treatment and Reuse**. 4th ed. New York: McGraw-Hill.

Monod, J. 1991. **Water treatment handbook**. Vol 1. 6th ed. Rueil-Malmaison: Degrémont, 136 – 145.

Narashimha, M., Brennan, M., Holtham, P.N., 2007a. A review of CFD modelling for performance predictions of hydrocyclone. **Engineering Applications of Computational Fluid Mechanics**, 1,109-125.

Narashimha, M., Brennan, M., Holtham, P.N., 2007b. Prediction of magnetite segregation in dense medium cyclone using computational fluid dynamics technique. **Mineral Processing**, 82, 41-56.

Ohasi, H., Maeda, S., 1958. The velocity distribution within a hydrocyclone operating without an air core. **Canadian Journal of Chemical Engineering**, 22, 200.

Pradipat Bumrungsri. 2007. Hybrid Process : **Hydrocyclone, Coagulantion-Flocculation and Floatation in water treatment process**. Génie des Procédés de l'Environnement. Institut National des Sciences Appliquées de Toulouse. Environmental management, Graduate school, Chulalongkorn university.

Puprasert, C. et al. 2004b. Potential of using Hydrocyclone and Hydrocyclone equipped with Grit pot as a pre-treatment in run-off water treatment. **Chemical Engineering and Processing** 43 : 67-83.

Rawle, A., 2002. The importance of particle size to the coating industry part I: particle size measurement, **Advances in Colour Science and Technology** 5(1), 1-12.

Reynolds and Richards. 1995. **Unit operation and processes in environmental engineering.** 2nd ed. Cengage Engineering.

Rodrigues, R.T. and Rubio, J. 2003. New basis for measuring the size distribution of bubbles. **Minerals Engineering**. 16, 757-765.

Rosa, J.J. and Rubio, J. 2005. The FF (flocculation-flotation) Process. **Minerals Engineering** 18 : 701 -707.

Sanada, T., Watanabe, M. and Fukano, T. 2005. Effects of viscosity on coalescence of a bubble upon impact with a free surface. **Chemical Engineering Science** 60 : 5372-5384.

Signal processing S.A., 2000. **DOP2000 User's manual**. Polytec GmbH. Switzerland.

Slack, M.D., et al., 2000. Advances in cyclone modelling using unstructured grids. **Chemical Engineering Research and Design**, 78(A), 1098-1104.

Vorasiri Siangsanun. 2006. **Hybrid process: hydrocyclone, coagulation-flocculation and flotation in water treatment process**. Department of Environmental Engineering. Faculty of Engineering. Chulalongjkorn university.

Tchobanoglous, G. et al. 2004. **Wastewater engineering: treatment, disposal and reuse**. 4th ed. Singapore: Metcalf&Eddy, Inc. McGraw-Hill

Udaya, B. K., et al., 2006. Simulation and experimental validation studies on hydrocyclone. **Mineral Engineering**, 20, 60-71.

Xu, R., 2002. Particle Chracterization: Light Scattering Methods. **Particle Technology Series**, vol 13. Kluwer Academic Publishers. 397p.

APPENDICES

APPENDIX A

MATERIAL

Appendix A-1: Characteristic of bentonite BENTONIL CV15T

Table A-1   Characteristic of bentonite BENTONIL CV15T

Property	
Appearance	Clear powder, beige to pink
Average particle size	0.4
Water content	14 (maximum)
Sieve of 75 µm (%)	4 (maximum wet)
Swelling	11 (minimum, test CTIF)
Density apparent non packed	0.7
Density apparent packed	0.9
Specific weight	2.2
pH gel to 5%	10

Appendix A-2: Characteristic and property of polymer FO107

Table A-2   Characteristic of polymer FO107 (FO9107)

Property	
Appearance	White powder
Cationic charge	Low
Molecular weight	8
Mesh size	2.0 mm
Approximative specific weight	0.8
Brookfield viscosity in cps	
5.0g/L	130 cps
2.5g/L	30 cps
1.0g/L	8 cps
Maximum concentration	15g/L
Usual concentration	5g/L
Dissolution time	60 min
Stability of this solution	1 day
Stability of dry product	12 months

Flocculation after coagulation, especially on water filters or drinking

Retention of fillers or pigments (kaolin, talc) in the paper,

Conditioning of sludge organic

Settling and filtration of metal derivatives under acidic

Flocculation of silica.
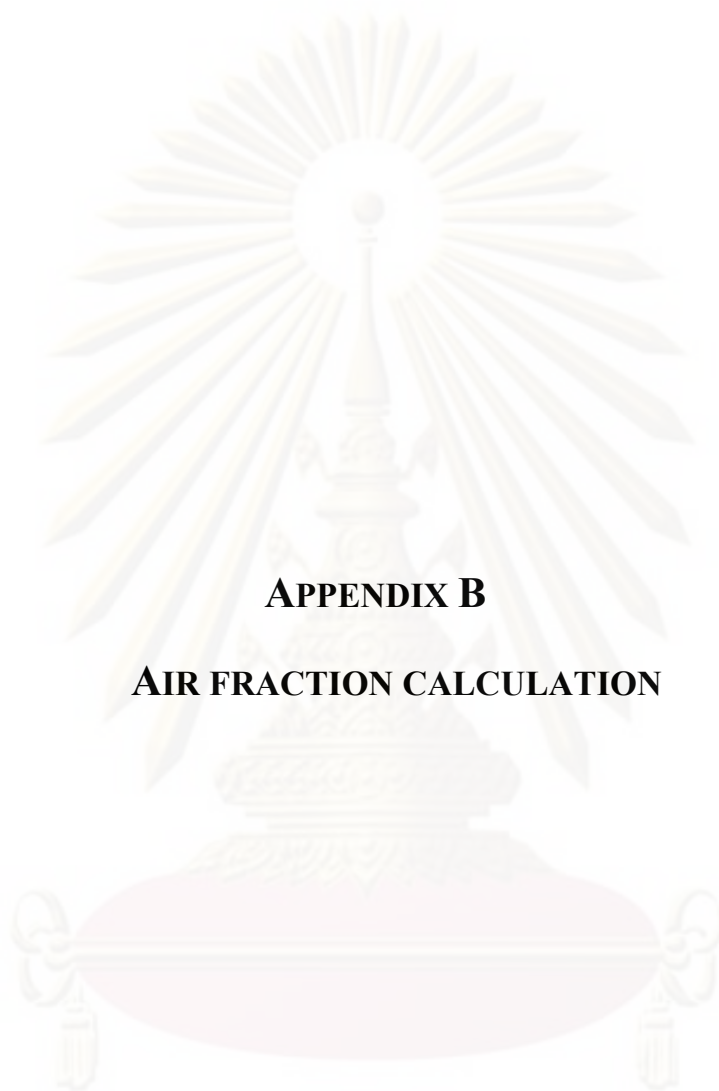
APPENDIX B

AIR FRACTION CALCULATION

Appendix B-I: Air fraction calculation

Henry's law for dissolved gases

The equilibrium or saturation concentration of gas dissolved in a liquid is a function of the type of gas and the partial pressure of the gas in contact with the liquid. The relationship between the mole fraction of the gas in the atmosphere above the liquid and the mole fraction of the gas in the liquid is given by the following from of Henry's law:

$$p_g = \frac{H}{P_T} x_g$$

When p_g = mole fraction of gas in air, $\dfrac{mole\ gas}{mole\ are}$

H = Henry's law constant, $\dfrac{atm(mole\ gas\,/\,mole\ air)}{(mole\ gas\,/\,mole\ water)}$

P_T = total pressure, usually 1.0 atm

x_g = mole fraction of gas in water, $\dfrac{mole\ gas}{mole\ water}$

$$= \frac{mole\ gas(n_g)}{mole\ gas(n_g) + mole\ water(n_w)}$$

For air p_g = 1.0 $\dfrac{mol\ gas}{mole\ air}$

H = 66400 $\dfrac{atm(mole\ gas\,/\,mole\ air)}{(mole\ gas\,/\,mole\ water)}$

x_g = $\dfrac{p_g \times P_T}{H}$

x_g = $\dfrac{1.0(mole\ air\,/\,mole\ air) \times 1.0\ atm}{66400atm\ \dfrac{(mole\ gas\,/\,mole\ air)}{(mole\ gas\,/\,mole\ water)}}$

$$= 1.506 \times 10^{-5}\ \frac{mole\ air}{mole\ water}$$

Air mole calculatioin

1 Liter of water contains $\dfrac{1000\ g}{18\ g\,/\,mole} = 55.6\ mole$

$$\frac{n_g}{n_g + n_w} = 1.506 \times 10^{-5} \; \frac{mole\;air}{mole\;water}$$

$$\frac{n_g}{n_g + 55.6} = 1.506 \times 10^{-5} \; \frac{mole\;air}{mole\;water}$$

$$n_g = 8.373 \times 10^{-4} \; \frac{mole\;air}{L}$$

Pressure (bars $\approx$ atm)	n_g (mole Air/L)
1.0	0.837×10^{-3}
2.0	1.675×10^{-3}
2.5	2.093×10^{-3}
3.0	2.512×10^{-3}
3.5	2.931×10^{-3}
4.0	3.350×10^{-3}

The saturated concentration of the air at the different pressure

Pressure (bars)	Concentration of Air (mg/l): C_{air}
1.0	24.26
2.0	48.52
2.5	60.63
3.0	72.77
3.5	84.91
4.0	97.05
4.5	109.17
5.0	121.30

Appendix B-II: Air fraction calculation

Pressure 4 bars the concentration of Air   =   97.05mg/L

The mass flow rate of air   = $C_{air} \times Q_{air\;pressurized\;water}$

$$= \quad 97.05 \frac{mg}{l} \times 148 \frac{l}{hr} \times \frac{1g}{1000mg}$$

$$= \quad 14.36 \text{ g/hr}$$

Mole air flow rate (mol/hr) weight $\quad = \quad$ Mass flow rate $\times$ Air molecular weight

$$= \quad 14.36 \frac{g}{hr} \times \frac{1}{28.97} \frac{mol}{g}$$

$$= \quad 0.4958 \text{ mol/hr}$$

Air flow rate (l/hr) $\quad = \quad 0.4958 \frac{mol}{hr} \times 24.04 \frac{l}{mol} (at\, 20°C)$

$$= \quad 11.919 \text{L/hr}$$

Air flow rate with 70% system efficiency $\quad = \quad 11.919 \times 0.7$

$$= \quad 8.343 \text{L/hr}$$

Air fraction $\quad = \quad \dfrac{Q_{air}}{Q_{raw\,water} + Q_{coagulant} + Q_{air\,pressurized\,water}}$

$$= \quad \dfrac{8.343 \dfrac{l}{hr}}{1000 + 0.488 + 148 \dfrac{l}{hr}}$$

$$= \quad 0.0073$$
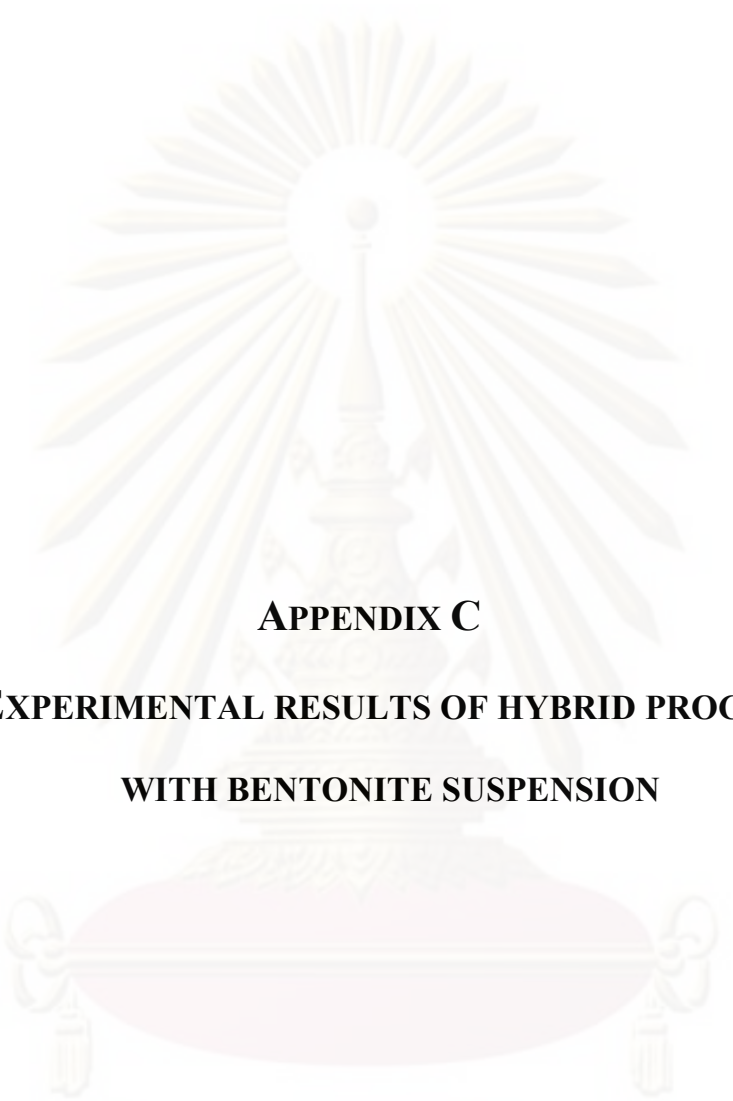
Table B-1   The air fraction in each condition for chapter V

Condition	Raw flow rate l/hr	Alum mg/l	Polymer mg/l	Air pressurized flow l/hr	Air flow rate l/hr	Air fraction
1	1000	30	0.1	100	6.341	0.0057
2	1000	70	0.1	100	6.341	0.0057
3	1000	30	0.5	100	6.341	0.0056
4	1000	70	0.5	100	6.341	0.0055
5	1000	70	0.1	50	3.171	0.0030
6	1000	70	0.1	200	12.683	0.0104
7	1000	70	0.2	100	6.341	0.0056
8	1000	70	0.2	100	6.341	0.0056
9	1000	0	0	50	3.171	0.0030
10	1000	0	0	100	6.341	0.0058
11	1000	0	0	150	9.512	0.0083
12	1000	0	0	200	12.683	0.0106

APPENDIX C

EXPERIMENTAL RESULTS OF HYBRID PROCESS

WITH BENTONITE SUSPENSION

Experimental results of hybrid process with bentonite suspension

Appendix C-I: Bentonite suspension 0.10g/L

Flow rate partition

Coagulant	Flow rate (l/hr)		Total flow l/hr	Air flow rate l/hr	Air fraction
	Centre	Wall			
Polymer 0.1	678	470	1148	8.315	0.0072
Polymer 0.5	687	407	1095	5.342	0.0049
Alum 15	610	440	1050	2.797	0.0011

Turbidity

Coagulant	Turbidity (NTU)		% turbidity removal		% separation efficiency
	Centre	wall	Centre	Wall	
Blank	22.33	0.00			
Polymer 0.1	4.83	4.83	78.37	78.37	No
Polymer 0.5	4.50	3.30	79.85	85.22	26.67
Alum 15	13.67	14.67	38.78	34.30	No

Suspended solid

Coagulant	Suspended solid (mg/l)		% suspended solid removal		% separation efficiency
	Centre	Wall	Centre	Wall	
Blank	0.100				
Polymer 0.1	0.063	0.060	37	40	4.76
Polymer 0.5	0.055	0.040	45	60	27.27
Alum 15	0.100	0.075	0.5	25	25.00

Suspended solid Mass balance calculation (mg/hr)

QC in = QC centre + QC wall

	Inlet	Centre	Wall	Outlet
Polymer 0.1mg/L	114.75	42.68	28.20	70.88
Polymer 0.5mg/L	109.48	37.80	16.30	54.10
Alum 15mg/L	104.96	60.95	33.01	93.96

Appendix C-II: Bentonite suspension 0.25g/L

Flow rate partition

Coagulant	Flow rate (l/hr)		Total flow l/hr	Air flow rate l/hr	Air fraction
	Centre	Wall			
Polymer 0.1	838.41	554.85	1393.26	22.16	0.0159
Polymer 0.5	799.37	418.57	1217.94	12.28	0.0101
Alum 5	730.00	511	1241	13.58	0.0107
Alum 15	702.86	442	1144.86	8.17	0.0057

Turbidity

Coagulant	Turbidity (NTU)		% Efficiency		% separation efficiency
	Centre	Wall	Centre	Wall	
Blank	55.665				
Polymer 0.1	30.67	32	44.90	42.51	0
Polymer 0.5	19.83	15.33	64.38	72.46	22.6929
Alum 5	29.67	23	46.70	58.68	22.4806
Alum 15	29.33	19	47.31	65.87	35.2199

Suspended solid

Coagulant	Suspended solid (mg/l)		% suspended solid removal		% separation efficiency
	Centre	Wall	Centre	Wall	
Blank	0.227				
Polymer 0.1	0.145	0.15	36.26	34.07	0
Polymer 0.5	0.158	0.155	30.55	31.87	1.8987
Alum 5	0.14	0.14	38.46	38.46	0
Alum 15	0.15	0.14	34.07	38.46	6.6667

Suspended solid Mass balance calculation (mg/hr)

QC in = QC centre + QC wall

	Inlet	Centre	Wall	Outlet
	3	1	8	2
Polymer 0.1mg/L	16.97	21.57	3.23	04.80
	2	1	6	1
Polymer 0.5mg/L	77.08	26.30	4.88	91.18
	2	1	7	1
Alum 5mg/L	82.33	02.20	1.54	73.74
	2	1	6	1
Alum 15mg/L	60.46	05.43	1.88	67.31

Appendix C-III: Bentonite suspension 0.50g/L

Flow rate partition

Coagulant + flocculant	Flow rate (l/hr)		Total flow (l/hr)	Air flow rate (l/hr)	Air Fraction
	Centre	Wall			
Blank	1000				
Alum 5 + Polymer 0	922.48	433.9	1356.38	20.09	0.0146
Alum 5 + Polymer 0.1	977.82	420.72	1398.54	22.47	0.0158
Alum 5 + Polymer 0.5	1024.14	250.7	1274.84	15.49	0.0119
Alum 15 + Polymer 0	753.03	474.22	1227.25	12.81	0.0091
Alum 15 + Polymer 0.1	782.09	466.67	1248.76	14.02	0.0099
Alum 15 + Polymer 0.5	918.79	283.69	1202.48	11.41	0.0081

Turbidity

Coagulant + flocculant	Turbidity (NTU)		% turbidity decreased		% separation efficiency
	Centre	Wall	Centre	Wall	
Blank	122				
Alum 5 + Polymer 0	74	75	39.34	38.52	0
Alum 5 + Polymer 0.1	68	63	44.26	48.36	7.35
Alum 5 + Polymer 0.5	43	41	64.75	66.39	4.65
Alum 15 + Polymer 0	65	68	46.72	44.26	0
Alum 15 + Polymer 0.1	66	68	45.90	44.26	0
Alum 15 + Polymer 0.5	41.5	51.5	65.98	57.79	0

Suspended solid

Coagulant + flocculant	Suspended solid (mg/l)		% SS removal		% separation
	Centre	Wall	Centre	Wall	
Blank	0.42				
Alum 5 + Polymer 0	0.23	0.22	45.24	47.62	4.35
Alum 5 + Polymer 0.1	0.26	0.27	38.10	35.71	0.00
Alum 5 + Polymer 0.5	0.25	0.23	40.48	45.24	8.00
Alum 15 + Polymer 0	0.27	0.29	35.71	30.95	0.00
Alum 15 + Polymer 0.1	0.26	0.25	38.10	40.48	3.85
Alum 15 + Polymer 0.5	0.225	0.245	46.43	41.67	0.00

Suspended solid Mass balance calculation (mg/hr)

QC in = QC centre + QC wall

	Inlet	Centre	Wall	Outlet
Alum 5 + Polymer 0	569.68	212.17	95.46	307.63
Alum 5 + Polymer 0.1	587.39	254.23	113.59	367.83
Alum 5 + Polymer 0.5	535.43	256.04	57.66	313.70
Alum 15 + Polymer 0	515.45	203.32	137.52	340.84
Alum 15 + Polymer 0.1	524.48	203.34	116.67	320.01
Alum 15 + Polymer 0.5	505.04	206.73	69.50	276.23
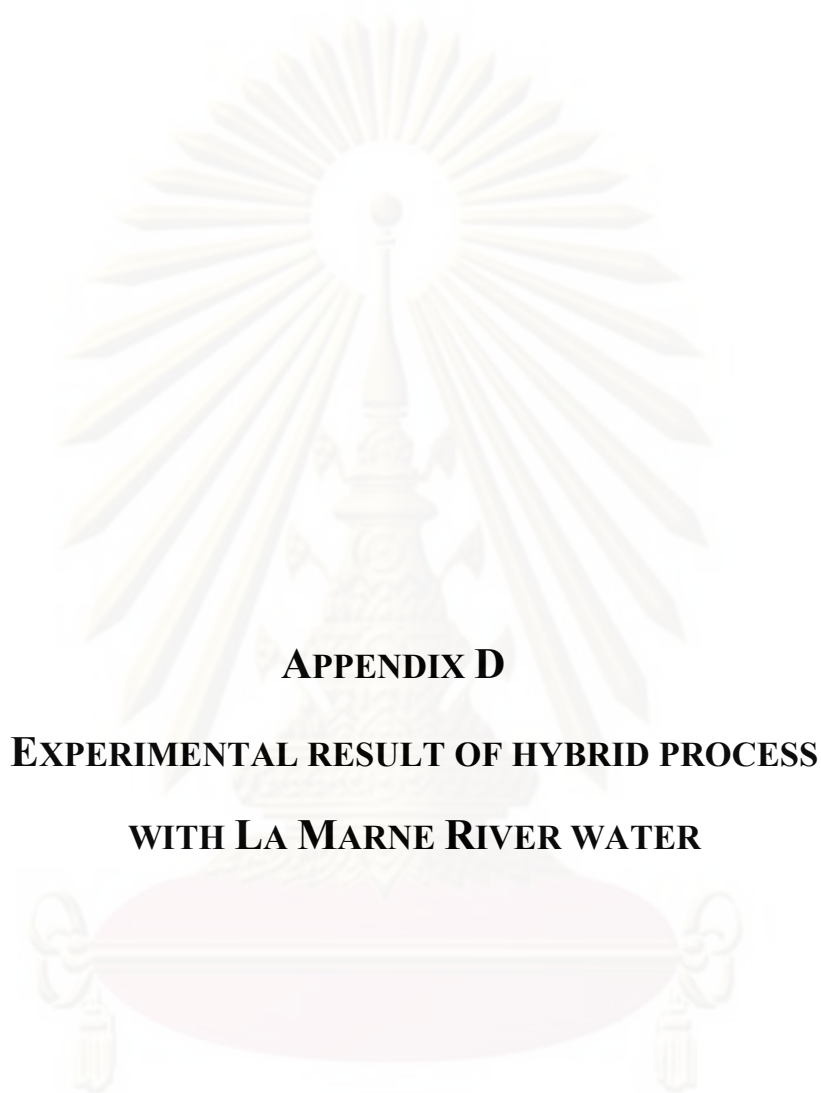
APPENDIX D

EXPERIMENTAL RESULT OF HYBRID PROCESS

WITH LA MARNE RIVER WATER

Appendix D-I: Jar test experiment with varied flocculation time

COAGULATION / SEDIMENTATION TEST							
Coagulant(s):		WAC HB (SM: 6.06532g/L)					
Polymer:		AN 905 (SM: 0.01883g/L)					
Beaker No.	Raw water	**1**	**2**	**3**	**4**	**5**	**6**
Dose coagulant (mg/l)		28	28	28	28	28	28
Dose polymer (mg/l)		0.1	0.5	0.1	0.5	0,1	0,5
Flocculation time		30 sec	30 sec	1 min	1 min	15 min	15 min
pH	8.06	8.00	7.96	7.98	7.95	7.95	7.94
Temperature (°C)	22,5	22.5	22.4	22.6	22.6	22.6	22.6
Flocs size		Poor-	Poor	Poor	Poor	Very good	excellent
Turbidity (NTU)	6.11 6.14	6.46 5.76	5.36 5.28	5.22 4.79	5.61 5.42	0.66 0.65	1.12 1.17
Average turbidity	6.13	6.11	5.32	6.00	5.51	0.65	1.14
DO 254nm NF (abs/5cm)	0.370	0.345	0.303	0.320	0.313	0.208	0.228
DO 254nm F (abs/5cm)	0.249	0.197	0.190	0.189	0.186	0.188	0.188
DO 254nm NF (abs/m)	7.400	6.900	6.060	6.400	6.260	4.160	4.560
DO 254nm F (abs/m)	4.980	3.940	3.800	3.780	3.720	3.760	3.760
Turbidity decreased (%)		0.3	13.2	2.1	10.1	89.4	81.4
DO NF reduction (%)		6.8	18.1	13.5	15.4	43.8	38.4
DO F reduction (%)		20.9	23.7	24.1	25.3	24.5	24.5

Remark: **Coagulation 1 min at 160tr/min**
Flocculation 30 sec at 15 min at 45tr/min
Sedimentation 10 min
F : Filtrated analysis
NF : Non filtrated analysis

Floc size observed	**N**	**Poor**	**Quite good**	**Good**	**Very good**	**Excellent**
	Non floc visible	≤ 0.5 mm	≈ 0.5 mm	0.5 to 1 mm	1 to 1.5 mm	> 1.5 mm

COAGULATION / SEDIMENTATION TEST
Coagulant(s): WAC HB (SM: 6.06532g/L)
Polymer: AN 905 (SM: 0.01883g/L)

Beaker No.	Raw water	1	2	3	4	5	6
Dose coagulant (mg/l)		40	40	40	40	40	40
Dose Polymer (mg/l)		0,1	0,5	0,1	0,5	0,1	0,5
Flocculation time		30 sec	30 sec	1 min	1 min	15 min	15 min
pH	7.92	7.81	7.79	7.79	7.80	7.80	7.80
Temperature (°C)	21,8	21.8	21.7	21.8	21.8	22	22
Flocs size		Poor	Poor	Quite good	Quite good	Very good	Excellent
Turbidity (NTU)	10 10.1	8.75 8.87	8.06 7.81	6.76 6.76	5.96 5.82	0.67 0.56	0.81 0.82
Average turbidity	10.05	8.81	5.32	6.76	5.89	0.61	0.81
DO 254nm NF (abs/5cm)	0.389	0.369	0.325	0.329	0.305	0.192	0.198
DO 254nm F (abs/5cm)	0.250	0.181	0.177	0.194	0.178	0.181	0.198
DO 254nm NF (abs/m)	7.780	7.380	6.500	6.580	6.100	3.840	3.960
DO 254nm F (abs/m)	5.000	3.620	3.540	3.880	3.560	3.620	3.960
Turbidity decreased (%)		12.3	47.1	32.7	41.4	93.9	91.9
DO NF reduction (%)		5.1	16.5	15.4	21.6	50.6	49.1
DO F reduction (%)		27.6	29.2	22.4	28.8	27.6	20.8

Coagulation 1 min at 160tr/min

Remark: **Floculation 30 sec at 15 min at 45tr/min**

Sedimentation 10 min

Floc size observed	Non	Poor	Quite good	Good	Very good	Excellent
-	Non floc visible	≤ 0.5 mm	≈ 0.5 mm	0.5 to 1 mm	1 to 1.5 mm	> 1.5 mm

COAGULATION / SEDIMENTATION TEST

Coagulant(s): WAC HB (SM: 6.06532g/L)
Polymer: AN 905 (SM: 0.01883g/L)

Beaker No.	Raw water	1	2	3	4	5	6
Dose coagulant (mg/l)		50	50	50	50	50	50
Dose Polymer (mg/l)		0.1	0.5	0.1	0.5	0.1	0.5
Flocculation time		30 sec	30 sec	1 min	1 min	15 min	15 min
pH	7.39	7.36	7.31	7.54	7.81	7.84	7.80
Temperature (°C)	22.5	22.6	22.6	22.6	22.6	22.6	22.6
Flocs size		Quite good	Quite good	Quite good	poor	Excellent	Excellent
Turbidity (NTU)	15.7 15.5	4.05 4.17	4.04 3.95	2.62 2.51	4.08 4.08	0.45 0.44	0.61 0.61
Average turbidity	15.60	4.11	4.00	2.57	4.08	0.46	0.61
DO 254nm NF (abs/5cm)	0.518	0.329	0.325	0.273	0.296	0.205	0.212
DO 254nm F (abs/5cm)	0.281	0.211	0.218	0.219	0.210	0.213	0.197
DO 254nm NF (abs/m)	10.360	6.580	6.500	5.460	5.920	4.100	4.240
DO 254nm F (abs/m)	5.620	4.220	4.360	4.380	4.200	4.260	3.940
Turbidity decreased (%)		73.7	74.4	83.5	73.8	97.1	96.1
DO NF reduction (%)		36.5	37.3	47.3	42.9	60.4	59.1
DO F reduction (%)		24.9	22.4	22.1	25.3	24.2	29.9

Remark: **Temps du jar-test :**
Coagulation 1 min at 160tr/min
Floculation 30 sec at 15 min at 45tr/min
Sedimentation 10 min

Floc size observed	N	Poor	Quite good	Good	Very good	Excellent
	Non floc visible	≤ 0.5 mm	≈ 0.5 mm	0.5 to 1 mm	1 to 1.5 mm	> 1.5 mm

COAGULATION / SEDIMENTATION TEST

Coagulant(s): WAC HB (SM: 6.06532g/L)
Polymer: AN 905 (SM: 0.01883g/L)

Beaker No.	Raw water	1	2	3	4	5	6
Dose coagulant (mg/l)		60	60	60	60	60	60
Dose Polymer (mg/l)		0.1	0.5	0.1	0.5	0.1	0.5
Flocculation time		30 sec	30 sec	1 min	1 min	15 min	15 min
pH	8.31	7.81	7.85	7.81	7.81	7.82	7.81
Température (°C)	22.6	22.5	22.5	22.5	22.5	22.6	22.7
Flocs size		Poor	Poor	Poor in sediment		Very good	Excellent
Turbidity (NTU)	5.64 5.72	3.77 3.79	4.53 4.48	2.33 2.39	2.39 2.26	0,49 0,48	0,53 0,54
Average turbidity	5.68	3.78	4.51	2.36	2.33	0.49	0.54
DO 254nm NF (abs/5cm)	0.352	0.294	0.294	0.247	0.241	0.173	0.176
DO 254nm F (abs/5cm)	0.249	0.176	0.174	0.175	0.176	0.176	0.174
DO 254nm NF (abs/m)	7.040	5.880	5.880	4.940	4.820	3.460	3.520
DO 254nm F (abs/m)	4.980	3.520	3.480	3.500	3.520	3.520	3.480
Turbidity decreased (%)		33.5	20.6	58.5	59.1	91.5	90.6
DO NF reduction (%)		16.5	16.5	29.8	31.5	50.9	50.0
DO F reduction (%)		29.3	30.1	29.7	29.3	29.3	30.1

Remark: Temps du jar-test :
Coagulation 1 min at 160tr/min
Floculation 30 sec at 15 min at 45tr/min
Sedimentation 10 min

	N	Poor	Quite good	Good	Very good	Excellent
Floc size observed	Non floc visible	≤ 0.5 mm	≈ 0.5 mm	0.5 to 1 mm	1 to 1.5 mm	> 1.5 mm

COAGULATION / SEDIMENTATION TEST

Coagulant(s): WAC HB (SM: 6.06532g/L)
Polymer: AN 905 (SM: 0.01883g/L)

Beaker No.	Raw water	1	2	3	4	5	6
Dose coagulant (mg/l)		40	40	50	50	60	60
Dose Polymer (mg/l)		0,1	0,5	0,1	0,5	0,1	0,5
Flocculation time		30 sec	30 sec	30 sec	30 sec	30 sec	30 sec
pH	7.98	7.88	7.88	7.87	7.84	7.79	7.81
Temperature (°C)	22,5	22.4	22.4	22.5	22.5	22.4	22.4
Flocs size		POOR-	POOR-	POOR+	POOR+	POOR+	POOR+
Turbidity (NTU)	5.12 4.99	4.75 4.78	4.55 4.79	4.37 4.37	4.57 4.65	4.12 3.93	3.86 3.70
Average turbidity	5.06	4.77	4.67	4.37	4.61	4.03	3.78
DO 254nm NF (abs/5cm)	0.329	0.325	0.320	0.304	0.312	0.296	0.285
DO 254nm F (abs/5cm)	0.251	0.185	0.180	0.178	0.176	0.172	0.172
DO 254nm NF (abs/m)	6.580	6.500	6.400	6.080	6.240	5.920	5.700
DO 254nm F (abs/m)	5.020	3.700	3.600	3.560	3.520	3.440	3.440
Turbidity decreased (%)		5.7	7.6	13.6	8.8	20.4	25.2
DO NF reduction (%)		1.2	2.7	7.6	5.2	10.0	13.4
DO F reduction (%)		26.3	28.3	29.1	29.9	31.5	31.5

Remark: Temps du jar-test :
Coagulation 1 min at 160tr/min
Floculation 30 sec at 45tr/min
Sedimentation 10 min

Floc size observed	N	Poor	Quite good	Good	Very good	Excellent
-	Non floc visible	≤ 0.5 mm	≈ 0.5 mm	0.5 to 1 mm	1 to 1.5 mm	> 1.5 mm

Beaker	EB	1	2	3	4	5	6	7	8	9	10	11	12
Dose coagulant (mg/L)		20	20	30	30	40	40	50	50	60	60	70	70
Dose polymer (mg/L)		0.1	0.5	0.1	0.5	0.1	0.5	0.1	0.5	0.1	0.5	0.1	0.5
Flocculation time		30 sec	30 sec	30 sec	30 sec	30 sec	30 sec	30 sec	30 sec	30 sec	30 sec	30 sec	30 sec
pH	8.15	8.10	8.07	7.99	7.98	7.93	7.92	7.83	7.86	7.87	7.84	7.80	7.78
Temperature (°C)	22.3	22.3	22.3	22.2	22.3	22.3	22.3	22.4	22.4	22.4	22.4	22.4	22.4
Flocs size		N	N	Poor-	Poor-	POOR-	POOR-	POOR	POOR	POOR+	POOR+	POOR+	POOR+
Turbidity (NTU)	6.26 6.08	6.28 6.28	6.61 6.84	6.60 6.42	6.49 6.39	5.80 5.58	5.68 5.66	5.44 5.91	6.07 5.67	4.41 4.41	4.65 4.67	2.78 2.57	2.80 2.61
Calculated turbidity	6.17	6.28	6.73	6.51	6.44	5.69	5.67	5.68	5.87	4.41	4.66	2.68	2.71
DO 254nm NF (abs/5cm)	0.350	0.354	0.343	0.352	0.348	0.338	0.338	0.320	0.317	0.288	0.296	0.239	0.239
DO 254nm F (abs/5cm)	0.252	0.198	0.217	0.186	0.189	0.178	0.179	0.188	0.177	0.176	0.179	0.171	0.171
DO 254nm NF (abs/m)	7.000	7.080	6.860	7.040	6.960	6.760	6.760	6.400	6.340	5.760	5.920	4.780	4.780
DO 254nm F (abs/m)	5.040	3.960	4.340	3.720	3.780	3.560	3.580	3.760	3.540	3.520	3.580	3.420	3.420
Turbidity removal (%)		-1.8	-9.0	-5.5	-4.4	7.8	8.1	8.0	4.9	28.5	24.5	56.6	56.2
DO NF removal (%)		-1.1	2.0	-0.6	0.6	3.4	3.4	8.6	9.4	17.7	15.4	31.7	31.7
DO F removal (%)		21.4	13.9	26.2	25.0	29.4	29.0	25.4	29.8	30.2	29.0	32.1	32.1

Appendix D-II: Jar test experiment with varied coagulant, flocculant and air pressurized water flow

Date   14-08-09

Condition

La Marne   Flow rate   1000   l/hr

Coagulant   WAC HB   **30**   mg/l   Scale   1.52   Flow rate   4.95   l/hr

Flocculant   AN 905   **0.1**   mg/l   Scale   2.37   Flow rate   6.43   l/hr

Air pressurized water flow rate   **100**   l/hr

- with static mixer

Sample	Turbidity NTU		Calculated turbidity	**Average Turbidity**	Filtrated Abs (abs/5cm)	Non Filtrated Abs (abs/5cm)	Paper wt g	Paper+mass g/l	**mass mg/l**	**Average SS (mg/l)**
Blank (1)	6.54			**6.31**	0.228	0.340	0.0764	0.0768	4.0	
(2)	6.07						0.0768	0.0764	-4.0	
(3)	6.1						0.0797	0.0800	3.0	**3.5**
Centre zone (1)	7.92	7.64	7.78		0.180	0.342	0.0849	0.0855	6.0	
(2)	8.13	7.98	8.06		0.172	0.359	0.0844	0.0862	18.0	
(3)	6.82	7.37	7.10	**7.64**	0.166	0.393	0.0880	0.0885	5.0	**9.7**
Wall zone (1)	5.70	6.22	5.96		0.170	0.324	0.0764	0.0774	10.0	
(2)	5.96	5.84	5.90		0.173	0.313	0.0778	0.0785	7.0	
(3)	4.80	4.94	4.87	**5.58**	0.164	0.295	0.0819	0.0827	8.0	**8.3**

The non filtrated absorbance shows the total dissolved organic material

Date   17-08-09

Condition
La Marne   Flow rate   1000   l/hr
Coagulant   **WAC HB**   **70**   mg/l   Scale   3.48   Flow rate   11.54   l/hr
Flocculant   **AN 905**   **0.1**   mg/l   Scale   2.37   Flow rate   6.43   l/hr
Air pressurized water flow rate   **100**   l/hr
- with static mixer

Sample	Turbidity NTU		Calculated turbidity	**Average Turbidity**	Filtrated Abs (abs/5cm)	Non Filtrated Abs (abs/5cm)	Paper wt g	Paper+mass g/l	**mass mg/l**	**Average SS (mg/l)**
Blank (1)	8.11			**8.46**	0.213	0.350	0.0939	0.0941	2.0	
(2)	8.80						0.0941	0.0937	-4.0	
(3)	8.41						0.0833	0.0837	4.0	**3.0**
Centre zone (1)	6.85	6.75	6.80		0.143	0.312	0.0928	0.0938	10.0	
(2)	9.32	10.20	9.76		0.146	0.414	0.0943	0.0959	16.0	
(3)	8.60	9.50	9.05	**8.54**	0.144	0.381	0.0844	0.0859	15.0	**13.7**
Wall zone (1)	3.50	3.50	3.50		0.141	0.228	0.0935	0.0933	-2.0	
(2)	3.20	3.30	3.25		0.136	0.219	0.0934	0.0936	2.0	
(3)	3.20	3.10	3.15	**3.30**	0.136	0.222	0.0943	0.0943	0.0	**1.0**

The non filtrated absorbance shows the total dissolved organic material

Date 14-08-09

Condition

La Marne Flow rate 1000 l/hr

Coagulant **WAC HB** **30** mg/l Scale 1.52 Flow rate 4.95 l/hr

Flocculant **AN 905** **0.5** mg/l Scale 8.33 Flow rate 32.13 l/hr

Air pressurized water flow rate **100** l/hr

- with static mixer

Sample	Turbidity NTU		Calculated Turbidity	**Average Turbidity**	Filtrated Abs (abs/5cm)	Non Filtrated Abs (abs/5cm)	Paper wt g	Paper+mass g/l	mass mg/l	**Average SS (mg/l)**
Blank (1)	6.53			**6.52**	0.201	0.433	0.0848	0.0852	4.0	
(2)	6.51						0.0823	0.0828	5.0	
(3)							0.0779	0.0788	9.0	**6.0**
Centre zone (1)	5.85	5.90	5.88		0.159	0.303	0.0771	0.0776	5.0	
(2)	6.39	7.01	6.70		0.169	0.323	0.0767	0.0769	2.0	
(3)	6.68	6.95	6.82	**6.46**	0.160	0.339	0.0767	0.0777	10.0	**5.7**
Wall zone (1)	5.47	4.88	5.18		0.174	0.285	0.0807	0.0807	0.0	
(2)	5.03	5.37	5.20		0.160	0.301	0.0837	0.0840	3.0	
(3)	5.67	5.58	5.63	**5.33**	0.182	0.310	0.0856	0.0857	1.0	**1.3**

The non filtrated absorbance shows the total dissolved organic material

Date   13-08-09

Condition
La Marne   Flow rate   1000 l/hr
Coagulant   **WAC HB**   **70** mg/l   Scale   3.48 Flow rate   11.54 l/hr
Flocculant   **AN 905**   **0.5** mg/l   Scale   8.33 Flow rate   32.13 l/hr
Air pressurized water flow rate   **100** l/hr
- with static mixer

Sample	Turbidity NTU		Calculated turbidity	**Average Turbidity**	Filtrated Abs (abs/5cm)	Non Filtrated Abs (abs/5cm)	Paper wt g	Paper+mass g/l	mass mg/l	**Average SS (mg/l)**
Blank (1)	5.60			**5.50**	0.216	0.374	0.0804	0.0801	-3.0	
(2)	5.51						0.0838	0.0836	-2.0	
(3)	5.39						0.0854	0.0851	-3.0	**error**
Centre zone (1)	5.51	5.44	5.48		0.146	0.262	0.0859	0.0865	6.0	
(2)	5.86	5.63	5.75		0.145	0.308	0.0886	0.0897	11.0	
(3)	7.09	6.76	6.93	**6.05**	0.143	0.365	0.0857	0.0865	8.0	**8.3**
Wall zone (1)	4.19	4.38	4.29		0.143	0.236	0.0782	0.0780	-2.0	
(2)	4.76	4.81	4.79		0.158	0.251	0.0773	0.0774	1.0	
(3)	4.48	4.76	4.62	**4.56**	0.146	0.318	0.0826	0.0827	1.0	**1.0**

note: The sample volume of the suspended solid test = 100 ml

Date   18-08-09

Condition

La Marne   Flow rate   1000 l/hr

Coagulant   **WAC HB**   **70** mg/l   Scale   3.48 Flow rate   11.54 l/hr

Flocculant   **AN 905**   **0.1** mg/l   Scale   2.37 Flow rate   6.43 l/hr

Air pressurized water flow rate   **50** l/hr

- with static mixer

Sample	Turbidity NTU		Calculated turbidity	**Average Turbidity**	Filtrated Abs (abs/5cm)	Non Filtrated Abs (abs/5cm)	Paper wt g	Paper+mass g/l	**mass mg/l**	**Average SS (mg/l)**
Blank (1)	5.80			**5.80**	0.195	0.361	0.0945	0.0947	2.0	
(2)	5.80						0.0940	0.0945	5.0	
(3)	5.90						0.0931	0.0934	3.0	**3.3**
Centre zone (1)	7.20	6.30	6.75		0.144	0.361	0.0934	0.0948	14.0	
(2)	6.80	6.40	6.60		0.141	0.320	0.0935	0.0945	10.0	
(3)	7.40	7.80	7.60	**6.98**	0.145	0.369	0.0930	0.0942	12.0	**12.0**
Wall zone (1)	5.80	5.80	5.80		0.140	0.307	0.0933	0.0942	9.0	
(2)	6.30	6.30	6.30		0.143	0.301	0.0942	0.0952	10.0	
(3)	5.40	5.80	5.60	**5.90**	0.144	0.313	0.0948	0.0955	7.0	**8.7**

Date   17-08-09

Condition

La Marne	Flow rate	1000	l/hr			
Coagulant	**WAC HB**	**70**	mg/l	Scale	3.48	Flow rate	11.54	l/hr
Flocculant	**AN 905**	**0.1**	mg/l	Scale	2.37	Flow rate	6.43	l/hr

Air pressurized water flow rate   **200** l/hr

- with static mixer

Sample	Turbidity NTU		Calculated turbidity	**Average Turbidity**	Filtrated Abs (abs/5cm)	Non Filtrated Abs (abs/5cm)	Paper wt g	Paper+mass g/l	**mass mg/l**	**Average SS (mg/l)**
Blank (1)	6.20			**6.30**	0.199	0.343	0.0933	0.0937	4.0	
(2)	6.40						0.0938	0.0940	2.0	
(3)	6.20						0.0934	0.0938	4.0	**3.3**
Centre zone (1)	7.60	7.60	7.60		0.130	0.324	0.0932	0.0945	13.0	
(2)	7.00	6.90	6.95		0.149	0.315	0.0941	0.0952	11.0	
(3)	6.90	7.80	7.35	**7.30**	0.136	0.323	0.0937	0.0949	12.0	**12.0**
Wall zone (1)	3.00	3.10	3.05		0.134	0.213	0.0927	0.0928	1.0	
(2)	3.30	3.30	3.30		0.126	0.212	0.0931	0.0934	3.0	
(3)	3.40	3.40	3.40	**3.25**	0.130	0.216	0.0939	0.0941	2.0	**2.0**

Date   18-08-09

Condition

La Marne	Flow rate	1000	l/hr				
Coagulant	**WAC HB**	**70**	mg/l	Scale	3.48	Flow rate	11.54 l/hr
Flocculant	**AN 905**	**0.2**	mg/l	Scale	2.37	Flow rate	6.43 l/hr
Air pressurized water flow rate			**100**	l/hr			

- with static mixer

Sample	Turbidity NTU		Calculated turbidity	**Average Turbidity**	Filtrated Abs (abs/5cm)	Non Filtrated Abs (abs/5cm)	Paper wt g	Paper+mass g/l	**mass mg/l**	**Average SS (mg/l)**
Blank (1)	6.30			**6.25**	0.195	0.359	0.0940	0.0948	8.0	
(2)	6.20						0.0938	0.0946	8.0	
(3)	6.60						0.0944	0.0949	5.0	**7.0**
Centre zone (1)	6.20	6.50	6.35		0.137	0.344	0.0931	0.0948	17.0	
(2)	6.10	6.40	6.25		0.141	0.348	0.0931	0.0941	10.0	
(3)	6.20	5.80	6.00	**6.20**	0.140	0.355	0.0932	0.0944	12.0	**13.0**
Wall zone (1)	3.10	3.20	3.15		0.133	0.246	0.0939	0.0944	5.0	
(2)	3.80	3.90	3.85		0.141	0.268	0.0946	0.0954	8.0	
(3)	3.90	3.90	3.90	**3.63**	0.139	0.272	0.0943	0.0953	10.0	**7.7**

Date _19-08-09_

Condition

La Marne   Flow rate _1000_ l/hr

Coagulant   **WAC HB** _70_ mg/l   Scale _3.48_ Flow rate _11.54_ l/hr

Flocculant   **AN 905** _0.2_ mg/l   Scale _2.37_ Flow rate _6.43_ l/hr

Air pressurized water flow rate _100_ l/hr

The volume of raw water in the tank _400_ l

- With static mixer and Coagulation in the raw water mixing tank and Injection of Flocculant before static mixer

Sample	Turbidity NTU		Calculated turbidity	**Average Turbidity**	Filtrated Abs (abs/5cm)	Non Filtrated Abs (abs/5cm)	Paper wt g	Paper+mass g/l	**mass mg/l**	**Average SS (mg/l)**
Blank (1)	5.80			**5.80**	0.212	0.328	0.0938	0.0940	2.0	
(2)	5.80						0.0934	0.0936	2.0	
(3)	5.70						0.0943	0.0945	2.0	**2.0**
Centre zone (1)	6.40	6.70	6.55		0.177	0.297	0.0936	0.0942	6.0	
(2)	6.70	6.50	6.60		0.172	0.298	0.0930	0.0934	4.0	
(3)	7.30	7.30	7.30	**6.82**	0.166	0.297	0.0933	0.0937	4.0	**4.7**
Wall zone (1)	6.40	7.00	6.70		0.182	0.318	0.0940	0.0945	5.0	
(2)	6.40	6.10	6.25		0.173	0.295	0.0939	0.0942	3.0	
(3)	6.90	6.90	6.90	**6.62**	0.163	0.300	0.0927	0.0933	6.0	**4.7**

BIOGRAPHY

My name is Vorasiri Siangsanun. I was born the 18th July 1979 at Nakhornratchasima, Thailand. I graduated a Bachelor degree in environmental engineering (B.Eng.) from Environmental Faculty of Suranaree University of Technology (2002) and graduated a Master degree in Environmental Engineering (M.Eng.) at Chulalongkorn university (2006) with a Franco-Thai program between Institut National des Sciences Appliquées de Toulouse (INSA-Toulouse),France and Chulalongkorn university, Bangkok Thailand. In 2007, I continued my study in Dual Ph.D. program which was the international cooperation between INSA Toulouse and Chulalonkorn University, Thailand.

This is the list of my publication

- V. Siangsanun, C. Guigui, J. Morchain, P. Marteil, C. Levecq, C. Puprasert, G.Hébrard.

"Velocity measurement in the hydrocyclone by oil droplet, Doppler Ultrasound Velocimetry and CFD modeling". Oral presentation in the 8th world congress of chemical engineering. 23-27 August 2009. Montréal, Canada.

- V. Siangsanun, C. Guigui, J. Morchain, P. Marteil, C. Levecq, C. Puprasert, G.Hébrard.

"Velocity measurement in the hydrocyclone by oil droplet, Doppler Ultrasound Velocimetry and CFD modeling". In the process of submission for the Canadian Journal of Chemical Engineering.